

this document downloaded from

vulcanhammer.info

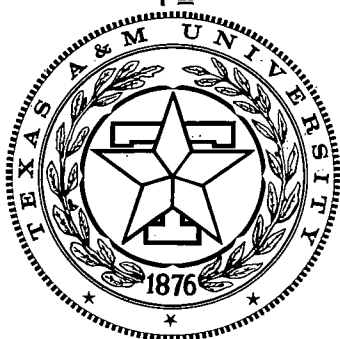
the website about
Vulcan Iron Works
Inc. and the pile
driving equipment it
manufactured

Visit our companion site
<http://www.vulcanhammer.org>

Terms and Conditions of Use:

All of the information, data and computer software ("information") presented on this web site is for general information only. While every effort will be made to insure its accuracy, this information should not be used or relied on for any specific application without independent, competent professional examination and verification of its accuracy, suitability and applicability by a licensed professional. Anyone making use of this information does so at his or her own risk and assumes any and all liability resulting from such use. The entire risk as to quality or usability of the information contained within is with the reader. In no event will this web page or webmaster be held liable, nor does this web page or its webmaster provide insurance against liability, for any damages including lost profits, lost savings or any other incidental or consequential damages arising from the use or inability to use the information contained within.

This site is not an official site of Prentice-Hall, Pile Buck, or Vulcan Foundation Equipment. All references to sources of software, equipment, parts, service or repairs do not constitute an endorsement.



TEXAS
TRANSPORTATION
INSTITUTE

TEXAS
HIGHWAY
DEPARTMENT

COOPERATIVE
RESEARCH

PILE DRIVING ANALYSIS— STATE OF THE ART

in cooperation with the
Department of Transportation
Federal Highway Administration
Bureau of Public Roads

RESEARCH REPORT 33-13 (FINAL)
STUDY 2-5-62-33
PILING BEHAVIOR

PILE DRIVING ANALYSIS STATE OF THE ART

by

Lee Leon Lowery, Jr.
Associate Research Engineer

T. J. Hirsch
Research Engineer

Thomas C. Edwards
Assistant Research Engineer

Harry M. Coyle
Associate Research Engineer

Charles H. Samson, Jr.
Research Engineer

Research Report 33-13 (Final)

*Research Study No. 2-5-62-33
Piling Behavior*

Sponsored by
The Texas Highway Department
in cooperation with the
U. S. Department of Transportation, Federal Highway Administration
Bureau of Public Roads

January 1969

TEXAS TRANSPORTATION INSTITUTE
Texas A&M University
College Station, Texas

Foreword

The information contained herein was developed on the Research Study 2-5-62-33 entitled "Piling Behavior" which is a cooperative research endeavor sponsored jointly by the Texas Highway Department and the U. S. Department of Transportation, Federal Highway Administration, Bureau of Public Roads, and also by the authors as evidenced by the number of publications during the past seven years of intense study and research. The broad objective of the project was to fully develop the computer solution of the wave equation and its use for pile driving analysis, to determine values for the significant parameters involved to enable engineers to predict driving stresses in piling during driving, and to estimate the static soil resistance to penetration on piling at the time of driving from driving resistance records.

The opinions, findings, and conclusions expressed in this report are those of the authors and not necessarily those of the Bureau of Public Roads.

Acknowledgments

Since this report is intended to summarize the research efforts and experience gained by the authors over a seven-year period, it is impossible to mention all of the persons, companies, and agencies without whose cooperation and support no "state of the art" in the analysis of piling by the wave equation would exist.

The greatest debt of gratitude is due Mr. E. A. L. Smith, Chief Mechanical Engineer of Raymond International (now retired), who not only first proposed the method of analysis but also maintained a continuing interest throughout the work and contributed significantly to the accomplishments of the research. His advice and guidance, based on his extensive field experience, and his intimate knowledge of the wave equation have proven invaluable throughout all phases of the research.

The authors gratefully acknowledge the assistance and support of Farland C. Bundy and Wayne Henneberger of the Bridge Division of the Texas Highway Department, who worked closely with the authors in accomplishing several of the projects. A debt of gratitude is due the Bass Bros. Concrete Company of Victoria, Ross Anglin and Son, General Contractors, and the California Company of New Orleans for their unselfish cooperation with all phases of the field work. It was indeed fortunate to have these foresighted and progressive businessmen as contractors on the various jobs. They willingly invested considerable amounts of their own time and effort to the accomplishment of the research projects.

Sincere thanks and our personal appreciation are extended to the Texas Highway Department and the U. S. Department of Transportation, Federal Highway Administration, Bureau of Public Roads, whose sponsorship made all the research and studies leading to this report a reality.

Several graduate students and research assistants contributed significantly to the accomplishment of this work. They were Tom P. Airhart, Gary N. Reeves, Paul C. Chan, Carl F. Raba, Gary Gibson, I. H. Sulaiman, James R. Finley, M. T. Al-Layla, and John Miller.

TABLE OF CONTENTS

	Page
LIST OF FIGURES	v
LIST OF TABLES	vi
CHAPTER	
I INTRODUCTION	1
II PILE DRIVING ANALYSIS	1
2.1 General	1
2.2 Smith's Numerical Solution of the Wave Equation	2
2.3 Critical Time Interval	4
2.4 Effect of Gravity	5
III PILE DRIVING HAMMERS	6
3.1 Energy Output of Impact Hammers	6
3.2 Determination of Hammer Energy Output	6
3.3 Significance of Driving Accessories	8
3.4 Explosive Pressure in Diesel Hammers	10
3.5 Effect of Ram Elasticity	11
IV CAPBLOCKS AND CUSHION BLOCKS	12
4.1 Method Used to Determine Capblock and Cushion Properties	12
4.2 Idealized Load-Deformation Properties	14
4.3 Coefficient of Restitution	14
V STRESS WAVES IN PILING	15
5.1 Comparison with Laboratory Experiments	15
5.2 Significance of Material Damping in the Pile	16
VI SOIL PROPERTIES	17
6.1 General	17
6.2 Equations to Describe Soil Behavior	17
6.3 Soil Parameters to Describe Dynamic Soil Resistance During Pile Driving	18
6.4 Laboratory Tests on Sands	19
6.5 Static Soil Resistance After Pile Driving (Time Effect)	20
6.6 Field Test in Clay	20
VII USE OF THE WAVE EQUATION TO PREDICT PILE LOAD BEARING CAPACITY AT TIME OF DRIVING	21
7.1 Introduction	21
7.2 Wave Equation Method	21
7.3 Comparison of Predictions with Field Tests	24
VIII PREDICTION OF DRIVING STRESSES	25
8.1 Introduction	25
8.2 Comparison of Smith's Numerical Solution with the Classical Solution	25
8.3 Correlation of Smith's Solution with Field Measurements	26
8.4 Effect of Hammer Type and Simulation Method	26
8.5 Effect of Soil Resistance	27
8.6 Effects of Cushion Stiffness, Coefficient of Restitution, and Pile Material Damping	27
8.7 Fundamental Driving Stress Considerations	27
8.8 Summary of Fundamental Driving Stress Considerations	31
IX USE OF THE WAVE EQUATION FOR PARAMETER STUDIES	32
9.1 Introduction	32
9.2 Significant Parameters	32
9.3 Examples of Parameter Studies	32
X SUMMARY AND CONCLUSIONS	36

APPENDIX A	38
DEVELOPMENT OF EQUATIONS FOR IMPACT STRESSES IN A LONG, SLENDER, ELASTIC PILE	38
A1 Introduction	38
A2 One Dimensional Wave Equation	38
A3 Boundary Conditions	39
A4 Solving the Basic Differential Equation	39
A5 Maximum Compressive Stress at the Head of the Pile	41
A6 Length of the Stress Wave	42
APPENDIX B	43
WAVE EQUATION COMPUTER PROGRAM UTILIZATION MANUAL	43
B1 Introduction	43
B2 Idealization of Hammers	43
B3 Ram Kinetic Energies	44
B4 Method of Including Coefficient of Restitution in Capblock and Cushion Springs	45
B5 Idealization of Piles	47
B6 Explanation of Data Input Sheets	47
B7 Comments on Data Input	50
APPENDIX C	56
OS/360 FORTRAN IV PROGRAM STATEMENTS	56
LIST OF REFERENCES	78

LIST OF FIGURES

Figure	Page
2.1 Method of Representing Pile for Purpose of Calculation (After Smith)	2
2.2 Load Deformation Relationships for Internal Springs	3
2.3 Load Deformation Characteristics Assumed for Soil Spring M	3
3.1 Typical Force vs Time Curve for a Diesel Hammer	6
3.2 Steam Hammer	11
3.3 Diesel Hammer	11
4.1 Stress Strain Curve for a Cushion Block	13
4.2 Dynamic and Static Stress Strain Curves for a Fir Cushion	13
4.3 Cushion Test Stand	14
4.4 Dynamic Stress Strain Curve for an Oak Cushion	14
4.5 Dynamic Stress Strain Curve for a Micarta Cushion	15
4.6 Stress vs Strain for Garlock Asbestos Cushion	15
5.1 Theoretical vs Experimental Solution	16
5.2 Theoretical vs Experimental Solution	16
5.3 Theoretical vs Experimental Solution	16
5.4 Theoretical vs Experimental Solution	16
5.5 Comparison of Experimental and Theoretical Solutions for Stresses	17
6.1 Model Used by Smith to Describe Soil Resistance on Pile	17
6.2 Load Deformation Characteristics of Soil	18
6.3 Load Deformation Properties of Ottawa Sand Determined by Triaxial Tests (Specimens Nominally 3 in. in Diameter by 6.5 in. High)	18
6.4 Increase in Strength vs Rate of Loading—Ottawa Sand	19
6.5 "J" vs "V" for Ottawa Sand	19
6.6 "Set up" or Recovery of Strength After Driving in Cohesive Soil (After Reference 6.7)	20
6.7 Pore Pressure Measurements in Clay Stratum—50 ft Depth	20
7.1 Ultimate Driving Resistance vs Blows per Inch for an Example Problem	22
7.2 Comparison of Wave Equation Predicted Soil Resistance to Soil Resistance Determined by Load Test for Piles Driven in Sands (Data from Table 7.1)	22
7.3 Comparison of Wave Equation Predicted Soil Resistance to Soil Resistance Determined by Load Tests for Piles Driven in Clay (Data from Table 7.2)	23
7.4 Comparison of Wave Equation Predicted Soil Resistance to Soil Resistance Determined by Load Tests for Piles Driven in Both Sand and Clay	24

7.5	Summary of Piles Tested to Failure in Sands (From Reference 7.2)	24
7.6	Wave Equation Ultimate Resistance vs Test Load Failure (From Reference 7.2)	25
8.1	Maximum Tensile Stress Along a Pile	25
8.2	Maximum Compressive Stress Along a Pile	26
8.3	Stress in Pile Head vs Time for Test Pile	26
8.4	Stress at Mid-length of Pile vs Time for Test Pile	27
8.5	Idealized Stress Wave Produced When Ram Strikes Cushion at Head of Concrete Pile	29
8.6	Reflection of Stress Wave at Point of a Long Pile	30
8.7	Reflection of Stress Wave at Point of a Short Pile	30
8.8	Effect of Ratio of Stress Wave Length on Maximum Tensile Stress for Pile with Point Free	31
9.1	Effect of Cushion Stiffness, Ram Weight, and Driving Energy on Stresses	33
9.2	Effect of Cushion Stiffness, Ram Weight, and Driving Energy on Permanent Set	34
9.3	Computer Analysis of Pile Hammer Effectiveness in Overcoming Soil Resistance, Ru, When Driving a Pile Under Varying Conditions	35
9.4	Evaluation of Vulcan 020 Hammer (60,000 ft-lb) for Driving a Pile to Develop Ultimate Capacity of 2000 Tons	35
9.5	Blows/In. vs RU (Total) for Arkansas Load Test Pile 4	35
A.1	Long Slender Elastic Pile	38
A.2	Ram, Cushion, Pile	39
B.1	Case I.—Ram, Capblock, and Pile Cap	43
B.2	Case II.—Ram, Capblock, Pile Cap, and Cushion	44
B.3	Case III.—Ram, Anvil, Capblock, and Pile Cap	44
B.4	Definition of Coefficient of Restitution	46
B.5	Pile Idealization	47
B.6	Example Problem	51
B.7	Normal Output (Option 15=1) for Prob. 1	53
B.8	Effect of Varying Cushion Stiffness	54
B.9	Summary Output for RU (Total) vs Blows/In. (Option 11=1) for Prob. 1 and 2	54
B.10	Normal Output for Single RU (Total) (Option 11=2) for Prob. 3	55
B.11	Detailed Output for Single RU (Total) (Option 15=2) for Prob. 4	55

LIST OF TABLES

Table		Page
3.1	Summary of Hammer Properties in Operating Characteristics	8
3.2	Effect of Cushion Stiffness on ENTHRU	9
3.3	Effect of Cushion Stiffness on FMAX	9
3.4	Effect of Cushion Stiffness on LIMSET	9
3.5	Effect of Removing Load Cell on ENTHRU, LIMSET, and Permanent Set of Pile	10
3.6	Effect of Coefficient of Restitution on ENTHRU (Maximum Point Displacement)	10
3.7	Effect of Coefficient of Restitution on ENTHRU	10
3.8	Effect of Breaking Ram Into Segments When Ram Strikes a Cushion or Capblock	11
3.9	Effect of Breaking Ram Into Segments When Ram Strikes a Steel Anvil	12
4.1	Typical Secant Moduli of Elasticity (E) and Coefficients of Restitution (e) of Various Pile Cushioning Materials	14
7.1	Errors Caused by Assuming $J(\text{point}) = 0.1$ and $J'(\text{side}) = \frac{J(\text{point})}{3}$ for Sand-Supported Piles Only	22
7.2	Errors Caused by Assuming $J(\text{point}) = 0.3$ and $J'(\text{side}) = \frac{J(\text{point})}{3}$ for Clay (for Clay-Supported Piles Only)	23
7.3	Errors Caused by Assuming a Combined $J(\text{point}) = 0.1$ for Sand and $J(\text{point}) = 0.3$ for Clay Using Equation 7.1 (for Piles Supported by Both Sand and Clay)	24
8.1	Variation of Driving Stress With Ram Weight and Velocity	28
8.2	Variation of Driving Stress With Ram Weight and Ram Energy	29
B.1	Drop Hammers and Steam Hammers	45
B.2	Diesel Hammers	46

Pile Driving Analysis-State of the Art

CHAPTER I

Introduction

The tremendous increase in the use of piles in both landbased and offshore foundation structures and the appearance of new pile driving methods have created great engineering interest in finding more reliable methods for the analysis and design of piles. Ever since Isaac published his paper, "Reinforced Concrete Pile Formula," in 1931,^{1,1*} it has been recognized that the behavior of piling during driving does not follow the simple Newtonian impact as assumed by many simplified pile driving formulas, but rather is governed by the one dimensional wave equation. Unfortunately, an exact mathematical solution to the wave equation was not possible for most practical pile driving problems.

In 1950, E. A. L. Smith^{1,2} developed a tractable solution to the wave equation which could be used to solve extremely complex pile driving problems. The solution was based on a discrete element idealization of the actual hammer-pile-soil system coupled with the use of a high speed digital computer. In a paper published in 1960,^{1,3} he dealt exclusively with the application of wave theory to the investigation of the dynamic behavior of piling during driving. From that time to the present the authors have engaged in research dealing with wave equation analysis. The major objectives of these studies were as follows:

1. To develop a computer program based upon a procedure developed by Smith to provide the engineer with a mathematical tool with which to investigate the behavior of a pile during driving.
2. To conduct field tests to obtain experimental data with which to correlate the theoretical solution.
3. To make an orderly theoretical computer investi-

*Numerical superscripts refer to corresponding items in the References.

gation of the influence of various parameters on the behavior of piles during driving and to present the results in the form of charts, diagrams or tables for direct application by office design engineers.

4. To present recommendations concerning good driving practices which would prevent cracking and spalling of prestressed concrete piles during driving.
5. To determine the dynamic load-deformation properties of various pile cushion materials which had tacitly been assumed linear.
6. To determine the dynamic load-deformation properties of soils required by the wave equation analysis.
7. To generalize Smith's original method of analysis and to develop the full potential of the solution by using the most recent and accurate parameter values determined experimentally.
8. To illustrate the significance of the parameters involved, such as the stiffness and coefficient of restitution of the cushion, ram velocity, material damping in the pile, etc., and to determine the quantitative effect of these parameters where possible.
9. To study and if possible evaluate the actual energy output for various pile driving hammers, the magnitudes of which were subject to much disagreement.
10. To develop the computer solution for the wave equation so that it may be used to estimate the resistance to penetration of piling at the time of driving from the driving records.
11. To develop a comprehensive users manual for the final computer program to enable its use by others.

CHAPTER II

Pile Driving Analysis

2.1 General

The rapidly increasing use of pile foundations and the appearance of new pile driving techniques have caused great interest among engineers in finding more reliable methods of pile analysis and design. As noted by Dunham,^{2,4} "A pile driving formula is an attempt to evaluate the resistance of a pile to the dynamic forces applied upon it during the driving and to estimate from this the statical longitudinal load that the pile can support safely as a part of the permanent substructure."

In 1851, Sanders (Army Corps of Engineers) proposed the first dynamic pile driving formula by equating the total energy of the ram at the instant of impact to the work done in forcing down the pile, that is, the product of the weight of the ram and the stroke was assumed equal to the product of the ultimate soil resistance by the distance through which the pile moved. Sanders applied a safety factor of 8 to this ultimate soil resistance to determine an assumed safe load capacity for the pile. Since that time, a multitude of formulas have been proposed, some of which are semirational, others being

strictly empirical. Many of the formulas proposed attempt to account for various impact losses through the cushion, capblock, pile, and soil.

When restricted to a particular soil, pile, and driving condition for which correlation factors were derived, dynamic formulas are often able to predict ultimate bearing capacities which agree with observed test loads. However, since several hundred pile driving formulas have been proposed there is usually the problem of choosing an appropriate or suitable one.^{2,3} Also distressing is the fact that in many cases no dynamic formula yields acceptable results; for example, long heavy piles generally show much greater ultimate loads than predicted by pile driving equations.^{2,5} This has become increasingly significant since prestressed concrete piles 172 ft long and 54 in. in diameter have been successfully driven,^{2,6} and more and more large diameter steel piles several hundred feet long are being used in offshore platforms. Numerous field tests have shown that the use of pile driving formulas may well lead to a foundation design ranging from wasteful to dangerous.^{2,4}

Driving stresses are also of major importance in the design of piles, yet compressive stresses are commonly determined simply by dividing the ultimate driving resistance by the cross-sectional area of the pile.^{2,7,2,8} Furthermore, conventional pile driving analyses are unable to calculate tensile stresses, which are of the utmost importance in the driving of precast or prestressed concrete piles. This method of stress analysis completely overlooks the true nature of the problem and computed stresses almost never agree with experimental values.^{2,7,2,9} Tensile failures of piles have been noted on numerous occasions^{2,7,2,10 2,11} and the absence of a reliable method of stress analysis has proven to be a serious problem.

Although most engineers today realize that pile driving formulas have serious limitations and cannot be depended upon to give accurate results, they are still used for lack of an adequate substitute. For further discussion of pile formulas in general, the reader is referred to the work of Chellis.^{2,5}

Isaacs^{2,1} is thought to have first pointed out the occurrence of wave action in piling during driving. He proposed a solution to the wave equation assuming that the point of the pile was fixed and that side resistance was absent. These assumptions were so restrictive that the solution was probably never used in practice. Cummings^{2,10} in an earlier writing noted that although the pile driving formulas were based on numerous erroneous assumptions and that only the wave equation could be expected to yield accurate results for all driving conditions, he also pointed out that such solutions involved "long and complicated mathematical expressions so that their use for practical problems would involve laborious, numerical calculations." In fact, with the advent of a multitude of different type driving hammers and driving conditions, an exact solution to the wave equation was not known.

2.2 Smith's Numerical Solution of the Wave Equation

In 1950, Smith^{2,2} proposed a more realistic solution to the problem of longitudinal impact. This solution is

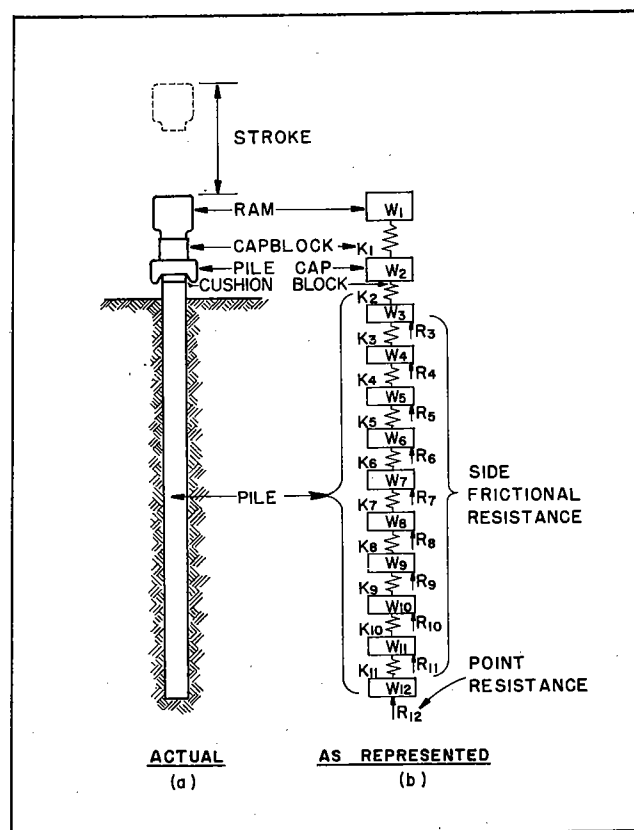


Figure 2.1. Method of representing pile for purpose of analysis (after Smith).

based on dividing the distributed mass of the pile into a number of concentrated weights $W(1)$ through $W(p)$, which are connected by weightless springs $K(1)$ through $K(p-1)$, with the addition of soil resistance acting on the masses, as illustrated in Figure 2.1(b). Time is also divided into small increments.

Smith's proposed solution involved the idealization of the actual continuous pile shown in Figure 2.1(a), as a series of weights and springs as shown in Figure 2.1(b). For the idealized system he set up a series of equations of motion in the form of finite difference equations which were easily solved using high-speed digital computers. Smith extended his original method of analysis to include various nonlinear parameters such as elastoplastic soil resistance including velocity damping and others.

Figure 2.1 illustrates the idealization of the pile system suggested by Smith. In general, the system is considered to be composed of (see Figure 2.1(a)):

1. A ram, to which an initial velocity is imparted by the pile driver;
2. A capblock (cushioning material);
3. A pile cap;
4. A cushion block (cushioning material);
5. A pile; and
6. The supporting medium, or soil.

In Figure 2.1(b) are shown the idealizations for the various components of the actual pile. The ram, cap-block, pile cap, cushion block, and pile are pictured as appropriate discrete weights and springs. The frictional soil resistance on the side of the pile is represented by a series of side springs; the point resistance is accounted for by a single spring at the point of the pile. The characteristics of these various components will be discussed in greater detail later in this report.

Actual situations may deviate from that illustrated in Figure 2.1. For example, a cushion block may not be used or an anvil may be placed between the ram and capblock. However, such cases are readily accommodated.

Internal Springs. The ram, capblock, pile cap, and cushion block may in general be considered to consist of "internal" springs, although in the representation of Figure 2.1(b) the ram and the pile cap are assumed rigid (a reasonable assumption for many practical cases).

Figures 2.2(a) and 2.2(b) suggest different possibilities for representing the load-deformation characteristics of the internal springs. In Figure 2.2(a), the material is considered to experience no internal damping. In Figure 2.2(b) the material is assumed to have internal damping according to the linear relationship shown.

External Springs. The resistance to dynamic loading afforded by the soil in shear along the outer surface of the pile and in bearing at the point of the pile is extremely complex. Figure 2.3 shows the load-deforma-

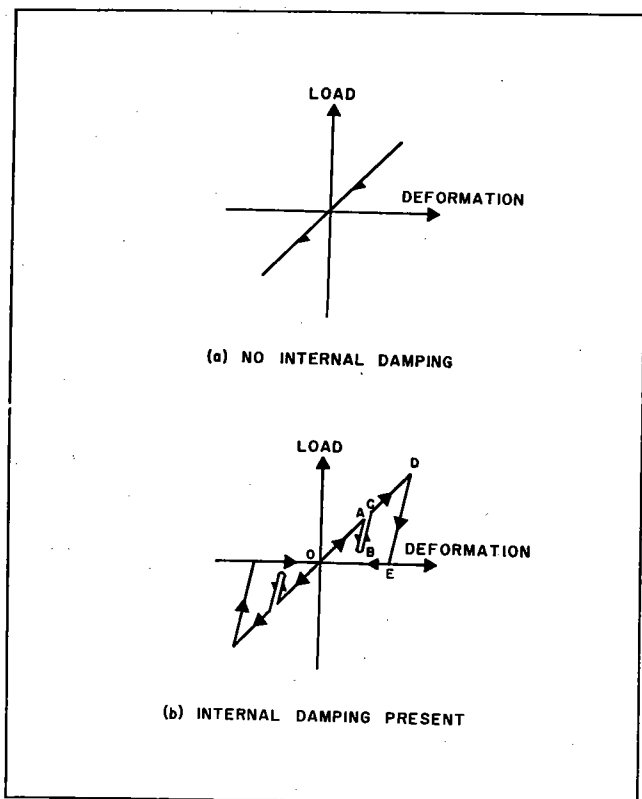


Figure 2.2. Load-deformation relationships for internal springs.

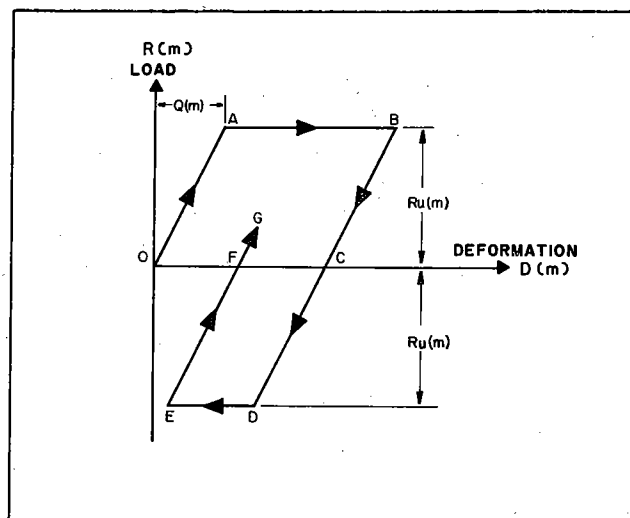


Figure 2.3. Load-deformation characteristics assumed for soil spring m .

tion characteristics assumed for the soil in Smith's procedure, exclusive of damping effects. The path OABC-DEFG represents loading and unloading in side friction. For the point, only compressive loading may take place and the loading and unloading path would be along OABCF.

It is seen that the characteristics of Figure 2.3 are defined essentially by the quantities "Q" and "Ru." "Q" is termed the soil quake and represents the maximum deformation which may occur elastically. "Ru" is the ultimate ground resistance, or the load at which the soil spring behaves purely plastically.

A load-deformation diagram of the type in Figure 2.3 may be established separately for each spring. Thus, $K'(m)$ equals $Ru(m)$ divided by $Q(m)$, where $K'(m)$ is the spring constant (during elastic deformation) for external spring m .

Basic Equations. Equations (2.3) through (2.7) were developed by Smith.^{2,2}

$$D(m,t) = D(m,t-1) + 12\Delta t V(m,t-1) \quad (2.3)$$

$$C(m,t) = D(m,t) - D(m+1,t) \quad (2.4)$$

$$F(m,t) = C(m,t) K(m) \quad (2.5)$$

$$R(m,t) = [D(m,t) - D'(m,t)] K'(m) [1 + J(m) V(m,t-1)] \quad (2.6)$$

$$V(m,t) = V(m,t-1) + [F(m-1,t) - F(m,t) - R(m,t)] \frac{g\Delta t}{W(m)} \quad (2.7)$$

where

() = functional designation;

m = element number;

t = number of time interval;

Δt = size of time interval (sec);

$C(m,t)$ = compression of internal spring m in time interval t (in.);

- $D(m,t)$ = displacement of element m in time interval t (in.);
 $D'(m,t)$ = plastic displacement of external soil spring m in time interval t (in.);
 $F(m,t)$ = force in internal spring m in time interval t (lb);
 g = acceleration due to gravity (ft/sec²);
 $J(m)$ = damping constant of soil at element m (sec/ft);
 $K(m)$ = spring constant associated with internal spring m (lb/in.);
 $K'(m)$ = spring constant associated with external soil spring m (lb/in.);
 $R(m,t)$ = force exerted by external spring m on element m in time interval t (lb);
 $V(m,t)$ = velocity of element m in time interval t (ft/sec); and
 $W(m)$ = weight of element m (lb).

This notation differs slightly from that used by Smith. Also, Smith restricts the soil damping constant J to two values, one for the point of the pile in bearing and one for the side of the pile in friction. While the present knowledge of damping behavior of soils perhaps does not justify greater refinement, it is reasonable to use this notation as a function of m for the sake of generality.

The use of a spring constant $K(m)$ implies a load-deformation behavior of the sort shown in Figure 2.2(a). For this situation, $K(m)$ is the slope of the straight line. Smith develops special relationships to account for internal damping in the capblock and the cushion block. He obtains instead of Equation 2.5 the following equation:

$$F(m,t) = \frac{K(m)}{[e(m)]^2} C(m,t) - \left[\frac{1}{[e(m)]^2} - 1 \right] K(m) C(m,t)_{\max} \quad (2.8)$$

where

$e(m)$ = coefficient of restitution of internal spring m ; and

$C(m,t)_{\max}$ = temporary maximum value of $C(m,t)$.

With reference to Figure 2.1, Equation (2.8) would be applicable in the calculation of the forces in internal springs $m = 1$ and $m = 2$. The load-deformation relationship characterized by Equation (2.8) is illustrated by the path OABCDEO in Figure 2.2(b). For a pile cap or a cushion block, no tensile forces can exist; consequently, only this part of the diagram applies. Intermittent unloading-loading is typified by the path ABC, established by control of the quantity $C(m,t)_{\max}$ in Equation (2.8). The slopes of lines AB, BC, and DE depend upon the coefficient of restitution $e(m)$.

The computations proceed as follows:

1. The initial velocity of the ram is determined from the properties of the pile driver. Other time-dependent quantities are initialized at zero or to satisfy static equilibrium conditions.
2. Displacements $D(m,1)$ are calculated by Equation (2.3). It is to be noted that $V(1,0)$ is the initial velocity of the ram.
3. Compressions $C(m,1)$ are calculated by Equation (2.4).
4. Internal spring forces $F(m,1)$ are calculated by Equation (2.5) or Equation (2.8) as appropriate.
5. External spring forces $R(m,1)$ are calculated by Equation (2.6).
6. Velocities $V(m,1)$ are calculated by Equation (2.7).
7. The cycle is repeated for successive time intervals.

In Equation (2.6), the plastic deformation $D'(m,t)$ for a given external spring follows Figure (2.3) and may be determined by special routines. For example, when $D(m,t)$ is less than $Q(m)$, $D'(m,t)$ is zero; when $D(m,t)$ is greater than $Q(m)$ along line AB (see Figure 2.3), $D'(m,t)$ is equal to $D(m,t) - Q(m)$.

Smith notes that Equation (2.6) produces no damping when $D(m,t) - D'(m,t)$ becomes zero. He suggests an alternate equation to be used after $D(m,t)$ first becomes equal to $Q(m)$:

$$R(m,t) = [D(m,t) - D'(m,t)] K'(m) + \frac{J(m) K'(m) Q(m) V(m,t-1)}{Q(m)} \quad (2.9)$$

Care must be used to satisfy conditions at the head and point of the pile. Consider Equation (2.5). When $m = p$, where p is number of the last element of the pile, $K(p)$ must be set equal to zero since there is no $F(p,t)$ force (see Figure 1.1). Beneath the point of the pile, the soil spring must be prevented from exerting tension on the pile point. In applying Equation (2.7) to the ram ($m = 1$), one should set $F(0,t)$ equal to zero.

For the idealization of Figure 2.1, it is apparent that the spring associated with $K(2)$ represents both the cushion block and the top element of the pile. Its spring rate may be obtained by the following equation:

$$\frac{1}{K(2)} = \frac{1}{K(2)_{\text{cushion}}} + \frac{1}{K(2)_{\text{pile}}} \quad (2.10)$$

A more complete discussion of digital computer programming details and recommended values for various physical quantities are given in the Appendices.

From the point of view of basic mechanics, the wave equation solution is a method of analysis well founded physically and mathematically.

2.3 Critical Time Interval

The accuracy of the discrete-element solution is also related to the size of the time increment Δt . Heising^{2,13} in his discussion of the equation of motion for free longitudinal vibrations in a continuous elastic bar, points

out that the discrete-element solution is an exact solution of the partial differential equation when

$$\Delta t = \frac{\Delta L}{\sqrt{E/\rho}}$$

where ΔL is the segment length. Smith^{3,2} draws a similar conclusion and has expressed the critical time interval as follows:

$$\Delta t = \frac{1}{19.648} \sqrt{\frac{W_{(m+1)}}{K_{(m)}}} \quad (2.11a)$$

or

$$\Delta t = \frac{1}{19.648} \sqrt{\frac{W_{(m)}}{K_m}} \quad (2.11b)$$

If a time increment larger than that given by Equation 2.11 is used, the discrete-element solution will diverge and no valid results can be obtained. As pointed out by Smith, in this case the numerical calculation of the discrete-element stress wave does not progress as rapidly as the actual stress wave. Consequently, the value of Δt given by Equation (2.11) is called the "critical" value.

Heising^{2,13} has also pointed out that when

$$\Delta t < \sqrt{\frac{\Delta L}{E/\rho}}$$

is used in a discrete-element solution, a less accurate solution is obtained for the continuous bar. As Δt becomes progressively smaller, the solution approaches the actual behavior of the discrete-element system (segment lengths equal to ΔL) used to simulate the pile.

This in general leads to a less accurate solution for the longitudinal vibrations of a slender continuous bar. If, however, the discrete-element system were divided into a large number of segments, the behavior of this simulated pile would be essentially the same as that of the slender continuous bar irrespective of how small Δt becomes, provided

$$\sqrt{\frac{\Delta L}{E/\rho}} \geq \Delta t > 0$$

This means that if the pile is divided into only a few segments, the accuracy of the solution will be more sensitive to the choice of Δt than if it is divided into many segments. For practical problems, a choice of Δt equal to about one-half the "critical" value appears suitable since inelastic springs and materials of different densities and elastic moduli are usually involved.

2.4 Effect of Gravity

The procedure as originally presented by Smith did not account for the static weight of the pile. In other words, at $t = 0$ all springs, both internal and external, exert zero force. Stated symbolically,

$$F(m,0) = R(m,0) = 0$$

If the effect of gravity is to be included, these forces must be given initial values to produce equilibrium of

the system. Strictly speaking, these initial values should be those in effect as a result of the previous blow. However, not only would it be awkward to "keep books" on the pile throughout the driving so as to identify the initial conditions for successive blows, but it is highly questionable that this refinement is justified in light of other uncertainties which exist.

A relatively simple scheme has been developed as a means of getting the gravity effect into the computations.

Smith suggests that the external (soil) springs be assumed to resist the static weight of the system according to the relationship

$$R(m,0) = [R_u(m)/R_u(\text{total})] [W(\text{total})] \quad (2.12)$$

where

$W(\text{total})$ = total static weight resisted by soil (lb); and

$R_u(\text{total})$ = total ultimate ground resistance (lb).

The quantity $W(\text{total})$ is found by

$$W(\text{total}) = W(b) + F(c) + \sum_{m=2}^{m=p} W(m) \quad (2.13)$$

where

$W(b)$ = weight of body of hammer, excluding ram (lb); and

$F(c)$ = force exerted by compressed gases, as under the ram of a diesel hammer (lb).

The internal forces which initially exist in the pile may now be obtained:

$$F(1,0) = W(b) + F(c) \quad (2.14)$$

and in general,

$$F(m,0) = F(m-1,0) + W(m) - R(m,0) \quad (2.15)$$

In the absence of compressed gases and hammer weight resting on the pile system, the right-hand side of Equation (2.14) is zero.

The amount that each internal spring m is compressed may now be expressed

$$C(m,0) = F(m,0)/K(m) \quad (2.16)$$

By working upward from the point, one finds displacements from

$$D(p,0) = R(p,0)/K'(p) \quad (2.17)$$

$$D(m,0) = D(m+1,0) + C(m,0) \quad (m \neq p) \quad (2.18)$$

For the inclusion of gravity, Equation (2.7) should be modified as follows:

$$V(m,t) = V(m,t-1) + [F(m-1,t) - F(m,t) - R(m,t) + W(m)] \frac{g\Delta t}{W(m)} \quad (2.19)$$

In order that the initial conditions of the external springs be compatible with the assumed initial forces $R(m,0)$ and initial displacements $D(m,0)$, plastic displacements $D'(m,0)$ should be set equal to $D(m,0) - R(m,0)/K'(m)$.

CHAPTER III

Pile Driving Hammers

3.1 Energy Output of Impact Hammer

One of the most significant parameters involved in pile driving is the energy output of the hammer. This energy output must be known or assumed before the wave equation or dynamic formula can be applied. Although most manufacturers of pile driving equipment furnish maximum energy ratings for their hammers, these are usually downgraded by foundation experts for various reasons. A number of conditions such as poor hammer condition, lack of lubrication, and wear are known to seriously reduce energy output of a hammer. In addition, the energy output of many hammers can be controlled by regulating the steam pressure or quantity of diesel fuel supplied to the hammer. Therefore, a method was needed to determine a simple and uniform method which would accurately predict the energy output of a variety of hammers in general use. Towards this purpose, the information generated by the Michigan State Highway Commission in 1965 and presented in their paper entitled "A Performance Investigation of Pile Driving Hammers and Piles" by the Office of Testing and Research, was used. These data were analyzed by the wave equation to determine the pile driver energy which would have been required to produce the reported behavior.^{3,3}

3.2 Determination of Hammer Energy Output

Diesel Hammers. At present the manufacturers of diesel hammers arrive at the energy delivered per blow by two different methods. One manufacturer feels that "Since the amount of (diesel) fuel injected per blow is constant, the compression pressure is constant, and the temperature constant, the energy delivered to the piling is also constant."^{3,1} The energy output per blow is thus computed as the kinetic energy of the falling ram plus the explosive energy found by thermodynamics. Other manufacturers simply give the energy output per blow as the product of the weight of the ram-piston W_R and the length of the stroke h , or the equivalent stroke in the case of closed-end diesel hammers.

The energy ratings given by these two methods differ considerably since the ram stroke h varies greatly thereby causing much controversy as to which, if either, method is correct and what energy output should be used in dynamic pile analysis.

In conventional single acting steam hammers the steam pressure or energy is used to raise the ram for each blow. The magnitude of the steam force is too small to force the pile downward and consequently it works only on the ram to restore its potential energy, $W_R \times h$, for the next blow. In a diesel hammer, on the other hand, the diesel explosive pressure used to raise the ram is, for a short time at least, relatively large (see Figure 3.1).

While this explosive force works on the ram to restore its potential energy $W_R \times h$, the initially large

explosive pressure also does some useful work on the pile given by:

$$E_e = \int F ds \quad (3.1)$$

where F = the explosive force, and

ds = the infinitesimal distance through which the force acts.

Since the total energy output is the sum of the kinetic energy at impact plus the work done by the explosive force.

$$E_{total} = E_k + E_e \quad (3.2)$$

where E_{total} = the total energy output per blow,

E_k = the kinetic energy of the ram at the instant of impact,

and E_e = the diesel explosive energy which does useful work on the pile.

It has been noted that after the ram passes the exhaust ports, the energy required to compress the air-fuel mixture is nearly identical to that gained by the remaining fall (d) of the ram.^{3,1} Therefore, the velocity of the ram at the exhaust ports is essentially the same as at impact, and the kinetic energy at impact can be closely approximated by:

$$E_k = W_R (h - d)$$

where W_R = the ram weight,

h = the total observed stroke of the ram, and

d = the distance the ram moves after closing the exhaust ports and impacts with the anvil.

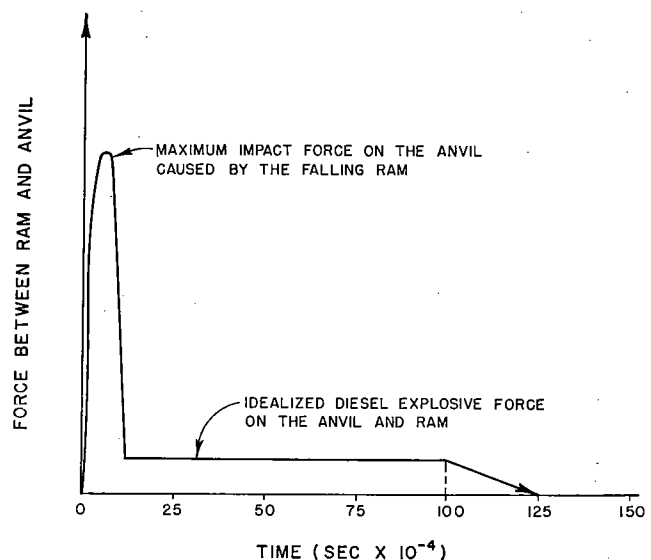


Figure 3.1. Typical force vs time curve for a diesel hammer.

The total amount of explosive energy $E_{e(\text{total})}$ is dependent upon the amount of diesel fuel injected, compression pressure, and temperature; and therefore, may vary somewhat.

Unfortunately, the wave equation must be used in each case to determine the exact magnitude of E_e since it not only depends on the hammer characteristics, but also on the characteristics of the anvil, helmet, cushion, pile, and soil resistance. However, values of E_e determined by the wave equation for several typical pile problems indicates that it is usually small in proportion to the total explosive energy output per blow, and furthermore, that it is on the same order of magnitude as $W_R \times d$. Thus, Equation (3.1) can be simplified by assuming:

$$E_e = W_R \times d \quad (3.4)$$

Substituting Equations (3.3) and (3.4) into Equation (3.1) gives:

$$E_{\text{total}} = E_k + E_e = W_R (h - d) + W_R d \quad (3.5)$$

so that:

$$E_{\text{total}} = W_R h \quad (3.6)$$

The results given by this equation were compared with experimental values and the average efficiency was found to be 100%.

Steam Hammers. Using the same equation for comparison with experimental values indicated an efficiency rating of 60% for the single-acting steam hammers, and 87% for the double-acting hammer, based on an energy output given by:

$$E_{\text{total}} = W_R h \quad (3.7)$$

In order to determine an equivalent ram stroke for the double-acting hammers, the internal steam pressure above the ram which is forcing it down must be taken into consideration. The manufacturers of such hammers state that the maximum steam pressure or force should not exceed the weight of the housing or casing, or the housing may be lifted off the pile. Thus the maximum downward force on the ram is limited to the total weight of the ram and housing.

Since these forces both act on the ram as it falls through the actual ram stroke h , they add kinetic energy to the ram, which is given by:

$$E_{\text{total}} = W_R h + F_R h \quad (3.8)$$

where W_R = the ram weight,

F_R = a steam force not exceeding the weight of the hammer housing, and

h = the observed or actual ram stroke.

Since the actual steam pressure is not always applied at the rated maximum, the actual steam force can be expressed as:

$$F_R = \left(\frac{P}{P_{\text{rated}}} \right) W_H \quad (3.9)$$

where W_H = the hammer housing weight,

p = the operating pressure, and

P_{rated} = the maximum rated steam pressure.

The total energy output is then given by

$$E_{\text{total}} = W_R h + \left(\frac{P}{P_{\text{rated}}} \right) W_H h \quad (3.10)$$

This can be reduced in terms of Equation (3.7) by using an equivalent stroke h_e which will give the same energy output as Equation (3.10).

Thus:

$$E_{\text{total}} = W_R h_e \quad (3.11)$$

Setting Equations (3.10) and (3.11) equal yields

$$\begin{aligned} W_R h_e &= W_R h + \left(\frac{P}{P_{\text{rated}}} W_H \right) h \\ &= h \left[W_R + \frac{P}{P_{\text{rated}}} W_H \right] \end{aligned}$$

or solving for the equivalent stroke:

$$h_e = h \left[1 + \frac{P}{P_{\text{rated}}} \times \frac{W_H}{W_R} \right] \quad (3.12)$$

Conclusions. The preceding discussion has shown that it is possible to determine reasonable values of hammer energy output simply by taking the product of the ram weight and its observed or equivalent stroke, and applying an efficiency factor. This method of energy rating can be applied to all types of impact pile drivers with reasonable accuracy.

A brief summary of this simple procedure for arriving at hammer energies and initial ram velocities is as follows:

Open End Diesel Hammers

$$E = W_R h (e)$$

$$V_R = \sqrt{2g(h-d)} (e)$$

where W_R = ram weight

V_R = initial ram velocity

h = observed total stroke of ram

d = Distance from anvil to exhaust ports

e = efficiency of open end diesel hammers, approximately 100% when energy is computed by this method.

Closed End Diesel Hammers

$$E^* = W_R h_e (e)$$

$$V_R = \sqrt{2g(h_e-d)} (e)$$

where W_R = ram weight

V_R = initial ram velocity

h_e = equivalent stroke derived from bounce chamber pressure gage

d = distance from anvil to exhaust ports

e = efficiency of closed end diesel hammers, approximately 100% when energy is computed by this method.

Double-Acting Steam Hammers

$$E = W_R h_e (e)$$

$$V = \sqrt{2g h_e (e)}$$

*Note: For the Link Belt Hammers, this energy can be read directly from the manufacturer's chart using bounce chamber pressure gage.

where W_R = ram weight

h_e = equivalent ram stroke

$$= h \left[1 + \frac{p}{P_{\text{rated}}} \times \frac{W_H}{W_R} \right]$$

h = actual or physical ram stroke

p = operating steam pressure

P_{rated} = maximum steam pressure recommended by manufacturer.

W_H = weight of hammer housing

e = efficiency of double-acting steam hammers, approximately 85% by this method.

Single-Acting Steam Hammers.

$E = W_R h (e)$

$V_R = \sqrt{2g h (e)}$

where W_R = ram weight

h = ram stroke

e = efficiency of single-acting steam hammers, normally recommended around 75% to 85%. In a study of the Michigan data, a figure of 60% was found. The writers feel the 60% figure is unusually low and would not recommend it as a typical value.

A summary of the properties and operating characteristics of various hammers is given in Table 3.1.

3.3 Significance of Driving Accessories

In 1965 the Michigan State Highway Commission completed an extensive research program designed to obtain a better understanding of the complex problem of pile driving. Though a number of specific objectives were given, one was of primary importance. As noted by Housel,^{3,2} "Hammer energy actually delivered to the pile, as compared with the manufacturer's rated energy, was the focal point of a major portion of this investigation of pile-driving hammers." In other words, they hoped to determine the energy delivered to the pile and to compare these values with the manufacturer's ratings.

The energy transmitted to the pile was termed "ENTHRU" by the investigators and was determined by the summation

$$\text{ENTHRU} = \Sigma F \Delta S$$

Where F , the average force on the top of the pile during a short interval of time, was measured by a specially designed load cell, and ΔS , the incremental movement of the head of the pile during this time interval, was found using displacement transducers and/or reduced from accelerometer data. It should be pointed out that ENTHRU is not the total energy output of the hammer blow, but only a measure of that portion of the energy delivered below the load-cell assembly.

Many variables influence the value of ENTHRU. As was noted in the Michigan report: "Hammer type and operating conditions; pile type, mass, rigidity, and length; and the type and condition of cap blocks were all factors that affect ENTHRU, but when, how, and how much could not be ascertained with any degree of

TABLE 3.1. SUMMARY OF HAMMER PROPERTIES AND OPERATING CHARACTERISTICS

Hammer Manufacturer	Hammer Type	Maximum Rated Energy (ft lb)	Ram Weight (lb)	Hammer Housing Weight (lb)	Anvil Weight (lb)	Maximum or Equivalent Stroke (ft)	d (ft)	Rated Steam Pressure (psi)	Maximum Explosive Pressure (lb)	Cap Block Normally Specified
Vulcan	#1	15,000	5,000	4,700		3.00				
	014	42,000	14,000	13,500		3.00				
	50C	15,100	5,000	6,800		3.02		120		
	80C	24,450	8,000	9,885		3.06		120		
	140C	36,000	14,000	13,984		2.58		140		
Link Belt	312	18,000	3,857		1188	4.66	0.50		98,000	5 Micarta disks 1" x 10 7/8" dia.
	520	30,000	5,070		1179	5.93	0.83		98,000	
MKT Corp	DE20	16,000	2,000		640	8.00	0.92		46,300	nylon disk 2" x 9" dia.
	DE30	22,400	2,800		775	8.00	1.04		98,000	nylon disk 2" x 19" dia.
	DE40	32,000	4,000		1350	8.00	1.17		138,000	nylon disk 2" x 24" dia.
Delmag	D-12	22,500	2,750		754	8.19	1.25		93,700	15" x 15" x 5" German Oak
	D-22	39,700	4,850		1147	8.19	1.48		158,700	15" x 15" x 5" German Oak

certainty." However, the wave equation can account for each of these factors so that their effects can be determined.

The maximum displacement of the head of the pile was also reported and was designated LIMSET. Oscillographic records of force vs time measured in the load cell were also reported. Since force was measured only at the load cell, the single maximum observed values for each case was called FMAX.

The wave equation can be used to determine (among other quantities) the displacement $D(m,t)$ of mass "m" at time "t", as well as the force $F(m,t)$ acting on any mass "m" at time "t." Thus the equation for ENTHRU at any point in the system can be determined by simply letting the computer calculate the equation previously mentioned:

$$\text{ENTHRU} = \Sigma F \Delta S$$

or in terms of the wave equation:

$$\text{ENTHRU}(m) = \Sigma \left[\frac{F(m,t) + F(m,t-1)}{2.0} \right] \times [D(m+1,t) - D(m+1,t-1)]$$

where ENTHRU (m) = the work done on any mass (m + 1),

m = the mass number, and

t = the time interval number.

ENTHRU is greatly influenced by several parameters, especially the type, condition, and coefficient of restitution of the cushion, and the weight of extra driving caps.

It has been shown,^{3,3} that the coefficient of restitution alone can change ENTHRU by 20%, simply by changing e from 0.2 to 0.6. Nor is this variation in e unlikely since cushion condition varied from new to "badly burnt" and "chips added."

The wave equation was therefore used to analyze certain Michigan problems to determine the influence of cushion stiffness, e, additional driving cap weights, driving resistance encountered, etc.

Table 3.5 shows how ENTHRU and SET increases when the load cell assembly is removed from Michigan piles.

TABLE 3.2. EFFECT OF CUSHION STIFFNESS ON ENERGY TRANSMITTED TO THE PILE (ENTHRU)

Ram Velocity (ft/sec)	RUT (kip)	ENTHRU (kip ft)			
		Cushion Stiffness (kip/in.)			
		540	1080	2700	27,000
8	30	3.0	3.0	3.0	2.9
	90	3.1	3.2	3.3	2.9
	150	3.0	3.2	3.3	3.0
12	30	6.6	6.4	7.1	6.4
	90	7.0	7.1	7.2	6.4
	150	6.9	7.2	7.4	6.7
16	30	11.8	11.9	12.2	11.3
	90	12.3	12.6	12.8	11.5
	150	12.4	12.9	13.2	11.4

TABLE 3.3. EFFECT OF CUSHION STIFFNESS ON THE MAXIMUM FORCE MEASURED AT THE LOAD CELL (FMAX)

Ram Velocity (ft/sec)	RUT (kip)	FMAX (kip)			
		Cushion Stiffness (kip/in.)			
		540	1080	2700	27,000
8	30	132	185	261	779
	90	137	185	261	779
	150	143	186	261	779
12	30	198	278	391	1,169
	90	205	278	391	1,169
	150	215	279	391	1,169
16	30	264	371	522	1,558
	90	275	371	522	1,558
	150	288	371	522	1,558

From Table 3.2, it can be seen that ENTHRU does not always increase with increasing cushion stiffness, and furthermore, the maximum increase in ENTHRU noted here is relatively small—only about 10%.

When different cushions are used, the coefficient of restitution will probably change. Since the coefficient of restitution of the cushion may affect ENTHRU, a number of cases were solved with "e" ranging from 0.2 to 0.6. As shown in Tables 3.6 and 3.7, an increase in "e" from 0.2 to 0.6 normally increases ENTHRU from 18 to 20%, while increasing the permanent set from 6 to 11%. Thus, for the case shown, the coefficient of restitution of the cushion has a greater influence on rate of penetration and ENTHRU than does its stiffness. This same effect was noted in the other solutions, and the cases shown in Tables 3.6 and 3.7 are typical of the results found in other cases.

As can be seen from Table 3.3, any increase in cushion stiffness also increases the driving stress. Thus, according to the wave equation, increasing the cushion stiffness to increase the rate of penetration (for example by not replacing the cushion until it has been beaten to a fraction of its original height or by omitting the cushion entirely) is both inefficient and poor practice because of the high stresses induced in the pile. It would be better to use a cushion having a high coefficient of restitution and a low cushion stiffness in order to increase ENTHRU and to limit the driving stress.

Unfortunately, the tremendous variety of driving accessories precludes general conclusions to be drawn

TABLE 3.4. EFFECT OF CUSHION STIFFNESS ON THE MAXIMUM DISPLACEMENT OF THE HEAD OF THE PILE (LIMSET)

Ram Velocity (ft/sec)	RUT (kip)	LIMSET (in.)			
		Cushion Stiffness (kip/in.)			
		540	1080	2700	27,000
8	30	1.09	1.08	1.08	1.13
	90	0.44	0.44	0.45	0.45
	150	0.32	0.33	0.33	0.33
12	30	2.21	2.14	2.19	2.25
	90	0.80	0.82	0.84	0.84
	150	0.55	0.57	0.58	0.58
16	30	3.62	3.59	3.63	3.68
	90	1.30	1.31	1.32	1.34
	150	0.85	0.87	0.88	0.90

TABLE 3.5 EFFECT OF REMOVING LOAD CELL ON ENTHRU, LIMSET, AND PERMANENT SET OF PILE

Case ³⁻³	Ram Velocity (ft/sec)	ENTHRU (kip ft)		LIMSET (in.)		PERMANENT SET (in.)	
		With Load Cell	Without Load Cell	With Load Cell	Without Load Cell	With Load Cell	Without Load Cell
DTP-15, 80.5	8	1.5	1.6	0.27	0.34	0.23	0.25
	12	3.3	3.6	0.53	0.67	0.57	0.57
	16	5.8	6.5	1.02	1.03	0.94	0.97
	20	9.1	10.1	1.54	1.54	1.43	1.47
DLTP-8, 80.2	8	3.1	3.8	0.62	0.71	0.51	0.62
	12	7.1	8.5	1.15	1.32	1.06	1.29
	16	12.5	15.1	1.91	2.10	1.82	2.15
	20	19.5	23.6	2.70	3.08	2.65	3.13

from wave equation analyses in all but the most general of terms.

Although the effect of driving accessories is quite variable, it was generally noted that the inclusion of additional elements between the driving hammer and the pile and/or the inclusion of heavier driving accessories consistently decreased both the energy transmitted to the head of the pile and the permanent set per blow of the hammer. Increasing cushion stiffness will increase compressive and tensile stresses induced in a pile during driving.

3.4 Explosive Pressure in Diesel Hammers

In order to account for the effect of explosive force in diesel hammers, the force between the ram and the anvil is assumed to reach some maximum due to the impact between the ram and anvil, and then decrease. However, should this impact force tend to decrease below some specified minimum, it is assumed that the diesel explosive pressure maintains this specified minimum force between the ram and anvil for a given time, after

which the force tapers to zero. As shown in Figure 3.1, the force between the ram and anvil reaches some maximum due to the steel on steel impact, afterwards the force decreases to the minimum diesel explosive force on the anvil. This force is maintained for 10 milliseconds, thereafter decreasing to zero at 12.5 milliseconds. The properties of this curve, including values of the minimum explosive force and time over which this force acts, were determined from the manufacturer's published literature for the diesel hammers.

The effect of explosive pressure was found to be extremely variable, possibly more so than the effect of the driving accessories, and few conclusions could be drawn. The only consistent effect that could be observed was that if the maximum impact force induced by the falling ram was insufficient to produce permanent set, the addition of explosive force had little or no effect on the solution. In other words, unless the particular hammer, driving accessories, pile, and soil conditions were such that it was possible to get the pile moving, the explosive force, being so much smaller than the maximum impact force, had no effect.

TABLE 3.6. EFFECT OF COEFFICIENT OF RESTITUTION ON MAXIMUM POINT DISPLACEMENT

Pile I.D.	RUT (kip)	Ram Velocity (ft/sec)	Maximum Point Displacement (in.)			Maximum Change (%)
			e = 0.2	e = 0.4	e = 0.6	
BLTP-6; 10.0	30	12	2.13	2.14	2.36	10
		16	3.38	3.47	3.58	6
		20	4.73	4.93	5.17	8
BLTP-6; 57.9	150	12	0.46	0.48	0.50	8
		16	0.73	0.76	0.81	10
		20	1.05	1.10	1.18	11

TABLE 3.7. EFFECT OF COEFFICIENT OF RESTITUTION ON ENTHRU

Pile I.D.	RUT (kip)	Ram Velocity (ft/sec)	ENTHRU (kip ft)			Maximum Change (%)
			e = 0.2	e = 0.4	e = 0.6	
BLTP-6; 10.0	30	12	6.0	6.5	7.3	18
		16	10.5	11.8	12.8	18
		20	16.5	17.4	20.0	17
BLTP-6; 57.9	150	12	6.7	7.2	8.2	18
		16	11.6	12.7	14.5	20
		20	18.2	19.7	22.4	19

However, the addition of explosive pressure increased the permanent set of the pile in some cases where the maximum impact force is sufficient to start the pile moving; on the other hand, its addition was found ineffective in an equal number of circumstances.

The explosive forces assumed to be acting within various diesel hammers are listed in Table 3.1. These forces were determined by experiment, personal correspondence with the hammer manufacturers, and from their published literature.

3.5 Effect of Ram Elasticity

In 1960, when Smith first proposed his numerical solution to the wave equation for application to pile driving problems, he suggested that since the ram is usually short in length, it can in many cases be represented by a single weight having infinite stiffness. The example illustrated in Figure 2.1 makes this assumption, since $K(1)$ represents the spring constant of only the capblock, the elasticity of the ram having been neglected. Smith also noted that if greater accuracy was desired, the ram could also be divided into a series of weights and springs, as is the pile.

As noted in Figures 3.2 and 3.3, there is a significant difference between the steam or drop hammers and diesel hammers, i.e., the steam hammer normally strikes a relatively soft capblock, whereas the diesel hammer involves steel on steel impact between the ram and anvil.

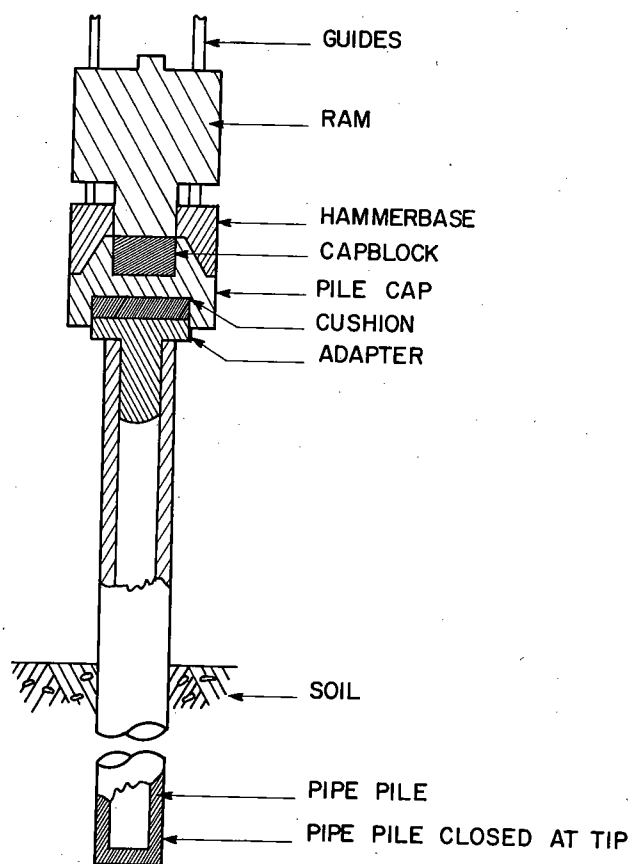


Figure 3.2. Steam hammer.

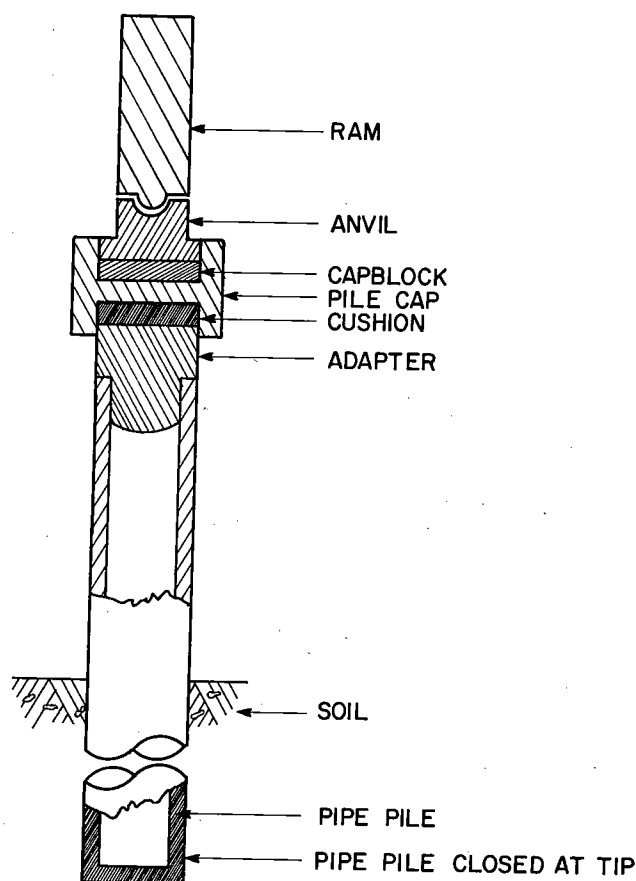


Figure 3.3. Diesel hammer.

To determine the influence of dividing the ram into a number of segments, several ram lengths ranging from 2 to 10 ft were assumed, driving a 100-ft pile having point resistance only. The total weight of the pile being driven varied from 1500 to 10,000 lb, while the ultimate soil resistance ranged from 0 to 10,000 lb. The cushion was assumed to have a stiffness of 2,000 kips per in.

Table 3.8 lists the results found for a typical problem solved in this study, the problem consisting of a 10-ft long ram traveling at 20 fps striking a cushion with a stiffness of 2000 kips per in. The pile used was a 100-ft 12H53 steel pile, driven by a 5,000-lb ram.

TABLE 3.8. EFFECT OF BREAKING THE RAM INTO SEGMENTS WHEN RAM STRIKES A CUSHION OR CAPBLOCK

Number of Ram Divisions	Length of Pile Segments (ft)	Maximum Compressive Force in Pile (kip)	Maximum Tensile Force in Pile (kip)	Maximum Point Displacement (in.)
1	10.0	305.4	273.9	3.019
1	5.0	273.8	245.9	3.042
1	2.5	265.6	224.8	3.053
1	1.25	263.1	219.0	3.057
2	1.25	262.6	218.8	3.058
10	1.25	262.9	218.5	3.059

TABLE 3.9. EFFECT OF BREAKING RAM INTO SEGMENTS WHEN RAM STRIKES A STEEL ANVIL

Anvil Weight	Ram Length	Number of Ram Divisions	Length of Each Ram Segment	Maximum Compressive Force on Pile			Maximum Point Displacement
				At Head	At Center	At Tip	
lb	ft		ft	kip	kip	kip	in.
2000	10	1	10.0	513	513	884	0.207
		2	5.0	437	438	774	0.159
		5	2.0	373	373	674	0.124
		10	1	375	375	678	0.125
	8	1	8.0	478	478	833	0.183
		4	2.0	359	359	648	0.117
		8	1.0	360	360	651	0.118
	6	1	6.0	430	430	763	0.155
		3	2.0	344	344	621	0.110
		6	1.0	342	342	616	0.109
	10	1	10.0	508	509	878	0.160
		2	5.0	451	451	789	0.159
		5	2.0	381	382	691	0.151
		10	1.0	371	372	681	0.153
1000	8	1	8.0	487	488	846	0.151
		4	2.0	443	444	785	0.144
		8	1.0	369	370	675	0.134
		10	0.8	337	338	665	0.133
	6	1	6.0	457	457	798	0.137
		3	2.0	361	362	666	0.128
		6	1.0	316	316	562	0.109
		10	0.6	320	320	611	0.113

No pile cap was included in the solution, the cushion being placed directly between the hammer and the head of the pile. Since the ram was divided into very short lengths, the pile was also divided into short segments.

As shown in Table 3.8, the solution is not changed to any significant extent whether the ram is divided into 1, 2, or 10 segments. The time interval was held constant in each case.

In the case of a diesel hammer, the ram strikes directly on a steel anvil rather than on a cushion. This makes the choice of a spring rate between the ram and anvil difficult because the impact occurs between two steel elements. The most obvious solution is to place a spring having a rate dictated by the elasticity of the ram and/or anvil. A second possible solution is to break the ram into a series of weights and springs as is the pile.

To determine when the ram should be divided, a parameter study was run in which the ram length varied between 6 and 10 ft, and the anvil weight varied from, 1,000 to 2,000 lb. In each case the ram parameter was

held constant and the ram was divided equally into segment lengths as noted in Table 3.9. These variables were picked because of their possible influence on the solution.

The pile used was again a 12H53 point bearing pile having a cushion of 2,000 kip per in. spring rate placed between the anvil and the head of the pile. The soil parameters used were $RU = 500$ kips, $Q = 0.1$ in., and $J = 0.15$ sec. per ft. These factors were held constant for all problems listed in Tables 3.8 and 3.9.

The most obvious result shown in Table 3.9 is that when the steel ram impacts directly on a steel anvil, dividing the ram into segments has a marked effect on the solution.

An unexpected result of the study was that even when the ram was short, breaking it into segments still effected the solution. As seen in Table 3.9, the solutions for forces and displacements for both 6 through 10 ft ram lengths continue to change until a ram segment length of 2 ft was reached for the 2,000-lb anvil and a segment length of 1 ft for the 1,000-lb anvil was reached.

CHAPTER IV

Capblock and Cushions

4.1 Methods Used to Determine Capblock and Cushion Properties

As used here, the word "capblock" refers to the material placed between the pile driving hammer and the steel helmet. The term "cushion" refers to the ma-

terial placed between the steel helmet and pile (usually used only when driving concrete piles).

Although a capblock and cushion serve several purposes, their primary function is to limit impact stresses in both the pile and hammer. In general, it has

been found that a wood capblock is quite effective in reducing driving stresses, more so than a relatively stiff capblock material such as Micarta. However, the stiffer Micarta is usually more durable and transmits a greater percentage of the hammer's energy to the pile because of its higher coefficient of restitution.

For example, when fourteen different cases of the Michigan study were solved by the wave equation, the Micarta assemblies averaged 14% more efficient than capblock assemblies of wood. However, the increased cushion stiffness in some of these cases increased the impact stresses to a point where damage to the pile or hammer might result during driving. The increase in stress was particularly important when concrete or prestressed concrete piles were driven. When driving concrete piles, it is also frequently necessary to include cushioning material between the helmet and the head of the pile to distribute the impact load uniformly over the surface of the pile head and prevent spalling.

To apply the wave equation to pile driving, Smith assumed that the cushion's stress-strain curve was a series of straight lines as shown in Figure 4.1. Although this curve was found to be sufficiently accurate to predict maximum compressive stresses in the pile, the shape of the stress wave often disagreed with that of the actual stress wave. To eliminate the effects of soil resistance several test piles were suspended horizontally above the ground. These test piles were instrumented with strain gages at several points along the length of the pile, and especially at the head of the pile. A cushion was placed at the head of the pile which was then hit by a horizontally swinging ram, and displacements, forces, and accelerations of both the ram and head of the pile were measured. Thus, by knowing the force at the head of the pile and the relative displacement between the ram and the head of the pile, the force exerted in the cushion

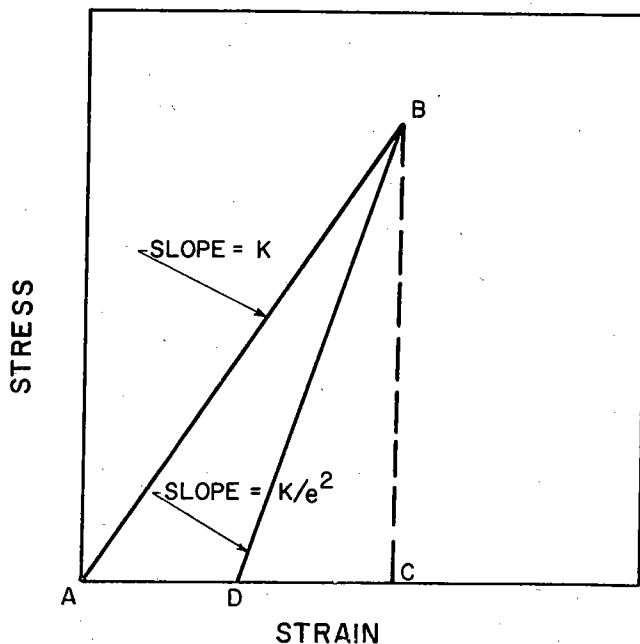


Figure 4.1. Stress-strain curve for a cushion block.

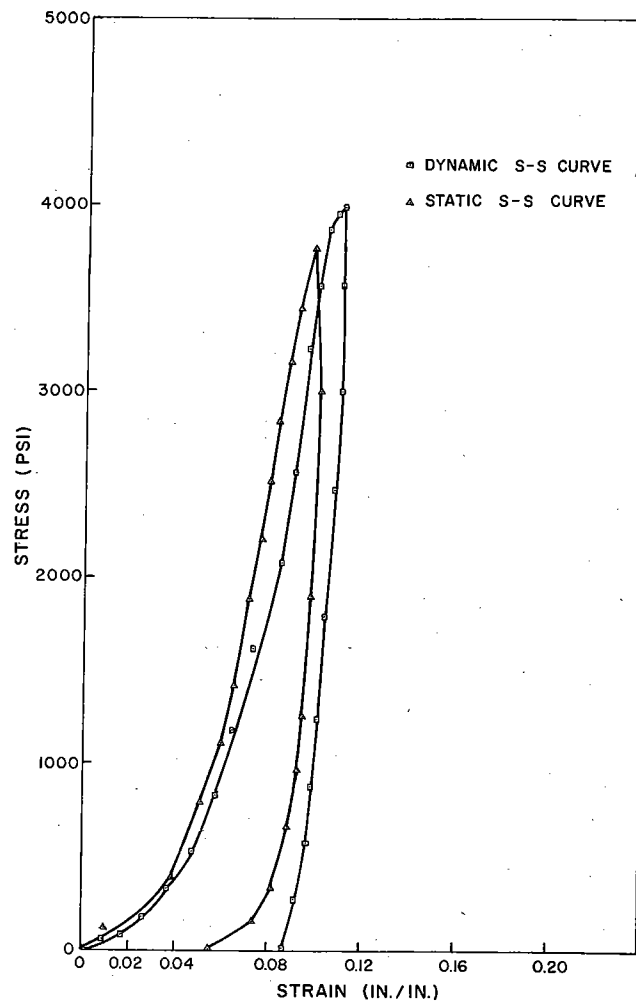


Figure 4.2. Dynamic and static stress-strain curves for a fir cushion.

and the compression in the cushion at all times could be calculated. Thus the cushion's stress-strain diagram could be plotted to determine whether or not it was actually a straight line.

Using this method, the dynamic stress-strain properties were measured for several types of cushions.

It was further determined that the stress-strain curves were not linear as was assumed by Smith, but rather appeared as shown in Figure 4.2. Because it was extremely difficult to determine the dynamic stress-strain curve by this method, a cushion test stand was constructed as shown in Figure 4.3 in an attempt to simplify the procedure.

Since it was not known how much the rigidity of the pedestal affected the cushion's behavior, several cushions whose stress-strain curve had been previously determined by the first method were checked. These studies indicated that the curves determined by either method were similar and that the cushion test stand could be used to accurately study the dynamic load-deformation properties of cushioning material.

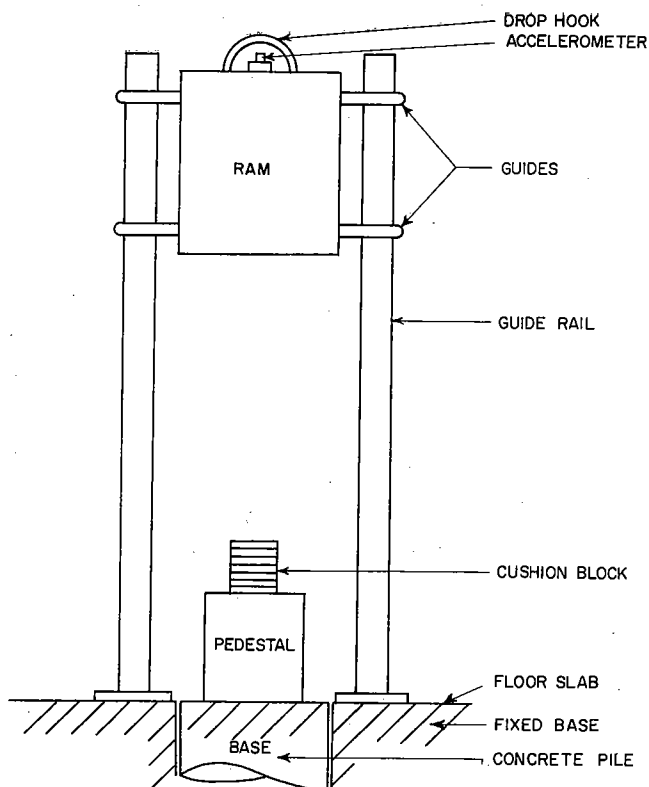


Figure 4.3. Cushion test stand.

Throughout this investigation, a static stress-strain curve was also determined for each of the cushions. Surprisingly, the static and dynamic stress-strain curves for wood cushions agreed remarkably well. A typical example of this agreement is shown in Figure 4.2. The stress-strain curves for a number of other materials commonly used as pile cushions and capblocks, namely oak, Micarta, and asbestos are shown by Figures 4.4-4.6.

4.2 Idealized Load-Deformation Properties

The major difficulty encountered in trying to use the dynamic curves determined for the various cushion materials was that it was extremely difficult to input the information required by the wave equation. Although the initial portion of the curve was nearly parabolic, the top segment and unloading portion were extremely complex. This prevented the curve from being input in equation form, and required numerous points on the curve to be specified.

Fortunately, it was found that the wave equation accurately predicted both the shape and magnitude of the stress wave induced in the pile even if a linear force-deformation curve was assumed for the cushion, so long as the loading portion was based on the secant modulus of elasticity for the material (as opposed to the initial, final, or average modulus of elasticity), and the unloading portion of the curve was based on the actual dynamic coefficient of restitution. Typical secant moduli of elasticity and coefficient of restitution values for various materials are presented in Table 4.1.

TABLE 4.1. TYPICAL SECANT MODULI OF ELASTICITY (E) AND COEFFICIENTS OF RESTITUTION (e) OF VARIOUS PILE CUSHIONING MATERIAL

	E psi	e
Micarta Plastic	450,000	.80
Oak (Green)	45,000*	.50
Asbestos Discs	45,000	.50
Fir Plywood	35,000*	.40
Pine Plywood	25,000*	.30
Gum	30,000*	.25

*Properties of wood with load applied perpendicular to wood grain.

4.3 Coefficient of Restitution

Although the cushion is needed to limit the driving stresses in both hammer and pile, its internal damping reduces the available driving energy transmitted to the head of the pile. Figure 4.1 illustrates this energy loss, with the input energy being given by the area ABC while the energy output is given by area BCD. This energy loss is commonly termed coefficient of restitution of the cushion "e", in which

$$e = \sqrt{\frac{\text{Area BCD}}{\text{Area ABD}}}$$

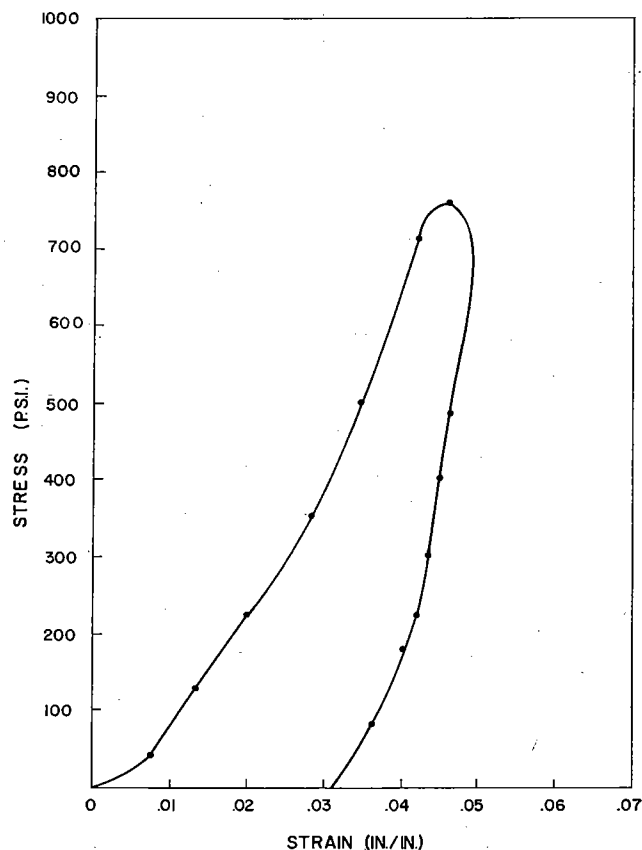


Figure 4.4. Dynamic stress-strain curve for an oak cushion.

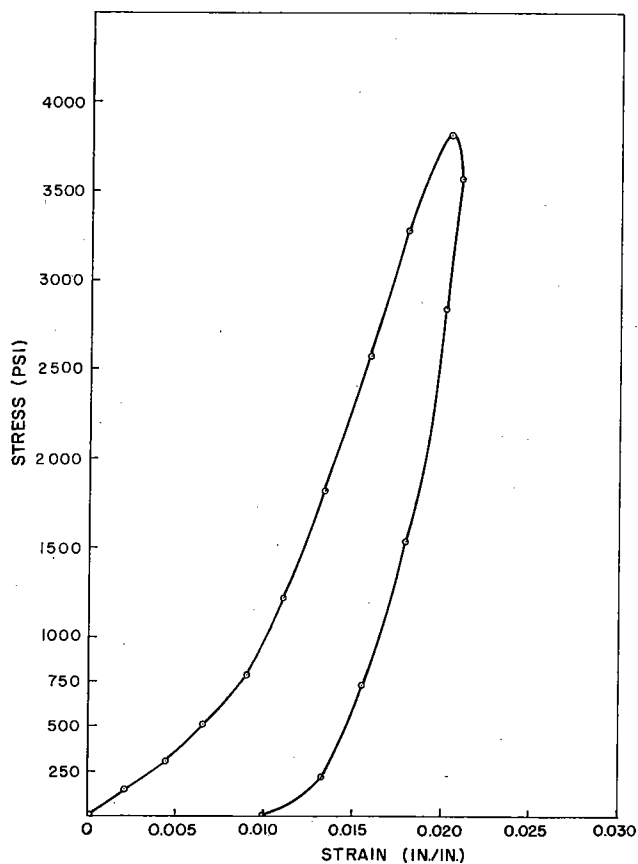


Figure 4.5. Dynamic stress-strain curve for a micarta cushion.

Once the coefficient of restitution for the material is known, the slope of the unloading curve can be determined as noted in Figure 4.1.

For practical pile driving problems, secant moduli

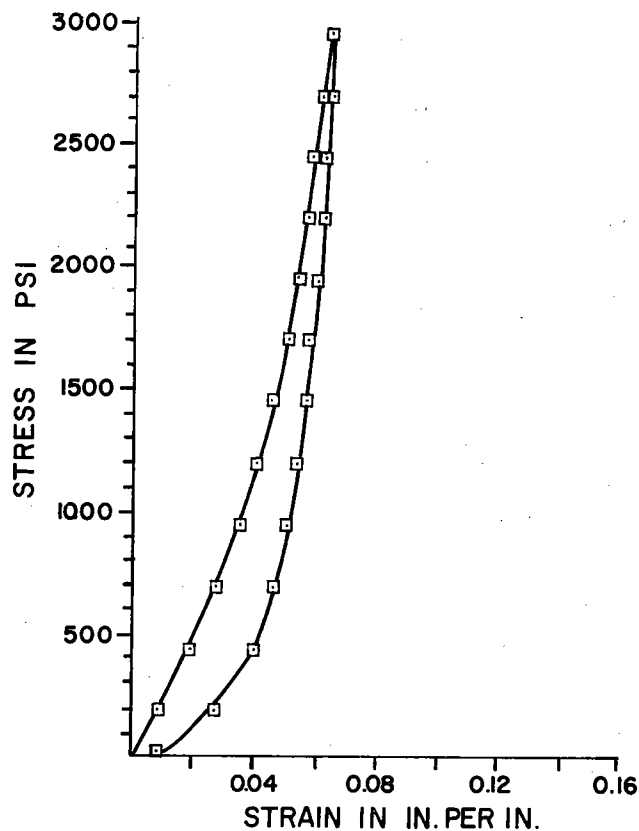


Figure 4.6. Stress vs strain for garlock asbestos cushion.

of elasticity values for well consolidated cushions should be used. Table 4.1 shows typical secant moduli of well consolidated wood cushions. Table 4.1 also lists the coefficient of restitution for the materials which should be used when analyzing the problem by the wave equation.

CHAPTER V

Stress Waves in Piling

5.1 Comparison with Laboratory Experiments

As noted in the preceding section, several test piles were instrumented and suspended horizontally above the ground. This example pile was a steel pile, 85 ft in length with a cross-sectional area of 21.46 sq. in. The cushion was oak, 7 in. thick. The ram had a weight of 2128 lb and a velocity of 13.98 fps. The cushion was clamped to the head of the pile and then struck by a horizontally swinging ram. The pile was instrumented with strain gages at six points along the pile, and displacements and accelerations of both the ram and head of the pile were also measured.

In order to utilize Smith's solution to the wave

equation, the following information is normally required:

1. The initial velocity and weight of the ram,
2. The actual dynamic stress-strain curve for the cushion,
3. The area and length of the pile, and
4. The density and modulus of elasticity of the pile.

Since the stress-strain curve for the cushion was unknown, the numerical solution was rewritten such that it was not needed. This was possible since the pile was instrumented with a strain gage approximately 1 ft from the head of the pile which recorded the actual stress

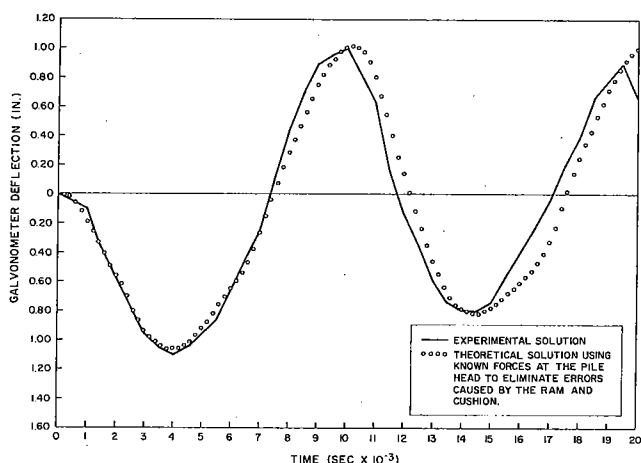


Figure 5.1. Theoretical vs experimental solution. Strain 25 ft from pile head.

induced in pile by the ram and cushion. The force measured at the head of the pile was then placed directly at the head of the pile and the wave equation was used to compute stresses and displacements at all of the gage points along the pile. Figures 5.1 and 5.2 present typical comparisons between the experimental results and wave equation solutions at two points on the pile, and illustrate the degree of accuracy obtained by use of the wave equation.

It must be emphasized that this excellent correlation between experimental and theoretical results was in effect obtained by using the actual dynamic load-deformation curve for that particular case. However, as mentioned earlier, the stress-strain curve for the cushion is normally assumed to be linear as shown in Figure 4.1.

To determine how much the use of the linear stress-strain curve will affect the solution, the previous case was rerun using the straight line stress-strain curves. As noted in Figures 5.3 and 5.4, the solutions for the linear and nonlinear cushion assumptions agreed favorably. The use of the straight line assumption is reasonable since it gives fairly accurate results for both maximum

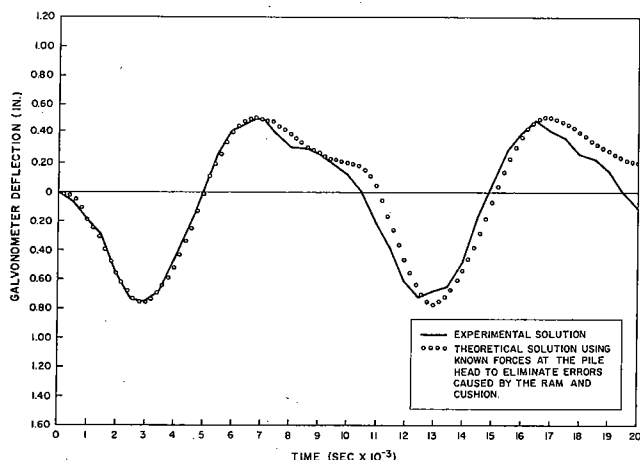


Figure 5.2. Theoretical vs experimental solution. Strain 52 ft from pile head.

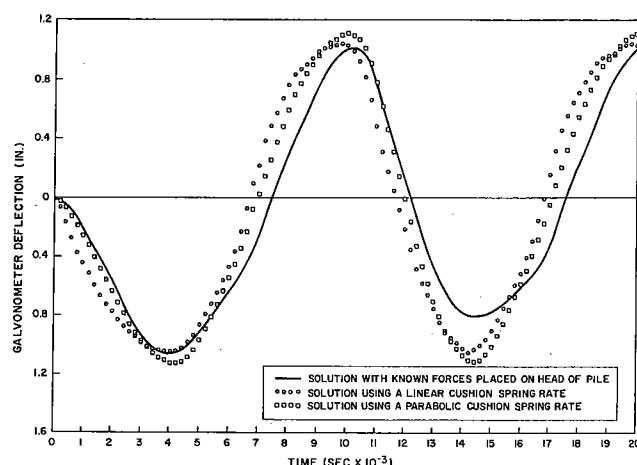


Figure 5.3. Theoretical vs experimental solution for strains 25 ft from the pile head.

tensile and compressive stresses. Furthermore, it predicts the shape of the stress wave reasonably well.

5.2 Significance of Material Damping in the Pile

Other parameters were often varied in an attempt to obtain more accurate results, one of which was the material damping capacity of the pile material. However, most suspended pile cases studied strongly indicated that damping would be negligible because of the extremely low rate of decay of the stress wave in the pile. The only pile in which damping was thought to be significant was a lightweight concrete pile with a static modulus of elasticity of 3.96×10^6 and a "sonic" modulus of elasticity of 4.63×10^6 psi. This problem was chosen since E_s was relatively larger than E , indicating the possibility of rather high damping. It can be seen in Figure 5.5 that the magnitude of the experimental results diminishes slightly after four cycles. The magnitude of the theoretical solution with damping neglected would not. Figure 5.5 compares the experimental and theoretical solutions for stresses when Smith's proposed method of damping is included. In this case, the ex-

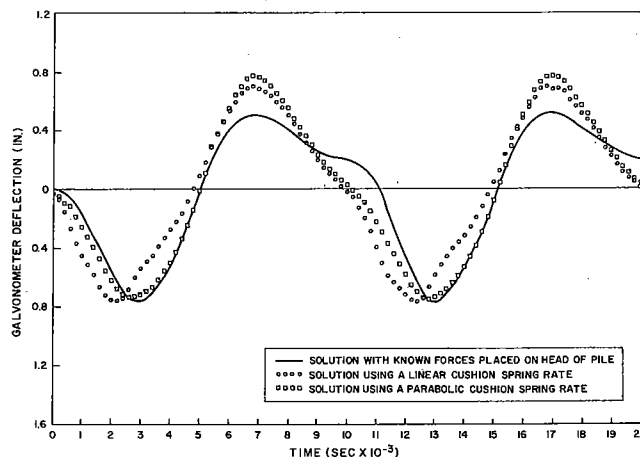


Figure 5.4. Theoretical vs experimental solution for strains 52 ft from the pile head.

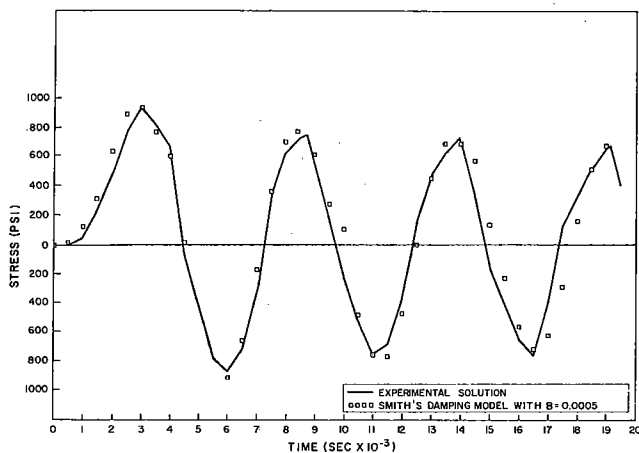


Figure 5.5. Comparison of experimental and theoretical solutions for stresses 25 ft from the pile head.

CHAPTER VI

Soil Properties

6.1 General

A limited amount of work has been done on soil properties and their effects on the wave equation solution of the piling behavior problem. A total of three research reports concerning soil properties have been published by the Texas Transportation Institute during the "Piling Behavior" study. Research Reports 33-7 and 33-7A^{6.1, 6.2} give the results of a series of laboratory dynamic (impact) and static tests conducted on saturated sands. Research Report 33-8^{6.3} gives the results of a field test on a full scale instrumented pile in clay. A brief summary of the results of these tests are given in this chapter.

6.2 Equations to Describe Soil Behavior

Examination of Equation (6.1) shows that Smith's equation describes a type of Kelvin rheological model as shown in Figure 6.1.

$$R(m,t) = \frac{[D(m,t) - D'(m,t)] K'(m)}{[1 + J(m) V(m,t-1)]} \quad (6.1)$$

The soil spring behaves elastically until the deformation $D(m,t)$ equals Q and then it yields plastically with a load-deformation property as shown in Figure 6.2(a). The dashpot J develops a resisting force proportional to the velocity of loading V . Smith has modified the true Kelvin model slightly as shown by Equation (6.2). This equation will produce a dynamic load-deformation behavior shown by path OABCDEF in Figure 6.2(b). If terms in Equation (6.1) are examined, it can be seen that Smith's dashpot force is given by

$$[D(m,t) - D'(m,t)] K'(m) [J(m) V(m,t-1)]$$

The dimensions of J are sec/ft and it is assumed to be independent of the total soil resistance or size of the pile.

perimental and theoretical solutions are in excellent agreement, both in wave shape and rate of decay.

Although it is extremely interesting to be able to predict the dynamic behavior of piling with such accuracy, most practically the primary interest is in the maximum stresses induced in the pile which occur during the first or second pass of the stress wave along the pile. During this time, the effects of damping are extremely small even for the lightweight aggregate pile, and are apparently of no practical importance. Whether this conclusion will be accurate for timber or other piles having much higher damping capacities than either steel or concrete piles is unknown. A higher damping capacity could affect the results earlier in the solution and thus be of significance.

It should be emphasized that the above conclusions are valid only for normal pile driving conditions. If the wave must be studied for an extended period of time, damping in the pile may be significant and should be accounted for.

It is also assumed to be constant for a given soil under given conditions as is the static shear strength of the soil from which R_u on a pile segment is determined. R_u is defined as the maximum soil resistance on a pile segment.

Smith notes that Equation (6.1) produces no damping when $D(m,t) - D'(m,t)$ becomes zero. He suggests an alternate equation to be used after $D(m,t)$ first becomes equal to $Q(m)$:

$$R(m,t) = [D(m,t) - D'(m,t)] K'(m) + J(m) R_u(m) V(m,t-1) \quad (6.2)$$

Care must be used to satisfy conditions at the point of the pile. Consider Equation (6.1) when $m = p$, where p is the number of the last element of the pile. $K(p)$ is used as the point soil spring and $J(p)$ as the point soil damping constant. Also at the point of the

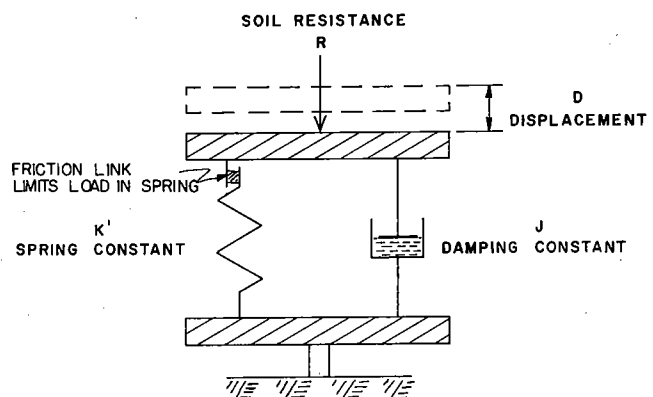
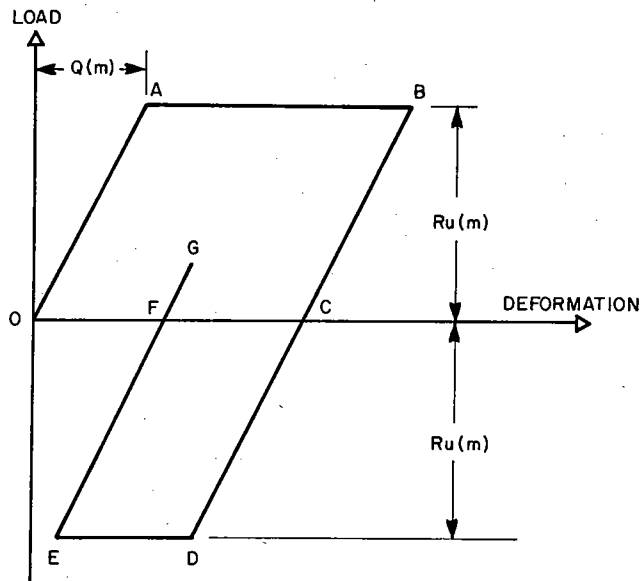


Figure 6.1. Model used by Smith to describe soil resistance on pile.

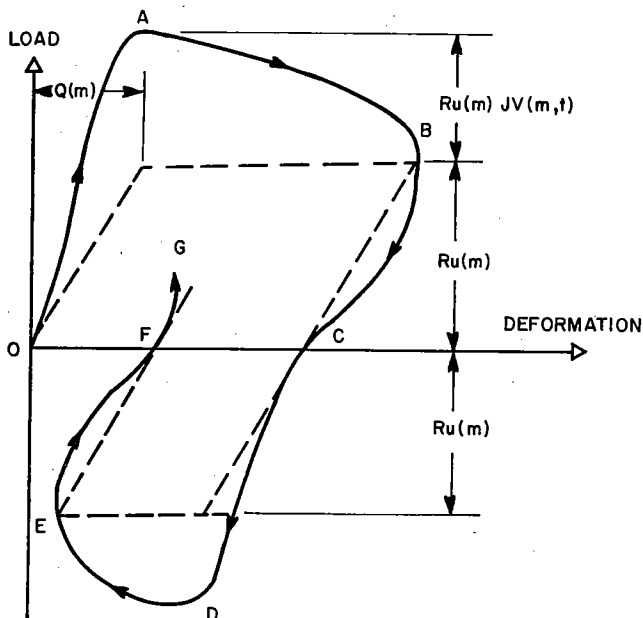
pile, the soil spring must be prevented from exerting tension on the pile point. The point soil resistance will follow the path OABCFG in Figure 6.2(b). It should be kept in mind that at the pile point the soil is loaded in compression or bearing. The damping constant $J(p)$ in bearing is believed to be larger than the damping constant $J(m)$ in friction along the side of the pile.

6.3 Soil Parameters to Describe Dynamic Soil Resistance During Pile Driving

The soil parameters used to describe the soil resistance in the wave equation are R_u , Q , and J .



(a) STATIC



(b) DYNAMIC

Figure 6.2. Load-deformation characteristics of soil.

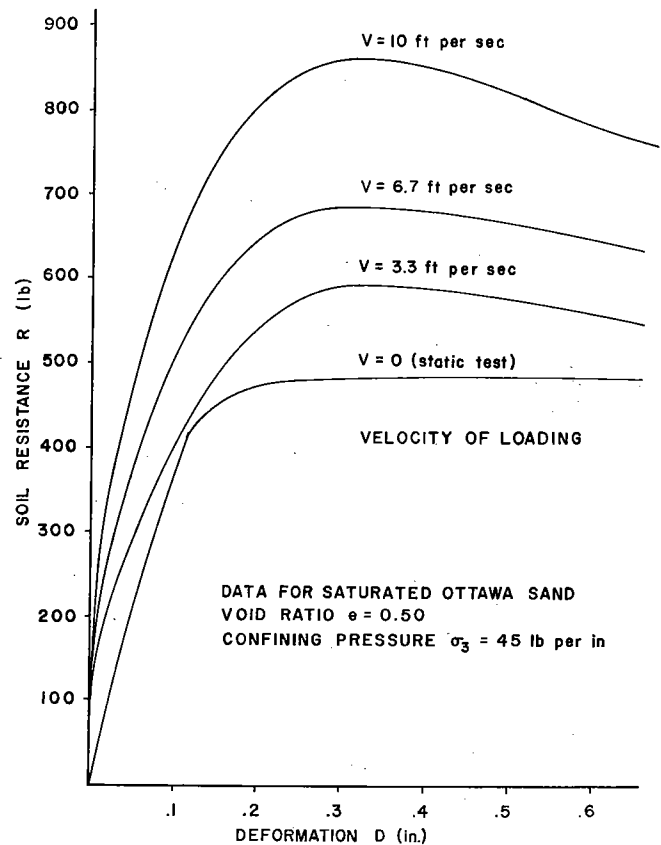


Figure 6.3. Load-deformation properties of Ottawa sand determined by triaxial tests (specimens nominally 3 in. in diam. by 6.5 in. high).

Soil Resistance " R_u ." For the side or friction soil resistance, R_u is determined by the maximum static soil adhesion or friction against the side of a given pile segment by:

$$R_u(m) = f_s \sum_o \Delta L \quad (6.3)$$

where

f_s = maximum soil adhesion or friction (lb/ft²),

\sum_o = perimeter of pile segment (ft), and

ΔL = length of pile segment (ft).

In cohesionless materials (sands and gravels)

$$f_s = \bar{\sigma} \tan \phi' \quad (6.4)$$

where

$\bar{\sigma}$ = effective normal stress against the side of the pile (lb per ft²), and

ϕ' = angle of friction between soil and pile (degrees).

In cohesive soils (clays) f_s during driving is the remolded adhesion strength between the soil and pile.

At the point of the pile R_u is determined by the maximum static bearing strength of the soil and is found by

$$R_u = (Q_u) (A_p) \quad (6.5)$$

where

Q_u = ultimate bearing strength of soil (lb/ft²), and

A_p = area of pile point (ft²).

In cohesive soils (clays) it is believed that the undisturbed strength of the soil may be used conservatively to determine Q_u , since the material at the pile point is in the process of being compacted and may even have a higher bearing value.

Quake "Q". The value of Q , the elastic deformation of the soil is difficult to determine for various types of soils conditions. Various sources of data indicate that values of Q in both friction and point bearing probably range from 0.05 in. to 0.15 in.

Chellis^{6.4} indicates that the most typical value for average pile driving conditions is $Q = 0.10$ in. If the soil strata immediately underlying the pile tip is very soft, it is possible for Q to go as high as 0.2 in. or more. At the present state of the art of pile driving technology it is recommended that a value of $Q = 0.10$ in. be used for computer simulation of friction and point soil resistance. However, in particular situations where more precise values of Q are known, they should be used.

Damping Constant "J". The Texas Transportation Institute has conducted static and dynamic tests on cohesionless soil samples to determine if Smith's rheological model adequately describes the load-deformation properties of these soils. Triaxial soil tests were conducted on Ottawa sand at different loading velocities. Figure 6.3 shows typical results from a series of such tests.

Figure 6.4 shows additional data concerning the increase in soil strength as the rate of loading is increased. Since these tests were confined compression tests it is believed that they simulate to some extent the soil behavior at the pile point. The J value increases as the sand density increases (void ratio e decreases) and it increases as the effective confining stress $\bar{\sigma}_3$ increases.

$$\bar{\sigma}_3 = \sigma_3 - u$$

where

σ_3 = total confining pressure, and
 u = pore water pressure.

For saturated Ottawa sand specimens, $J(p)$ varied from about 0.01 to 0.12. When the sand was dry $J(p)$ was nominally equal to zero. These values of $J(p)$ for

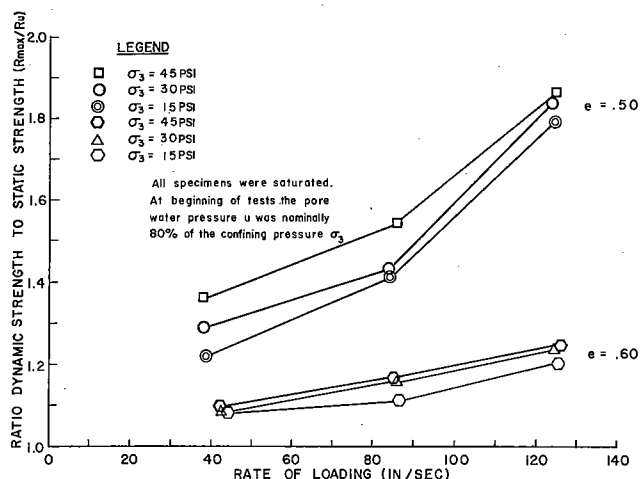


Figure 6.4. Increase in strength vs rate of loading-Ottawa sand.

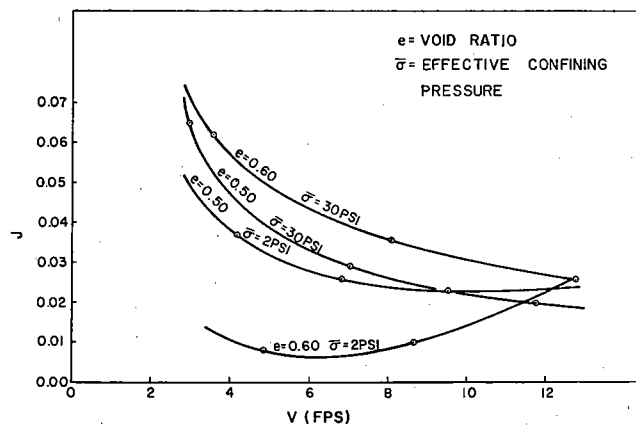


Figure 6.5. "J" versus "V" for Ottawa sand.

sand are in reasonable agreement with those recommended by Smith^{6.5} and Forehand and Reese^{6.6} (0.1 to 0.4).

The value of $J(p)$ for cohesive soils (clays) is not presently known. The very limited data available indicate it is at least equal to that for sand. Forehand and Reese believe it ranges from 0.5 to 1.0.

There are no data now available to indicate the value of $J(m)$ in friction along the side of the pile. Smith believes it is smaller than $J(p)$ and recommends $J(m)$ values in friction of about 1/3 those at the point. Research is under way at Texas A&M University which should indicate the value of J in friction. At the present time $J(m)$ in friction or adhesion is assumed to be 1/3 of $J(p)$.

6.4 Laboratory Tests on Sands

During the laboratory tests in saturated sands, attention was given to the determination of the soil damping constant. The peak dynamic resistance of the soil at the pile point can be represented in equation form for Smith's mathematical model as follows:

$$P_{\text{dynamic}} = P_{\text{static}} [1 + (J)(V)] \quad (6.6)$$

where: P_{dynamic} = peak load developed in dynamically loaded sample at a constant velocity, V ;

P_{static} = peak load developed in statically loaded sample;

J = a damping constant; and

V = impact velocity of the dynamic load.

The laboratory tests on sands were conducted in such a manner that P_{dynamic} , P_{static} , and V were measured, and consequently it was possible to evaluate J for a given set of test conditions.

The laboratory tests conducted on saturated sands were conducted with the sand sample subjected to triaxial confinement. Particular attention was given to the effects of variable loading velocities, initial sample densities, and effective initial confining pressures. The machine used for testing was developed for this particular research and a complete description of the machine

and the instrumentation used is given in Research Report 33-7A.^{6.2}

The results of the study of Ottawa sand are summarized in Figure 6.5. Application of Smith's mathematical model with the experimental data yields a damping factor, J , which varies from 0.01 to 0.07. For two other sands tested, Arkansas sand and Victoria sand, the value of J varied from 0.04 to 0.15. These values of J are not constant, and therefore Smith's equation did not accurately predict peak dynamic loads for the ranges of loading velocities (3 to 12 fps) used in these tests.

Additional tests have been conducted on these sands at loading velocities from 0 to 3 fps. Also, a series of tests have been conducted on clays at loading velocities of from 0 to 12 fps. This work has been accomplished under a new research study entitled "Bearing Capacity of Axially Loaded Piles." The tests on clays have shown that the use of Smith's original equation (Equation 6.2) yields a variable J value as was the case in sands. However, if Smith's equation is modified by raising the velocity, V , to some power, n , less than 1.0, a reasonably constant value of J can be obtained for the full range of loading velocities of from 0 to 12 fps. The proposed modified equation is as follows:

$$P_{\text{dynamic}} = P_{\text{static}} [1 + (J)(V)^n] \quad (6.7)$$

6.5 Static Soil Resistance After Pile Driving (Time Effect)

Immediately after driving, the total static soil resistance or bearing capacity of the pile equals the sum of the R_u values discussed previously. Thus, $R_u(\text{total})$ is the bearing capacity immediately after driving.

$$R_u(\text{total}) = \sum_{m=1}^{m=p} R_u(m)$$

where

$R_u(m)$ = soil adhesion or friction on segments $m = 1$ to $m = p - 1$ (lb), (note that this is the strength of the disturbed or remolded soil along the side of the pile), and

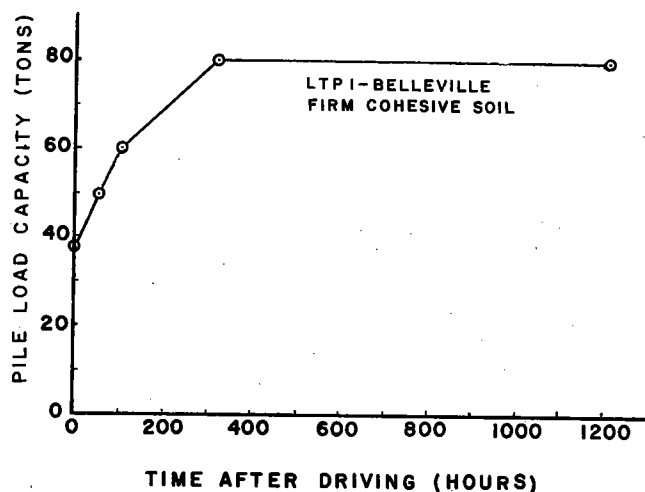


Figure 6.6. "Setup" or recovery of strength after driving in cohesive soil (after reference 6.7).

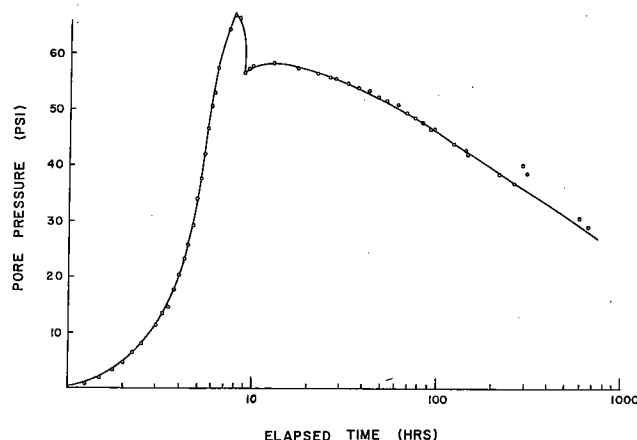


Figure 6.7. Pore pressure measurements in clay stratum —50' depth.

$R_u(p)$ = bearing or compressive strength of soil at the pile point $m = p$ (lb). Note this is taken as the strength of the soil in an undisturbed condition which should be conservative.

As time elapses after driving, $R_u(m)$ for $m = 1$ to $p - 1$ may increase as the disturbed or remolded soil along the side of the pile reconsolidates and the excess pore water pressure dissipates back to an equilibrium condition. In cohesive soils (clays) the increase in strength upon reconsolidation (sometimes referred to as "setup") is often considerable.

The bearing capacity of the pile will increase as the remolded or disturbed clay along the side of the pile reconsolidates and gains strength, since the adhesion or friction strength of clay is generally restored with the passage of time. Loading tests at increasing intervals of time show that ultimate adhesion is approximately equal to the undisturbed cohesion. Therefore, the amount of increase in bearing capacity with time is related to the sensitivity and reconsolidation of the clay*.

Figure 6.6 illustrates the time effect or "setup" of a pile driven in a cohesive soil. In cohesionless soils (sands and gravels) the friction strength of the soil will usually change very little. Normally, the value of $R_u(p)$ at the pile point changes very little.

6.6 Field Test in Clay

The purpose of the field test study^{6.3} was to investigate the failure mechanisms of clay soils subjected to dynamic and static loading. A test pile instrumented with pressure transducers, strain gages, and accelerometers was driven into a saturated clay at a site in Beaumont, Texas.^{6.5}

Measurements of strains and accelerations of the pile were taken during driving. Pore pressure measurements were made at the pile-soil interface for a continuous period of 30 days after driving. Figure 6.7 shows a typical plot of pore pressure versus elapsed time in the clay stratum at a 50 ft depth. Strain measurements were

*Sensitivity of clay = $\frac{\text{undisturbed strength}}{\text{remolded strength}}$

made during static load tests at 13 days and 30 days after driving. Soil borings were made for the in-situ, remolded, and reconsolidated conditions, and at specific radial distances from the pile. Conventional tests were conducted on the soil samples to measure the changes in engineering properties for the different conditions.

A mode of failure was established in this study for a cohesive soil involved in the load response of a pile-soil system. The behavior of the soil in this study indicates that soil disturbances which involve new soil particle arrangement and altered engineering properties are limited to a distance from the center of the pile of approximately 4.5 radii.^{6,5} This relationship can be expressed as follows:

$$\frac{r}{r_1} < 4.5 \quad (6.8)$$

where: r = radial distance from pile center; and
 r_1 = radius of pile.

Results of this study also suggest that the time after driving required for piles of different radii to attain comparable percentages of their ultimate bearing capacity can be expressed as follows:

$$\frac{r_1^2}{r_2^2} = \frac{T_1}{T_2} \quad (6.9)$$

where: r_1 = radius of pile 1;

r_2 = radius of pile 2;

T_1 = time for pile 1 to attain a stated percentage of ultimate bearing capacity; and

T_2 = time for pile 2 to attain the same percentage of ultimate bearing capacity.

CHAPTER VII

Use of the Wave Equation to Predict Pile Load Bearing Capacity At Time of Driving

7.1 Introduction

In general, engineers are interested in the static load carrying capacity of the driven pile. In the past the engineer has often had to rely on judgement based on simplified dynamic pile equations such as the Hiley or Engineering News formulas. By the wave equation method of analysis a much more realistic engineering estimate can be made using information generated by the program.

The previous chapters have shown how the hammer pile-soil system can be simulated and analyzed by the wave equation to determine the dynamic behavior of piling during driving. *With this simulation the driving stresses and penetration of the pile can be computed.*

7.2 Wave Equation Method

In the field the pile penetration or permanent set per blow (in. per blow) is observed and this can be translated into the static soil resistance through the use of the wave equation.

Consider the following example:

PILE: 72 ft steel step taper pile

HAMMER: No. 00 Raymond

Efficiency = 80%

Ram Weight = 10,000 lb

Energy = 32,500 ft lb

CAPBLOCK: Micarta

$K = 6,600,000$ lb/in.

$e = 0.8$

ASSUMED SOIL PARAMETERS:

$J(p)$ point = 0.15 sec/ft $Q(p)$ point = 0.10 in.

$J(m)$ side = 0.05 sec/ft $Q(m)$ side = 0.10 in.

Soil is a soft marine deposit of fine sand, silt, and muck, with the pile point founded on a dense layer of sand and gravel.

ASSUMED SOIL DISTRIBUTION:

Curve I: 25% side friction (triangular distribution) 75% point bearing.

Curve II: 10% side friction (triangular distribution) 90% point bearing.

This information is used to simulate the system to be analyzed by the wave equation. A total soil resistance $R_u(\text{total})$ is assumed by the computer for analysis in the work. It then computes the pile penetration or "permanent set" when driven against this $R_u(\text{total})$. The reciprocal of "permanent set" is usually computed to convert this to blows per in.

The computer program then selects a larger $R_u(\text{total})$ and computes the corresponding blows per in. This is done several times until enough points are generated to develop a curve relating blows per in. to $R_u(\text{total})$ as shown in Figure 7.1 (two curves for the two different assumed distributions of soil resistance are shown).

In the field if driving had ceased when the resistance to penetration was 10 blows per in. (a permanent set equal to 0.1 in. per blow), then the ultimate pile load bearing capacity immediately after driving should have been approximately 370 to 380 tons as shown on Figure 7.1. It is again emphasized that this $R_u(\text{total})$ is the total static soil resistance encountered during driving, since the increased dynamic resistance was considered in the analysis by use of J . If the soil resistance is predominantly due to cohesionless materials such as sands and gravels, the time effect or soil "setup" which tends to increase the pile bearing capacity will be small

FILE: 72 ft. Step Taper, 12 ft. steps, No. 1 to No. 6
HAMMER: No. 00 Raymond
SHELL: Step Taper Corrugated
CAPBLOCK: Micarta; Coeff. of Rest. = .80; K = 6,600,000 psi
DISTRIBUTION OF RESISTANCE:
Curve I: 25% Side (Triangular Distribution); 75% Point
Curve II: 10% Side (Triangular Distribution); 90% Point
CONSTANTS:
J (Point) = 0.15; J (Side) = 0.05
Q (Point) = 0.10; Q (Side) = 0.10

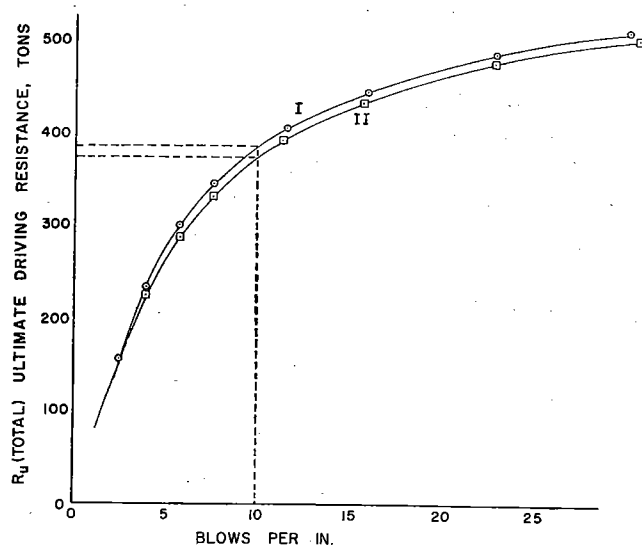


Figure 7.1. Ultimate driving resistance vs blows per inch for an example problem.

or negligible. If the soil is a cohesive clay, the time effect or soil "setup" might increase the bearing capacity as discussed in Chapter VI. The magnitude of this "setup" can be estimated if the "sensitivity" and reconsolidation of the clay is known. It can also be conservatively disregarded since the "setup" bearing capacity is usually greater than that predicted by a curve similar to Figure 7.1.

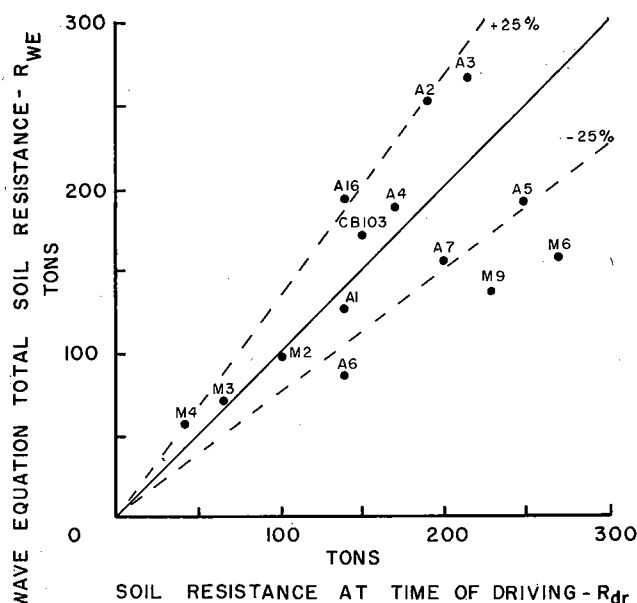


Figure 7.2. Comparison of wave equation predicted soil resistance to soil resistance determined by load tests for piles driven in sands. (Data from table 7.1.)

In developing the curves of Figure 7.1, it was necessary to assume the following soil parameters:

1. Distribution of soil resistance
2. Soil Quake "Q"
3. Soil damping constant "J"

As illustrated by Curves I and II on Figure 7.1, small variations in the distribution of soil resistance between side friction and point bearing will not affect the wave equation results significantly. All that is re-

TABLE 7.1. ERRORS CAUSED BY ASSUMING $J(\text{point}) = 0.1$ AND $J'(\text{side}) = \frac{J(\text{point})}{3}$ FOR SAND (For Sand-Supported Piles Only)

Location	Load Test Pile	R_{dr}^* (Resistance at Time of Driving) (kips)	R_{WE} (Indicated Soil Resistance) (kips)	% Error in R_{dr} $\left(\frac{R_{WE} - R_{dr}}{R_{dr}} \right) (100)$
Arkansas	1	280	255	- 9
	2	380	495	+30
	3	430	530	+23
	4	340	370	+ 9
	5	500	380	-24
	6	280	170	-39
	7	400	310	-23
	16	280	380	+36
Copano Bay	103	300	320	+ 7
Muskegon	2	200	195	- 3
	3	110	145	+32
	4	85	110	+29
	6	540	310	-43
	9	470	270	-43
Total				13501
Mean or Average % Error =				$\frac{13501}{14} = 25\%$

* R_{dr} for piles driven in sands was assumed equal to the actual load test measurements since no "setup" was considered.

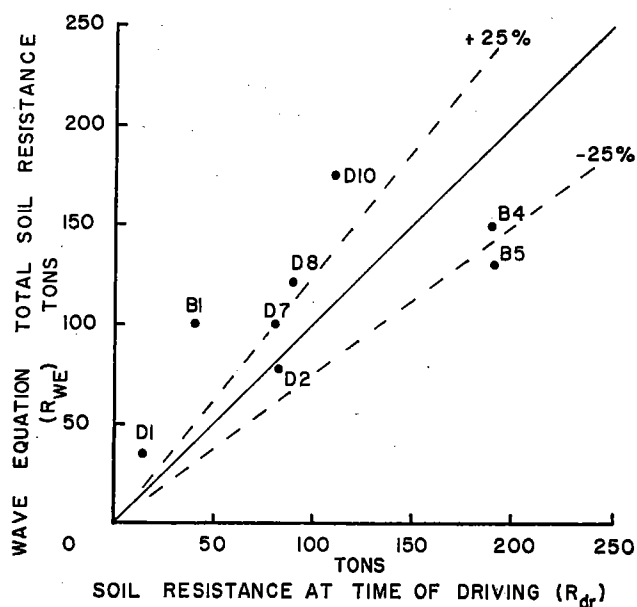


Figure 7.3. Comparison of wave equation predicted soil resistance to soil resistance determined by load tests for piles driven in clay. (Data from table 7.2.)

quired is a reasonable estimate of the situation. For most conditions an assumption of soil quake $Q = 0.1$ in. is satisfactory (see Chapter VI). The value of $J(m)$ is assumed to be $1/3$ of $J(p)$.

7.3 Comparison of Predictions with Field Tests

Correlations of wave equation solutions with full-scale load tests to failure have provided a degree of

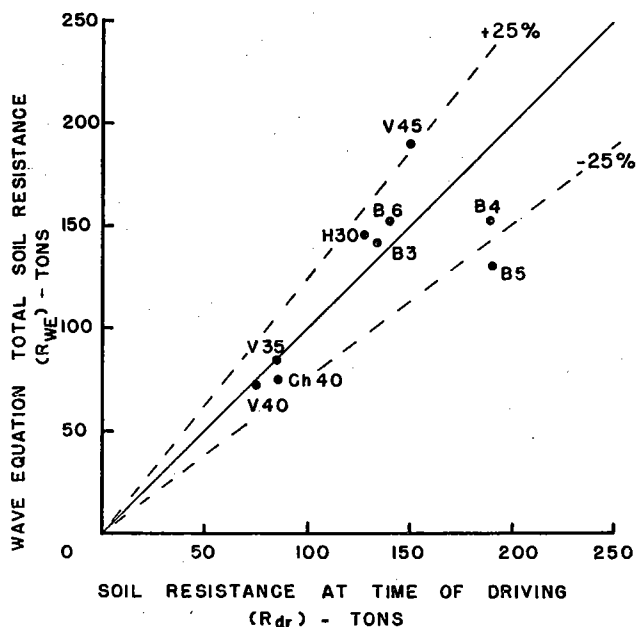


Figure 7.4. Comparison of wave equation predicted soil resistance to soil resistance determined by load tests for piles driven in both sand and clay. (Data from table 7.3.)

confidence in the previously described method of predicting static bearing capacity.

For the sand-supported piles (Table 7.1) damping constants of $J(\text{point}) = 0.1$ and $J'(\text{side}) = J(\text{point})/3$ were found to give the best correlation. Figure 7.2 shows the accuracy of the correlation to be approximately $\pm 25\%$. In Table 7.2, for clay-supported piles

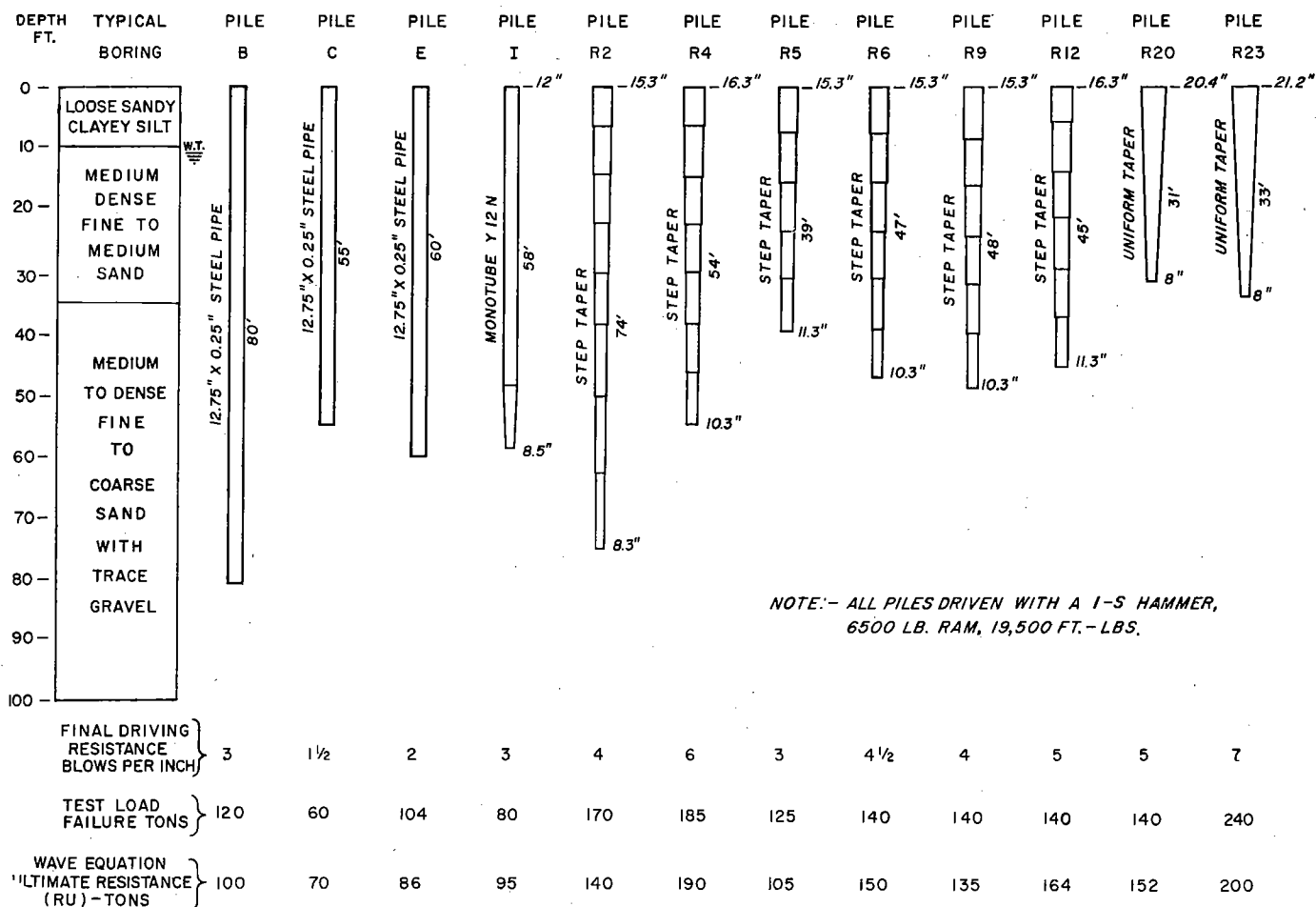
TABLE 7.2. ERROR CAUSED BY ASSUMING $J(\text{point}) = 0.3$ AND $J'(\text{side}) = \frac{J(\text{point})}{3}$ FOR CLAY (For Clay-Supported Piles Only)

Location	Load Test Pile	R_{lt} (Load Test Resistance) (kips)	R_{dr}^{***} (Resistance at time of driving) (kips)	R_{WE} (Indicated soil resistance) (kips)	% Error in R_{dr} $\left(\frac{R_{WE} - R_{dr}}{R_{dr}} \right) (100)$
Belleville	1**	160	80	200	+150
	4*	690	379	305	-19
	5*	692	381	260	-32
Detroit	1**	56	28	70	+156
	2	330	165	155	-6
	7	318	159	205	+29
	8	360	180	240	+33
	10	450	225	250	+11
					Total = 436
					Average % Error = $\frac{436}{8} = 54.5\%$

*90% clay-supported piles.

**The test values for these piles were questionable.

*** R_{dr} for piles driven in clay were actual load test measurements corrected to account for soil "set-up."



$Q = 0.1$ in. and $J(\text{point}) = 0.15$, $J(\text{side}) = 0.05$. Soil resistance was assumed to be 50% at the point and 50% friction distributed uniformly over the embedded length below a depth of 10 ft. Hammer efficiency assumed to be 80%.

Figure 7.5. Summary of piles tested to failure in sands.

TABLE 7.3. ERRORS CAUSED BY ASSUMING A COMBINED $J(\text{point}) = 0.1$ FOR SAND AND $J(\text{point}) = 0.3$ FOR CLAY USING EQ. 7.1 (For Piles Supported by Both Sand and Clay)

Location	Load Test Pile	$\Delta R_{\text{clay}} \times 0.3$	$\Delta R_{\text{sand}} \times 0.1$	$J(\text{point})$ (sec/ft)	R_{lt} (Load Test Resistance) (kips)	R_{dr}^{**} (Resistance at Time of Driving) (kips)	R_{WB} (Indicated Soil Resistance) (kips)	% Error in R_{dr} $\left(\frac{R_{\text{WB}} - R_{\text{dr}}}{R_{\text{dr}}} \right) (100)$
Victoria	35	0.090	0.070	0.16	208	176	170	- 3%
	40	0.087	0.071	0.16	160	136	148	+ 9%
	45	0.093	0.069	0.16	352	300	380	+ 27%
Chocolate Bayou	40	0.126	0.058	0.18	210	166	150	- 10%
	60	0.120	0.060	0.18	*	*	740	
Houston Copano Bay	30	0.153	0.049	0.20	340	255	290	+ 14%
Belleville	58	0.252	0.016	0.27	*	*	260	
	3	0.102	0.066	0.17	342	284	265	- 7%
	4	0.270	0.010	0.28	690	379	305	- 20%
	5	0.270	0.010	0.28	692	381	260	- 32%
	6	0.192	0.036	0.23	412	280	305	+ 9%
Muskegon	7	0.090	0.070	0.16	*	*	320	
	8	0.090	0.070	0.16	*	*	295	

Total = 131

$$\text{Average \% Error} = \frac{131}{9} = 14.5\%$$

*Indicates piles which exceeded the testing equipment's capacity, and could not be load-tested to failure.

** R_{dr} for these piles were actual load test measurements corrected to account for soil "setup."

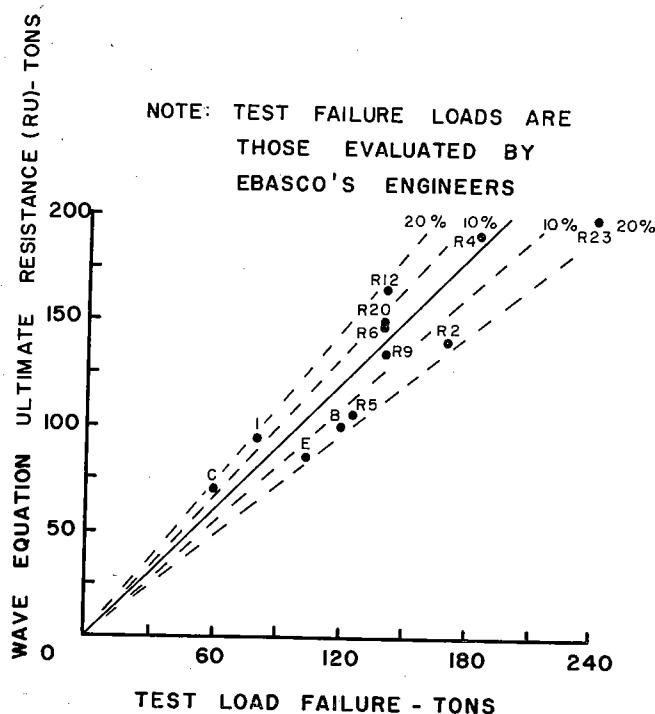


Figure 7.6. Wave equation ultimate resistance vs test load failure (after Ref. 7.2, data from Fig. 7.5) (sands).

the damping constants $J(\text{point}) = 0.3$ and $J'(\text{side}) = J(\text{point})/3$ gave the best correlation. The accuracy of the correlation is shown in Figure 7.3 to be approximately $\pm 50\%$.

If more than one soil was involved the damping constant used was a weighted average calculated from

$$J(\text{point}) = \Sigma [R_i \times J(\text{point})_i] \quad (7.1)$$

where R_i = the ratio of the amount of resistance of each type of soil "i", to the total soil resistance, both determined after setup has ceased, and

$$J'(\text{side}) = \frac{J(\text{point})}{3}$$

Table 7.3 shows the damping constant that was calculated from Equation 7.1 using $J(\text{point}) = 0.3$ for clay and $J(\text{point}) = 0.1$ for sand. The accuracy of the correlation, as shown in Figure 7.4 was approximately $\pm 25\%$.

Mosley^{7.2} has found a similar correlation with 12 piles driven in sand. Figure 7.5 is a summary of the piles tested. Figure 7.6 shows that all resistances on these piles fall within $\pm 20\%$ of that predicted by the wave equation.

CHAPTER VIII

Prediction of Driving Stresses

8.1 Introduction

In Appendix A the exact solution for the stress wave introduced into a long slender elastic pile is derived using the classical one-dimensional wave equation. The solution of this equation depends upon certain assumptions. It is assumed that the pile is prismatic with lateral dimensions small in comparison to its length (Poisson's effects can be neglected), that the pile and cushion material are linearly elastic, and the ram has infinite rigidity (assumed to be a rigid body). The equation which governs the stress amplitude in most practical cases, shows that the magnitude of the stress induced at the head of the pile, by the falling ram, is directly proportional to the velocity of the ram at impact. The equation further shows that the stiffnesses of the cushion and pile also have a significant effect on the magnitude of the stress generated. The soil resistance on the side and at the point of the pile will also affect the magnitude of the stresses in the pile.

Chapter II discusses Smith's numerical solution of the one-dimensional wave equation. This particular technique for solving the wave equation is much simpler for application to problems which can have inelastic cushions and material properties as well as soil on the side and point of the pile. Chapter V discusses the generation of stress waves in piling, the significance of material damping in the pile and the effects of pile dimensions on driveability.

This chapter demonstrates the validity of Smith's

numerical solution by comparing its results with the theoretical solution of Appendix A and with field data.

8.2 Comparison of Smith's Numerical Solution with the Classical Solution

For the purpose of correlation, consider a concrete pile, square in cross-section, with an area of 489 in.² and 90 ft long. The modulus of elasticity of the pile material is assumed to be 5×10^6 psi. The pile is considered to be free at the top with the bottom end fixed rigidly against movement. No side resistance is present.

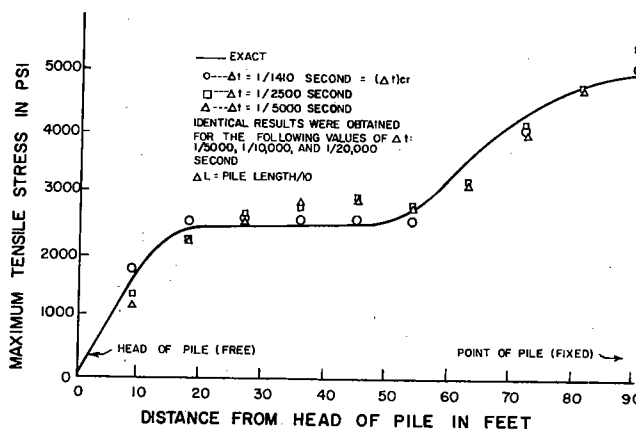


Figure 8.1. Maximum tensile stress along the pile.

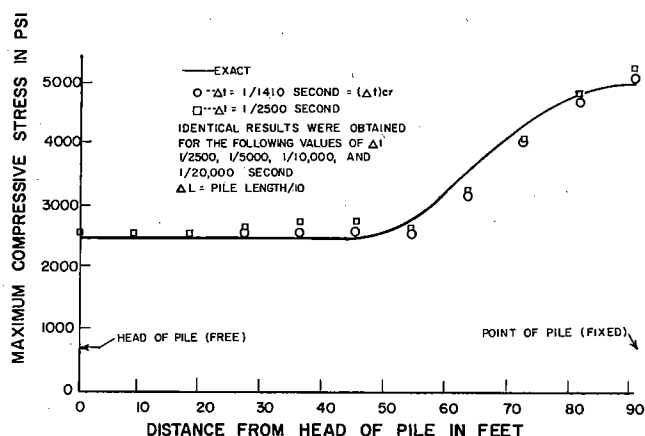


Figure 8.2. Maximum compressive stress along the pile.

The following information is also applicable to the correlation:

- Weight of the ram = 11,500 lb,
- Velocity of the ram = 14.45 fps
- Cushion block stiffness = 3,930,000 lb/in.,
- Coefficient of restitution of the cushion block = 1.00

Solutions have been obtained for the exact solution of the one-dimensional wave equation and for Smith's numerical method using 10 segments. Previous studies^{8.1} had shown that segment lengths of $L/10$ would yield accurate results. Figures 8.1 and 8.2 show comparisons of the maximum tensile stress and maximum compressive stress, respectively, versus position along the length of the pile. Note the time interval used (time differencing interval used in the numerical solution) for solutions shown is varied from $1/1410$ seconds (this is the critical time differencing interval) to $1/20,000$ seconds. Note that when the differencing interval became very small, i.e., $1/5000$ seconds, the accuracy of the solution was not improved. Note also that the numerical solution is very close to the exact solution. Other comparisons have been made for the stresses at other points in the pile and for other combinations of the end boundary conditions.^{8.1} Heising^{8.2} and Smith^{8.3} have shown that the discrete-element numerical solution is an exact solution of the one-dimensional wave equation when

$$\Delta t = \frac{\Delta L}{\sqrt{E/\rho}}$$

where,

- Δt = critical time differencing interval,
- ΔL = segment length,
- E = modulus of elasticity, and
- ρ = mass density of the pile material.

This time interval is the "critical" time interval. For practical problems, a choice of Δt = one-half the "critical value," appears suitable since inelastic springs, materials of different densities, and elastic moduli are usually involved.

8.3 Correlations of Smith's Solution with Field Measurements

In previous reports^{8.4, 8.5} the writers have shown several correlations of the wave equation with stresses measured in piles during the time of driving in the field. Typical examples of these correlations are shown in Figures 8.3 and 8.4. The significant conclusions drawn from these tests are as follows:

1. The maximum compressive stresses occurred at the head of the pile.
2. Maximum tensile stresses were found to occur near the midpoint of the piles.
3. The computed compressive stresses and displacements agree very well with the measured data.
4. The computed tensile stresses appeared high but in view of the unknown dynamic properties of the soil, concrete, and cushioning materials involved in the problem, the quantitative comparisons shown were considered good.

8.4 Effect of Hammer Type and Simulation Method

It has been shown^{8.7} (see Chapter III) that the ram of a pile hammer can be idealized as a rigid body provided it strikes on a capblock or cushion. If the ram strikes directly on steel, as in the case of the diesel hammers, the accuracy of the solution for stresses is improved by breaking the ram into segments.

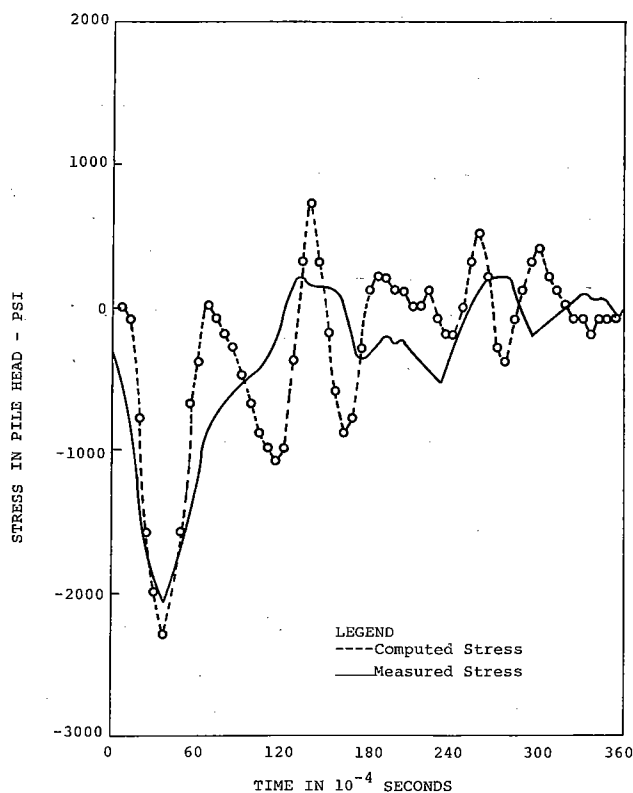


Figure 8.3. Stress in pile head vs time for test pile.

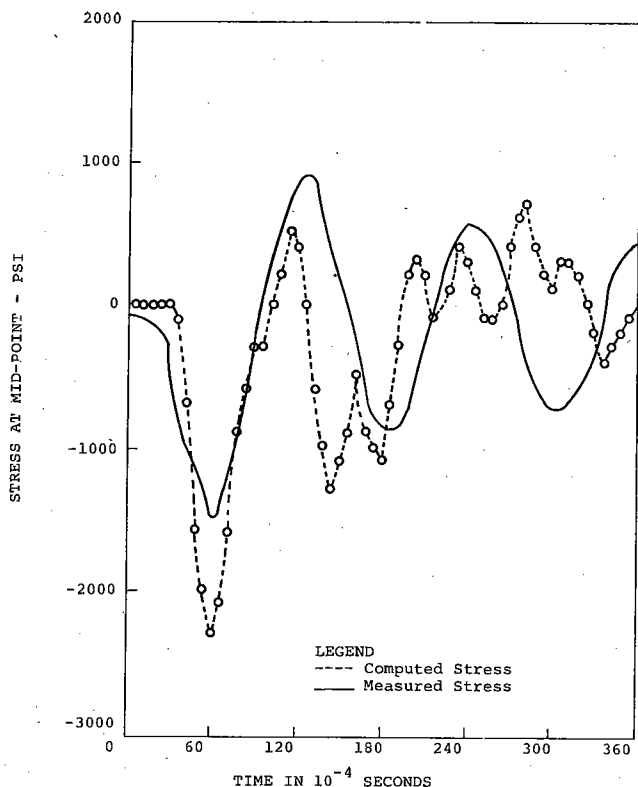


Figure 8.4. Stress at mid-length of pile vs time for test pile.

For diesel hammers, the explosive force used to raise the hammer for the next blow does work on the pile and should be included.

In all hammer simulations, all parts which are in the force transmission chain should be included. The housing and other parts which do not serve to transmit the driving energy may be neglected.

Refer to Appendix B, Tables B.1 and B.2, for recommended values for use in the simulation.

8.5 Effect of Soil Resistance

If soil borings are available, the distribution of the soil resistance on the pile should be estimated from soil shear strength data. In general, piles in uniform cohesive soils will have the soil resistance distributed uniformly in side friction with about 10 to 20% point resistance. Cohesionless soils can generally be simulated with a triangular friction distribution with about 40% in side friction and 60% of the total resistance at the point. The actual distributions used will, of course, depend on the properties of the soils, pile length, type, etc., and should be studied for each case. It is important to note, however, that the soil distribution will affect the magnitude of the driving stresses. This is particularly true for the reflected tensile stresses. In most investigations for driving stresses, it is best to vary the distribution over the expected range and choose the most conservative result. Reflected tensile stresses are highest when the soil resistance acting at the pile point is small.

8.6 Effects of Cushion Stiffness, Coefficient of Restitution, and Pile Material Damping

It has been shown^{8.6} (see Chapter IV) that the actual load deformation curve for a cushion is not a straight line, but is parabolic. However, a straight line which has a slope given by the secant modulus will give reasonably accurate results. The cushion's dynamic coefficient of restitution was found to agree with commonly recommended values. It has also been shown that the effect of internal damping in the concrete and steel piles will usually have a negligible effect on the driving stresses.

8.7 Fundamental Driving Stress Considerations

The purpose of this discussion is to briefly describe and discuss the phenomena of impact stresses during driving.

Compressive Stresses. High compressive stress at the head of the pile can be caused by the following:

1. Insufficient cushioning material between the pile driving ram and the pile will result in a very high compressive stress on impact.
2. When a pile is struck by a ram at a very high velocity, or from a very high drop, a stress wave of high magnitude is produced. This stress is directly proportional to the ram velocity.

If the pile is idealized as a long elastic rod, with an elastic cushion on top an equation for the compressive stress can be developed (see Appendix A). The approximate equations for the maximum compressive stress at the pile head are as follows:

Notations used are:

- $\sigma_o \text{ max}$ = maximum compressive stress at pile head (psi),
- W = ram weight (lb),
- V = ram impact velocity (in./sec),
= $\sqrt{2gh}$,
- h = ram free fall (in.),
- g = acceleration due to gravity,
386 in./sec²,
- K = cushion stiffness (lb/in.),
= $\frac{A_c E_c}{t_c}$
- A_c = cross-sectional area of cushion (in.²),
- E_c = modulus of elasticity of cushion (psi),
- t_c = initial uncompressed thickness of cushion (in.),
- t = time (sec),
- A = cross-sectional area of pile (in.²),
- E = modulus of elasticity of pile (psi),
- L_p = length of pile (in.),
- γ = unit weight of pile (lb/in.³),

$$n = \frac{K}{2A} \sqrt{\frac{g}{E\gamma}}$$

$$p = \sqrt{\frac{Kg}{W}}$$

Case I. $n < p$

$$\sigma_o \text{ max} = \frac{-KV}{A} \frac{e^{-nt}}{\sqrt{p^2 - n^2}} \sin (t \sqrt{p^2 - n^2}) \quad (8.1)$$

where t is found from the expression

$$\tan (t \sqrt{p^2 - n^2}) = \frac{\sqrt{p^2 - n^2}}{n}$$

Case II. $n = p$

$$\sigma_o \text{ max} = - \left[\frac{KV}{nA} - \frac{W}{A} \right] e^{-1} \quad (8.2)$$

Case III. $n > p$

$$\sigma_o \text{ max} = - \frac{KV}{A} \frac{e^{-nt}}{\sqrt{n^2 - p^2}} \sinh (t \sqrt{n^2 - p^2}) \quad (8.3)$$

where t is found from the expression

$$\tanh (t \sqrt{n^2 - p^2}) = \frac{\sqrt{n^2 - p^2}}{n}$$

Equations (8.1), (8.2), or (8.3) can be used to determine the maximum compressive stress at the pile head. For most practical pile problems n will be less than p and Equation (8.1) will be used. However, this is not always the case. For a given pile these equations can be used to determine a desirable combination of ram weight W , ram velocity V , and cushion stiffness K so as not to exceed a given allowable compressive stress at the pile head.

To illustrate the use of the equations consider the following situation.

Given:

Concrete Pile

$$L_p = 65 \text{ ft}$$

$$A = 200 \text{ in.}^2$$

$$\gamma = 0.0868 \text{ lb/in.}^3 \text{ (150 lb/ft}^3\text{)}$$

$$E = 5.00 \times 10^6 \text{ psi}$$

Green oak cushion, grain horizontal

$$A_c = 200 \text{ in.}^2$$

$$E_c = 45,000 \text{ psi (for properties of wood see Chapter IV)}$$

$$t_c = 3.0 \text{ in.}$$

$$K = \frac{A_c E_c}{t_c} = 3.0 \times 10^6 \text{ lb/in.}$$

Steel ram

$$W = 5000 \text{ lb}$$

$$h = 36 \text{ in.}$$

$$V = \sqrt{2gh} = 167 \text{ in./sec}$$

$$g = 386 \text{ in./sec}^2$$

Calculations:

$$n = \frac{K}{2A} \sqrt{\frac{g}{E\gamma}} = 224 \text{ sec}^{-1}$$

$$p = \sqrt{\frac{Kg}{W}} = 481 \text{ sec}^{-1}$$

Since $n < p$ Equation 8.1 of Case I applies.

$$\tan (t \sqrt{p^2 - n^2}) = \frac{\sqrt{p^2 - n^2}}{n}$$

$$= \frac{425}{224} = 1.896$$

$$\text{so } t \sqrt{p^2 - n^2} = 62.2^\circ \text{ or } 1.085 \text{ radians}$$

$$t = .00255 \text{ sec}$$

Using Equation 8.1

$$\sigma_o \text{ max} = \frac{-KV}{A} \frac{e^{-nt}}{\sqrt{p^2 - n^2}} \sin (t \sqrt{p^2 - n^2})$$

$$= \frac{3 \times 10^6 \times 167 e^{-244 \times .00255}}{200 \times 425} (\sin 62.2^\circ)$$

$$\sigma_o \text{ max} = 2920 \text{ psi}$$

Using these equations, Tables 8.1 and 8.2 were developed to illustrate the effect of ram weight and velocity on driving stresses. Table 8.1 shows the variation of the driving stress (compressive) with the ram weight and ram velocity. It can be seen that the stress magnitude also increases with ram weight, however, this is usually not of serious consequence. Table 8.2 shows the variation of driving stress (compression) with ram weight and ram driving energy. At a constant driving energy the driving stress decreases as the ram weight increases. Therefore, it is better to obtain driving energy with a heavy ram and short stroke than use a light ram and large stroke.

3. When the top of the pile is not perpendicular to the longitudinal axis of the pile, the ram impacting force will be eccentric and may cause very high stress concentrations.

4. If the reinforcing steel in a concrete pile is not cut flush with the end of the pile, high stress concentrations may result in the concrete adjacent to the reinforcing. The ram impact force may be transmitted to the concrete through the projecting reinforcing steel.

5. Lack of adequate spiral reinforcing at the head of a concrete pile and also at the pile point may lead

TABLE 8.1. VARIATION OF DRIVING STRESS WITH RAM WEIGHT AND VELOCITY

Result from Equation 8.1 for 65 ft long concrete pile, 200 in.² area, and 3 in. wood cushion. Stresses shown are maximum compression at pile head. $E_c = 45,000 \text{ psi}$.

Ram Weight lb	Ram Velocity, ft/sec—Stroke, ft			
	11.4 - 2	13.9 - 3	16.1 - 4	18.0 - 5
2,000	1,790 psi	2,200 psi	2,540 psi	2,840 psi
5,000	2,380 psi	2,920 psi	3,380 psi	3,780 psi
10,000	2,830 psi	3,470 psi	4,000 psi	4,480 psi
20,000	3,250 psi	3,980 psi	4,600 psi	5,150 psi

TABLE 8.2. VARIATION OF DRIVING STRESS WITH RAM WEIGHT AND RAM ENERGY

Results from Equation 8.1 for 65 ft long concrete pile, 200 in.² area, and 3 in. wood cushion. Stresses shown are maximum compression at pile head. $E_c = 45,000$ psi.

Ram Weight lb	Driving Energy ft - lb	
	20,000	40,000
2,000	4,010 psi	5,680 psi
5,000	3,380 psi	4,780 psi
10,000	2,830 psi	4,000 psi
20,000	2,290 psi	3,250 psi

to spalling or splitting. In prestressed concrete piles anchorage of the strands is being developed in these areas, and transverse tensile stresses are present. If no spiral reinforcing is used, the pile head may spall or split on impact of the ram.

6. Fatigue of the pile material can be caused by a large number of blows at a very high stress level.

7. If the top edges and corners of a concrete pile are not chamfered the edges or corners are likely to spall on impact of the ram.

Yielding of steel or spalling of concrete at the point of the pile can be caused by extremely hard driving resistance at the point. This type resistance may be encountered when founding the pile point on bed rock. Compressive stress under such driving conditions can be twice the magnitude of that produced at the head of the pile by the hammer impact (see Figure 8.2).

Tension. Transverse cracking of a concrete pile due to a reflected tensile stress wave is a complex phenomenon usually occurring in long piles (50 ft or over). It may occur in the upper end, midlength, or lower end of the pile. It can occur when driving in a very soft soil or when the driving resistance is extremely hard or rigid at the point such as in bearing on solid rock.

When a pile driver ram strikes the head of a pile or the cushion on top, a compressive stress is produced at the head of the pile. This compressive stress travels down the pile at a velocity

$$c = \sqrt{E/\rho}$$

where

c = velocity of the stress wave through the pile material in in./sec,

E = modulus of elasticity of the pile material in psi, and

ρ = mass density of the pile material in lb-sec²/in.⁴

The intensity of the stress wave (σ_c max.) can be determined by Equations 8.1, 8.2, or 8.3 and depends on the weight of the ram, velocity of the ram, stiffness of the cushion, and stiffness of the pile. Since in a given concrete pile the stress wave travels at a constant velocity (about 13,000 to 15,000 ft/sec) the length of the stress wave (L_s) will depend on the length of time (t_s) the ram is in contact with the cushion or pile head. A heavy ram will stay in contact with the cushion or pile head for a longer time than a light ram, thus producing a longer stress wave. If a ram strikes a thick soft cush-

ion, it will also stay in contact for a longer period of time than when it strikes a thin hard cushion. For Case I (when $n < p$ which is typical for most practical concrete pile conditions) the length of the stress wave can be calculated by the equation which follows.

$$L_s = ct_s$$

or

$$L_s = \frac{c}{\sqrt{p^2 - n^2}} \pi \quad (8.4)$$

where L_s = length of stress wave (in.) and

t_s = time of contact of ram (sec).

Figure 8.5(b) shows the compressive stress wave building up while the ram is in contact with the cushion. After the ram rebounds clear of the cushion, the compressive stress wave is completely formed and travels down the length of the pile as shown by Figure 8.5(c). When the compressive stress wave reaches the point of the pile, it will be reflected back up the pile in some manner depending on the soil resistance. If the point of the pile is experiencing little or no resistance from the soil, it will be reflected back up the pile as a tensile stress wave as shown in Figure 8.6(a). If the point of the pile is completely free, the reflected tensile wave will be of the same magnitude and length as the initial compressive wave. As shown in Figure 8.6(a) these two waves may overlap each other. The net stress at a particular point on the pile at a particular time will be the algebraic sum of the initial compressive (—) stress wave and reflected tensile (+) stress wave. Whether

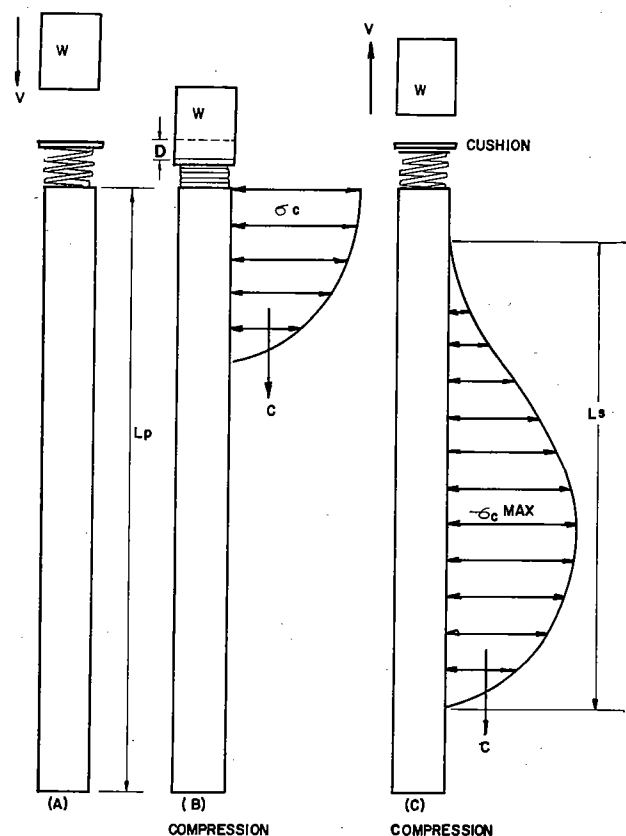


Figure 8.5. Idealized stress wave produced when ram strikes cushion at head of concrete pile.

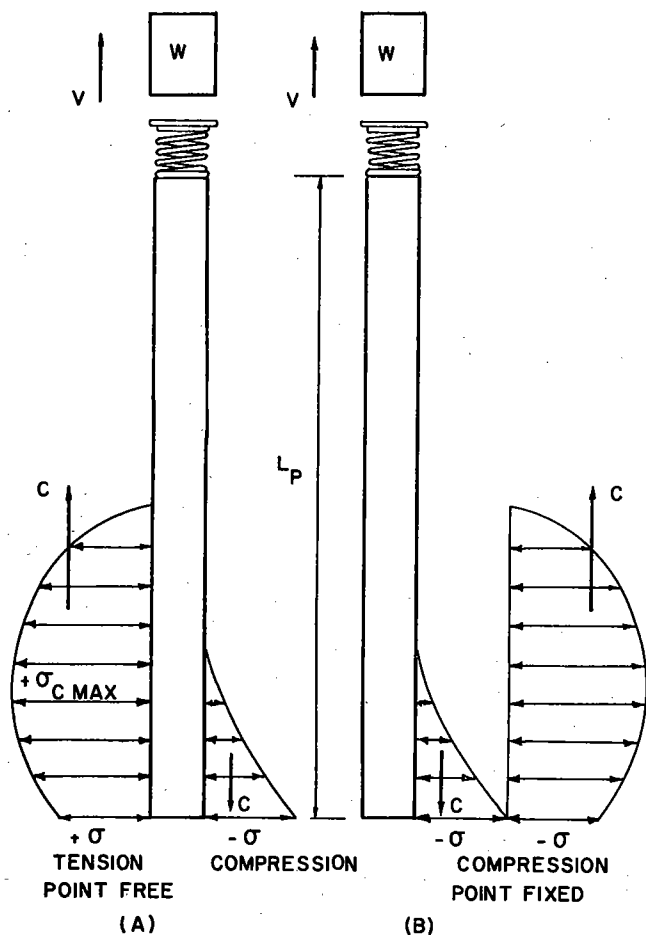


Figure 8.6. Reflection of stress wave on a long pile.

or not the pile will ever experience critical tensile stresses will depend on the pile length (L_p) relative to the length of the stress wave (L_s) and on material damping. If the pile is long compared to the length of the stress wave, critical tensile stresses may occur at certain points. When a heavy ram strikes a thick soft cushion, the stress wave may be around 150 ft in length. When a light ram strikes a thin hard cushion it may be only 50 or 60 ft in length.

The results of a theoretical study on ideal piles with the point free of soil resistance has shown that the maximum reflected tensile stress ($\sigma_t \text{ max.}$) can be computed approximately by Equations 8.5 and 8.6 given below.

$$\sigma_t \text{ max.} = \sigma_o \text{ max.} \quad (8.5)$$

when $L_s/L_p \leq 2$

and $\sigma_t \text{ max.} = \frac{8 \sigma_o \text{ max.}}{(L_s/L_p)^3} \quad (8.6)$

when $L_s/L_p \geq 2$

Figure 8.8 shows in dimensionless parameters how $\sigma_t \text{ max.}$ is affected by $\sigma_o \text{ max.}$, the length of the stress wave L_s , and the length of the pile L_p . The data points shown were computed using stress wave theory (Ap-

pendix A) and piles with a free point. These values are conservative since material damping of the pile and soil resistance will tend to reduce them.

If the point soil resistance is hard or very firm, the initial compressive stress wave traveling down the pile will be reflected back up the pile also as a compressive stress wave, as shown in Figure 8.6(b). If the point of the pile is fixed from movement, the reflected compressive stress wave will be on the same magnitude and length as the initial compressive stress wave. As shown in Figure 8.6(b) these two stress waves may overlap each other at certain points. The net compressive stress at a particular point at a particular time will be the algebraic sum of the initial compressive (—) stress wave and the reflected compressive (—) stress wave. (Note that under these conditions the maximum compressive stress at the pile point can be twice that produced at the pile head by ram impact.) Tensile stress will not occur here until the compressive stress wave is reflected from the free head of the pile back down the pile as a tensile stress wave (similar to the reflection shown at the free point in Figure 8.6(a)). It is possible for critical tensile stress to occur near the pile head in this case; however, damping characteristics of the surrounding soil may reduce the magnitude of this reflected tensile stress wave by this time. Such failures have occurred, however.

Figure 8.7 shows the reflection of the initial compressive (—) stress wave from the point of a relatively short pile. If the pile is short compared to the length of the stress wave (L_s) critical tensile stresses are not likely to occur. In Figure 8.7(a) the reflected tensile (+) stress wave overlaps the initial compressive (—) stress wave coming down the pile. Since the net stress at any point is the algebraic sum of the two, they tend to cancel each other and critical tension is not likely to occur. A similar phenomenon will occur when the reflected compressive (—) stress wave from the point is likely to find the ram still in contact with the pile head when it arrives there. In such a case, little or no reflected tensile stress wave will occur. In Figure 8.7(b) the initial compressive (—) stress wave is being reflected

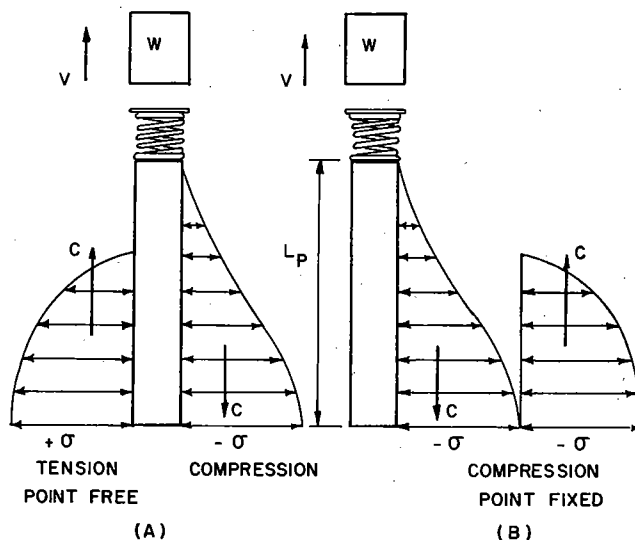


Figure 8.7. Reflection of stress wave along a short pile.

from the fixed point also as a compressive (—) stress wave. In this case also, little or no reflected tensile stress will occur.

The cases illustrated by Figures 8.6 and 8.7 are highly idealized and simplified, but they should indicate some of the basic factors which can cause tensile stress failures in concrete piles. In summary, tensile cracking of concrete piles can be caused by the following:

1. When insufficient cushioning material is used between the pile driver's steel helmet or cap and the concrete pile, a stress wave of high magnitude and of short length is produced, both characteristics being undesirable.

2. When a pile is struck by a ram at a very high velocity, or from a very high drop, a stress wave of high magnitude is produced. The stress is proportional to the ram velocity.

3. When the tensile strength of the concrete pile is too low to resist a reflected tensile stress, severe cracking can occur.

4. When little or no soil resistance at the point of long piles is present during driving, critical tensile stresses may occur in the lower half or near mid-length of the pile.

5. When hard driving resistance is encountered at the point of long piles, critical tensile stresses may occur in the upper half of the pile when the tensile stress is reflected from the pile head.

Torsion. Spiral or transverse cracking of concrete piles can be caused by a combination of torsion and reflected tensile stress. Diagonal tensile stress resulting from a twisting moment applied to the pile can by itself cause pile failure. However, if reflected tensile stresses occur during driving and they combine with diagonal tensile stress due to torsion the situation can become even more critical. Torsion on the pile may be caused by the following:

1. The helmet or pile cap fitting too tightly on the pile, preventing it from rotating slightly due to soil action on the embedded portion of the pile.

2. Excessive restraint of the pile in the leads and rotation of the leads.

8.8 Summary of Fundamental Driving Stress Considerations

From the preceding discussion some very basic and fundamental considerations have been revealed.

These fundamentals for good design and driving practices for piles and particularly for concrete piles can be summarized as follows:

1. Use adequate cushioning material between the pile driver's ram and the pile head. For concrete piles three or four inches of wood cushioning material (green oak, gum, pine or fir plywood, etc.) may be adequate for short (50 ft or less) piles with reasonably good point soil resistances. Six to eight inches or more of wood cushioning material may be required when driving longer concrete piles in very soft soil. The wood cushioning material should be placed on top of the pile with the grain horizontal and inspected to see that it is in good condition. When it begins to become highly compressed, charred or burned, it should be replaced. Some specifications require a new cushion on

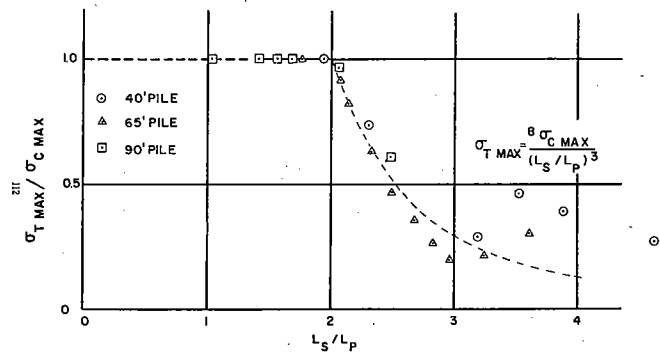


Figure 8.8. Effect of ratio of stress wave length on maximum tensile stress for pile with point free.

every pile. If driving is extremely hard, the cushion may have to be replaced several times during driving of a single pile. Use of an adequate cushion is usually a very economical means of controlling driving stresses.

2. Driving stresses can be reduced by using a heavy ram with a low impact velocity (short stroke) to obtain the desired driving energy rather than a light ram with a high impact velocity (large stroke). Driving stresses are proportional to the ram impact velocity. The maximum compressive stress can be determined approximately by Equations (8.1), (8.2), or (8.3).

3. Reduce the ram velocity or stroke during early driving when light soil resistance is encountered. Anticipate soft driving or at the first sign of easy driving reduce the ram velocity or stroke to avoid critical tensile stresses. This is very effective when driving long concrete piles through very soft soil layers. When the point of the pile is free of resistance, the maximum tensile stress can be determined approximately by using Equations (8.5) or (8.6).

4. If pre-drilling or jetting is permitted in placing concrete piles, ensure that the pile point is well seated with reasonable soil resistance at the point before full driving energy is used. Driving and jetting of concrete piles should not be done simultaneously.

5. Ensure that the pile driving helmet or cap fits loosely around pile top so that the pile may rotate slightly without binding within the driving head to prevent torsional stress.

6. Ensure that the pile is straight and not cambered. High flexural stresses may result during driving of a crooked pile.

7. Ensure that the top of the pile is square or perpendicular to the longitudinal axis of the pile.

8. Cut ends of prestressing or reinforcing steel in concrete piles flush with the end of the pile head to prevent their direct loading by the ram stroke.

9. Use adequate spiral reinforcing at the head and tip of concrete piles to reduce tendency of pile to split or spall.

10. Use adequate amount of prestress in prestressed concrete piles or reinforcement in ordinary precast concrete piles to resist reflected tensile stresses.

11. Chamfer top and bottom edges and corners of concrete piles to reduce tendency of concrete to spall.

CHAPTER IX

Use of the Wave Equation for Parameter Studies

9.1 Introduction

The wave equation can be used effectively to evaluate the effects of the numerous parameters which affect the behavior of a pile during driving. For example: the determination of the optimum pile driver to drive a given pile to a specified soil resistance, the determination of the pile stiffness which will yield the most efficient use of a specified pile hammer and cushion assembly, the determination of the optimum cushion stiffness to make the most efficient utilization of a specified pile hammer and driving assembly to drive a specific pile, and to determine the effects of various distributions of soil side and point resistance on the pile bearing capacity, driving stresses, and penetration per blow.

9.2 Significant Parameters

The parameters which are known to significantly affect the behavior of a pile during driving are as follows:

- (1) The pile driving hammer
 - a. stiffness and weight of the pile driver's ram.
 - b. the energy of the falling ram which is dependent upon the ram weight, the effective drop and the mechanical efficiency of the hammer.
 - c. in the case of a diesel hammer, the weight of the anvil and the impulse of the explosive force.
 - d. the stiffness of the capblock, which is dependent upon its mechanical properties, thickness, cross sectional area, and mechanical conditioning effects caused by repeated blows of the hammer.
 - e. the weight of the pile helmet and the stiffness of the cushion between the helmet and the pile. In the case of steel piles the cushion is usually omitted.
 - f. the coefficient of restitution of the capblock and cushion influence the shape of the wave induced in the pile and hence affects the magnitude of the stresses which are generated.
- (2) The pile
 - a. the length of the pile.
 - b. the stiffness of the pile which is a function of its cross sectional area and the modulus of elasticity of the pile material.
 - c. the weight of the pile, specifically the distribution of the weight.
 - d. the existence of physical joints in the pile which cannot transmit tension.

- (3) The soil
 - a. soil quake at the point.
 - b. soil quake in side friction.
 - c. damping constant of the soil at the point.
 - d. damping constant of the soil in friction.
 - e. distribution of point and side frictional resistance.

9.3 Examples of Parameter Studies

The most notable parameter study which has been reported to date is that presented by Hirsch.^{9.1} In that report, the results of 2,106 problems are presented graphically. This study was oriented toward providing information on the effects of ram weight and energy, stiffness of cushion blocks, length of pile, soil resistance, and distribution of soil resistance on the driving behavior of representative square concrete piles. Figures 9.1 and 9.2 show representative curves from this study. The results of this study have played a very significant part in formulating recommended driving practices for prestressed concrete piles.^{9.2}

Parameter studies of this type have been used by others. McClelland, Focht, and Emrich^{9.3} have used the wave equation to investigate the characteristics of available pile hammers for obtaining pile penetrations sufficient to support the heavy loads required in offshore construction. The parameters varied in this study were the pile length above the mud line, pile penetration, and the ratio of the soil resistance at the pile point to the total soil resistance, (see Figure 9.3 (a)). The results of this study enabled the authors to determine the pile driving limit versus the design load capacity as shown in Figure 9.4 (a) and (b). Figure 9.3 (b) shows the results of one study to determine the effects of varying the unembedded portion of a pile whose total length was held constant. Figure 9.3 (c) is for the same pile, but with the unembedded length held constant and the embedded length varied. Figure 9.3 (d) gives the results when the ratio of point soil resistance to total resistance is varied.

In Research Report 33-10^{9.4} the writers used the wave equation to determine the soil damping values for various soils encountered in field tests. In this particular parameter study the pile, hammer-soil system was held constant and the soil damping values were varied. By generating an ultimate soil resistance, R_u (total) versus blows/in. curve the appropriate soil damping properties could be determined by comparing the computer generated solution with the measured data taken from a full-scale field test pile (see Figure 9.5). This study yielded representative values of the soil damping constants for the soil at the point of the pile and the soil in side friction.

It is not necessary that all parameters for a particular pile installation be known. For example, several

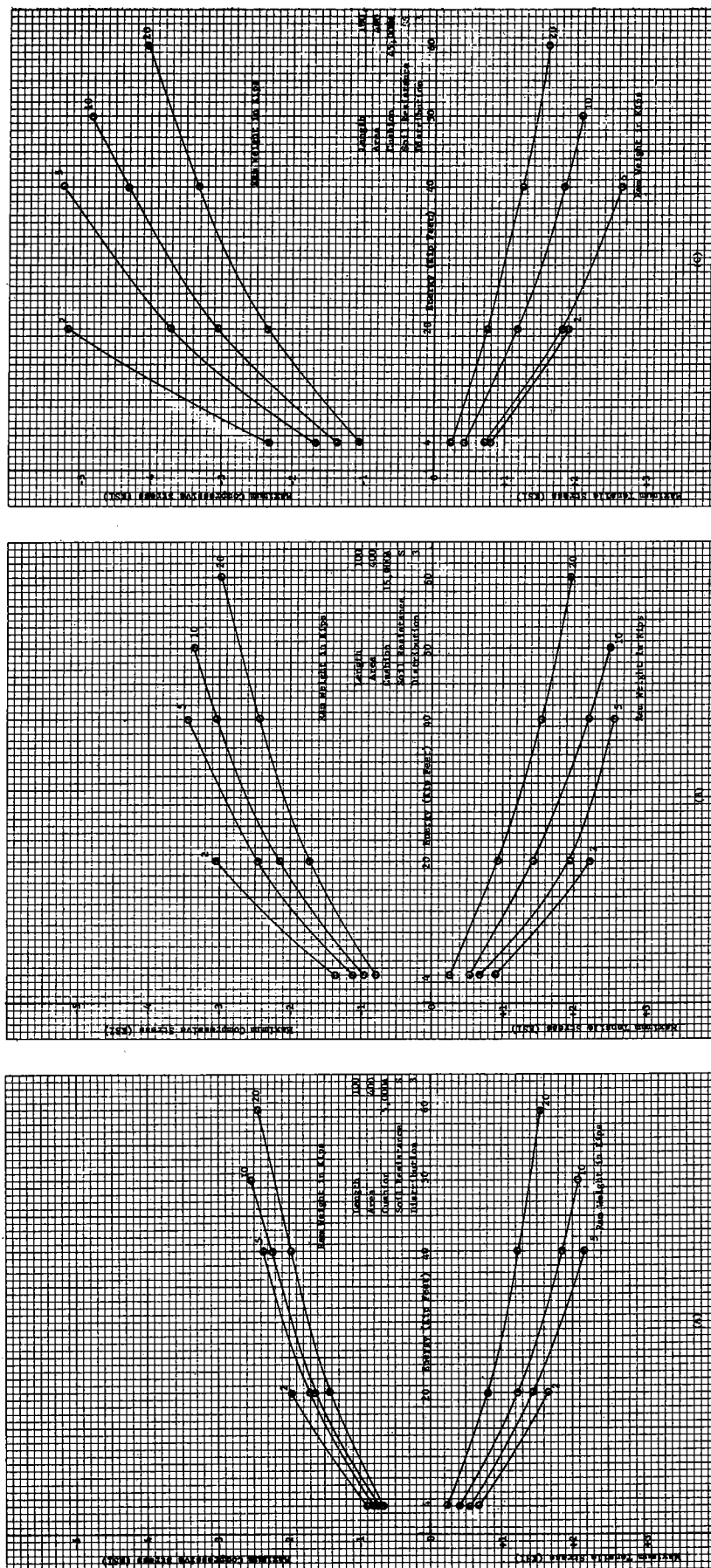


Figure 9.1. Effect of cushion stiffness, ram weight and driving energy on stresses. Square pile with uniformly distributed soil resistance of 107 tons.

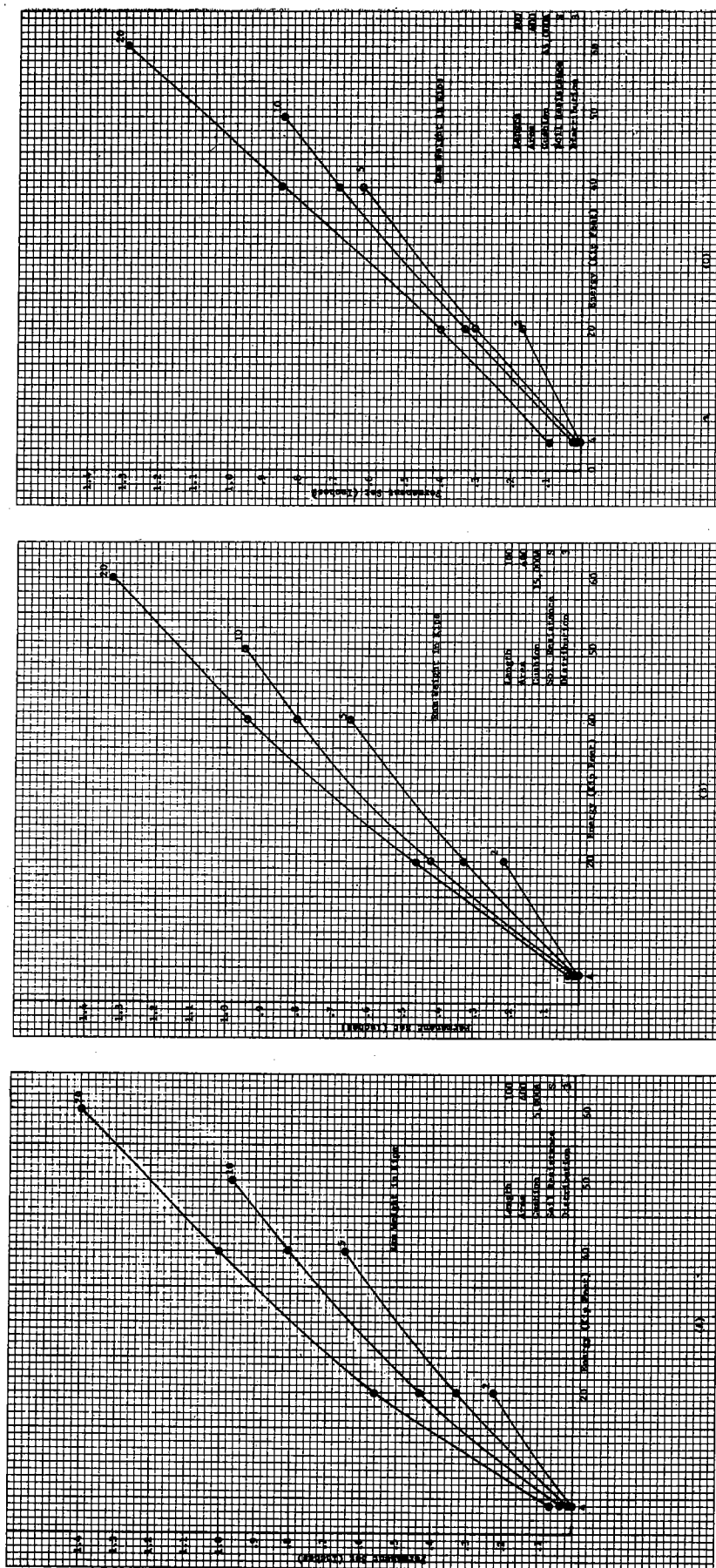


Figure 9.2. Effect of cushion stiffness, ram weight and driving energy on permanent set. Square pile with uniform soil resistance of 107 tons.

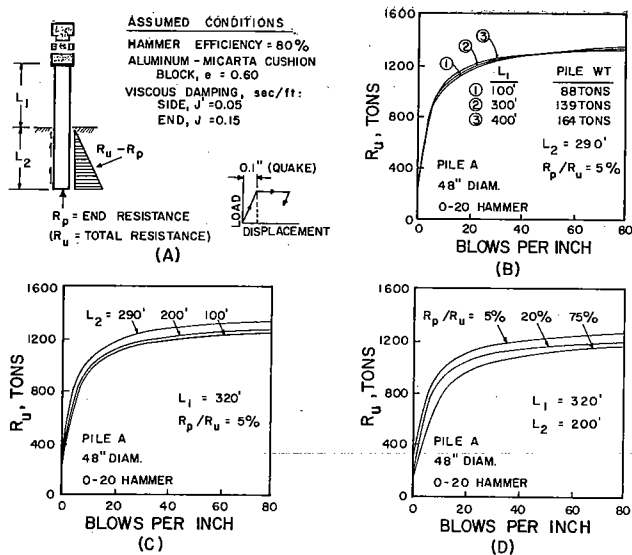


Figure 9.3. Computer analysis of pile hammer effectiveness in overcoming soil resistance, R_u , when driving pile under varying conditions: (A) computer input representing conditions of problem; (B) variations in pile length above ground; (C) variations in pile penetration; (D) variations in distribution of soil resistance, R_u (from Ref. 9.3).

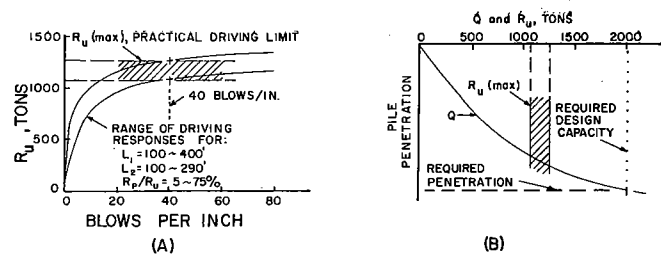


Figure 9.4. Evaluation of 0-20 hammer (60,000 ft-lb) for driving pile to develop ultimate capacity of 2000 tons: (A) summary of wave equation analysis (Fig. 9.3) establishing approximate pile driving limit, R_u (max); (B) comparison of R_u (max) with required design capacity (from Ref. 9.3).

problems can be solved in which the unknown parameter is varied between the upper and lower limits. These limits can usually be established with a reasonable amount of engineering judgement. Parameter studies of this type were conducted by the authors^{9,5} in studies of the effect of ram elasticity and in the correlation and analysis of the Michigan pile data.

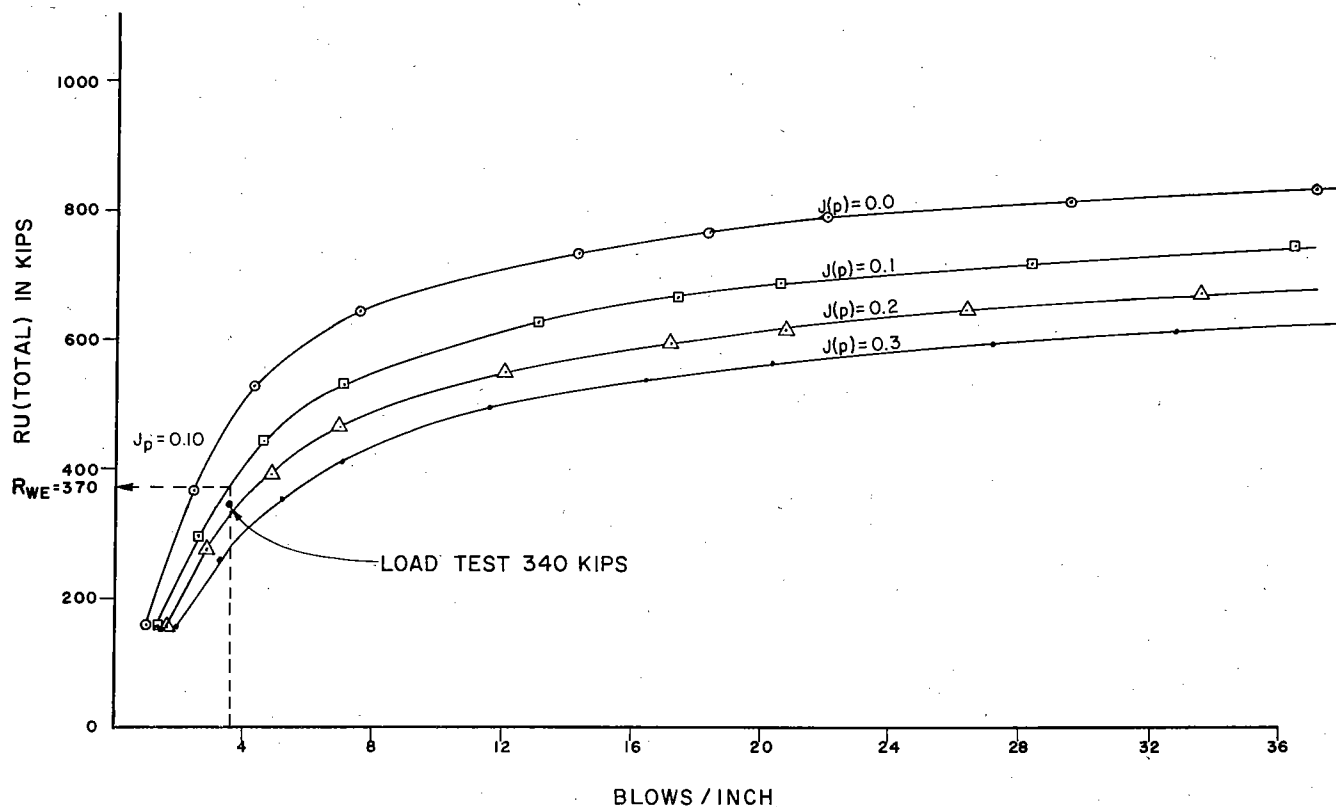


Figure 9.5. Blows/inch vs. R_u (total) for Arkansas load test pile 4.

CHAPTER X

Summary and Conclusions

The numerical computer solution of the one dimensional wave equation can be used with reasonable confidence for the analysis of pile driving problems. The wave equation can be used to predict impact stresses in a pile during driving and can also be used to estimate the static soil resistance on a pile at the time of driving from driving records.

By using this method of analysis, the effects of significant parameters such as type and size of pile driving hammer, driving assemblies (capblock, helmet, cushion block, etc.), type and size of pile, and soil condition can be evaluated during the foundation design stage. From such an analysis appropriate piles and driving equipment can be selected to correct or avoid expensive and time consuming construction problems such as excessive driving stresses or pile breakage and inadequate equipment to achieve desired penetration or bearing capacity.

A thorough discussion of the significant parameters involved in pile driving has been presented in this report. Some of the significant conclusions are as follows:

1. The elasticity of the ram was found to have a negligible effect on the solution in the case of steam, drop, and other hammers in which steel on steel impact between the ram and anvil is not present. However, in the case of diesel hammers, steel on steel impact does occur, and in this case, if the elasticity of the ram is disregarded, a conservative solution for driving stresses and permanent set results. When the elasticity of the ram is accounted for, maximum driving stresses and point displacements may be reduced as much as 20%.

2. Comparisons with the Michigan pile study indicated that a relatively simple yet accurate method of determining the energy output for pile driving hammers can be used. It was determined that for the cases investigated, a simple equation relating energy output for both diesel and steam hammers gave accurate results. This equation is

$$E = (W_R) (h) (e)$$

where

W_R = ram weight,

h = actual observed total ram stroke (or the equivalent stroke for double acting steam hammers and closed end diesel hammers), and

e = efficiency of the hammer in question.

The efficiencies determined during the course of this investigation were 100% for diesel hammers, 87% for double acting steam hammers, and 60% for single acting steam hammers. The writers feel that 60% was unusually low for the single acting hammer and would not recommend it as a typical value. An efficiency of 80% is believed to be more typical for the single acting steam hammer.

3. Comparisons between field test results and the numerical solution of the wave equation proposed by Smith were indeed encouraging. To date, the wave

equation has been compared with the results of thousands of actual field tests performed throughout the country. Among the more significant were the comparisons with the Michigan pile study which dealt almost exclusively with extremely long, slender steel piles, a wide variety of prestressed concrete piles driven in the Gulf Coast area for the Texas Highway Department. Extensive correlation and research has and is being conducted by many contractors, petroleum companies, and others interested in the economical design of pile foundations.

4. The driving accessories significantly affect the piling behavior. For this reason, their selection should be carefully considered and analyzed whenever possible.

5. The effect of explosive pressure in diesel hammers varies greatly depending on the condition and characteristics of the hammer, anvil, helmet, cushion, pile, and soil resistance, especially regarding the increased permanent set per blow claimed by the manufacturer. In general, when the driving resistance is large (which is usually the case near the end of driving) the explosive pressure does not have a large effect on the pile penetration per blow.

6. Three methods were used to determine cushion properties in this report. These included actual full-scale cushion tests dynamically loaded between a ram and pile, tests performed using a cushion test stand in which a ram was dropped on the cushion specimen which had been placed on a concrete pedestal atop a large concrete base embedded in the floor, and finally static tests. It was found that the two dynamic testing methods used yielded almost identical results. It was also found that for a given material, the dynamic curves during the loading of the specimens were almost identical to the corresponding static curves. Static tests can be used to determine cushion stiffness, but not for the coefficient of restitution. Typical properties are presented in Chapter IV.

7. It was shown in Chapter IV that the stress-strain diagrams for the material used as cushions are not linearly related to compression. Instead, the curve is closely parabolic during the loading phase. However, use of the exact load-deformation curve for the cushion is both time consuming and cumbersome, and its use is relatively impractical.

8. It was found that the load-deformation diagram of the cushion could be idealized by a straight line having a slope based on the secant modulus of elasticity of the material.

9. The dynamic coefficient of restitution for the cushion materials studied herein were found to agree generally with commonly recommended values.

10. When the wave equation was compared with the results of laboratory experiments, the numerical solution to the wave equation proposed by Smith was found to be extremely accurate.

11. The effect of internal damping in concrete and

steel piles was found to be negligible for the cases studied, although, if necessary, it can be accurately accounted for by the wave equation.

12. The effect of pile dimensions on ability to drive the pile varied greatly. In general, it was found that the stiffer the pile, the greater soil resistance to penetration it can overcome.

13. The wave equation can be used to estimate soil resistance on a pile *at the time of driving*. Before long-term bearing capacity can be extrapolated from this soil resistance at the time of driving, however, engineers must consider the effect of soil "setup" or possible soil "relaxation" which is a function of time, soil type and condition, and size or type of pile, and other time effects which might be of importance.

APPENDIX A

Development of Equations for Impact Stresses in a Long, Slender, Elastic Pile

A1 Introduction

The study of the behavior of piling has received considerable attention in the past, but only since 1960 when Smith^{1,3} adapted the general theory of stress wave propagation to pile driving problems, was it possible to accurately determine the magnitudes of stress induced in the pile during driving. Smith's method utilized a high-speed electronic digital computer to generate the solution, and while the calculations involved are simple, it can often prove to be an expensive method of solution. Therefore, it is the purpose of this Appendix to develop a series of equations from which a solution to a limited number of piles can be obtained without the use or expense of a computer.

A2 One Dimensional Wave Equation

Unlike a number of other approaches to the problem, wave theory does not involve a formula in the usual sense, but rather is based on the classical, one-dimensional wave equation.

$$\frac{\partial^2 u}{\partial t^2} = c^2 \frac{\partial^2 u}{\partial x^2} \quad (\text{A.1a})$$

where

c = the stress wave velocity = $\sqrt{E/\rho}$,

E = the modulus of elasticity of the pile material,

ρ = the mass density of the pile,

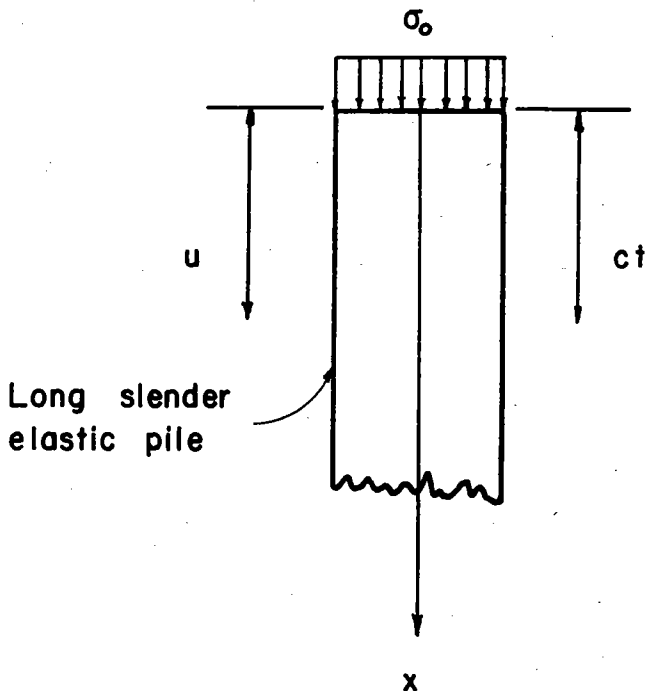


Figure A.1.

u = the longitudinal displacement of a point on the pile in the X-direction, and

t = time.

Figure A1 demonstrates the variables mentioned above.

It has been shown that any function $f(x + ct)$, or $f(x - ct)$ is a solution to the above differential equation. Further, the general solution is given by

$$u = f(x + ct) + f_1(x - ct)$$

From this solution, it can be shown that

$$\sigma = - \frac{E}{c} \frac{du}{dt} \quad (\text{A.1b})$$

where

σ = the stress in the pile.

The negative sign is used to denote compressive stress. Usually an elastic cushion is placed between the pile driving ram and the head of the pile in order to reduce the impact stresses in the pile (Figure A2). The falling ram first strikes the cushion which in turn applies a force to the head of the pile. The sum of the forces on the hammer are given by

$$F_v = W - P = M \frac{d^2 z}{dt^2}$$

where

M = the ram mass,

W = the ram weight,

P = force exerted between the head of the pile and the cushion,

t = time, and

z = displacement of the ram.

This equation can now be written in the form

$$P = M \left(g - \frac{d^2 z}{dt^2} \right) \quad (\text{A.2})$$

where

g = acceleration due to gravity, and

$W = Mg$

Considering the ram as being infinitely stiff, the displacement of the ram, z , and the displacement of the head of the pile u_0 defines the total compression in the cushion at any time. Therefore,

$$\text{Cushion compression} = z - u_0$$

Assuming the cushion to be linearly elastic, with a spring constant of K lb per in., then the cushion compression is given by:

$$\text{Cushion compression} = P/K.$$

Therefore,

$$z = u_0 + \frac{P}{K} \quad (\text{A.3})$$

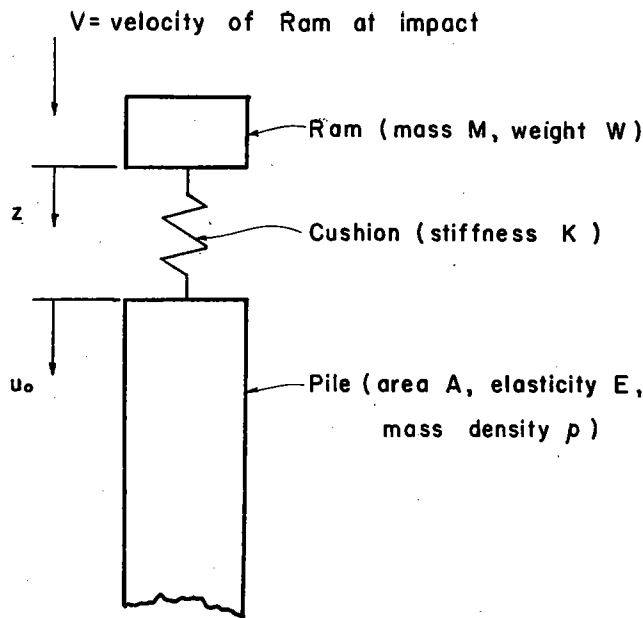


Figure A.2.

Differentiating Equation A.3 with respect to time we find

$$\frac{d^2z}{dt^2} = \frac{d^2u_o}{dt^2} + \left(\frac{1}{K} \right) \frac{d^2P}{dt^2} \quad (A.4)$$

Combining Equation A.2 and A.4 gives

$$P = M \left[g - \frac{d^2u_o}{dt^2} - \frac{1}{K} \frac{d^2P}{dt^2} \right] \quad (A.5)$$

Noting Equation A.1(b) it follows that

$$\sigma_o = - \frac{E}{c} \frac{du_o}{dt} \quad (A.6)$$

where

σ_o = the stress at the pile head, and

u_o = the displacement of the pile head.

Since σ_o equals $-\frac{P}{A}$, where A is the cross-sectional area of the pile, it is seen that

$$P = \frac{AE}{c} \frac{du_o}{dt} \quad (A.7)$$

Differentiating Equation A.7 twice with respect to time gives

$$\frac{d^2P}{dt^2} = \frac{AE}{c} \frac{d^3u_o}{dt^3} \quad (A.8)$$

Substituting Equations A.7 and A.8 into Equation A.5 yields

$$\frac{AE}{c} \frac{du_o}{dt} = M \left[g - \frac{d^2u_o}{dt^2} - \frac{AE}{cK} \frac{d^3u_o}{dt^3} \right]$$

Since V_o is equal to $\frac{du_o}{dt}$, where V_o is the velocity of the head of the pile, it is found that

$$\frac{AEV_o}{c} = M \left[g - \frac{dV_o}{dt} - \frac{AE}{cK} \frac{d^2V_o}{dt^2} \right] \quad (A.9)$$

Equation A.9 may be rewritten in the following form:

$$\frac{Md^2V_o}{dt^2} + \frac{McK}{AE} \frac{dV_o}{dt} + KV_o = \frac{cKMg}{AE} \quad (A.10)$$

which is the basic differential equation to be solved.

A3 Boundary Conditions

In order to satisfy the boundary conditions, it is necessary to set $V_o = 0$ at time $t = 0$. Further, at $t = 0$ we find that

$$\dot{z} = V$$

and

$$\dot{u}_o = 0$$

where V is the initial ram velocity and the dotted quantities denote differentiation with respect to time. From Equation A.3, we see that at $t = 0$,

$$P = K(z - u_o)$$

Differentiating this equation with respect to time, we find

$$\dot{P} = K(\dot{z} - \dot{u}_o)$$

and

$$\dot{P} = KV \text{ at } t = 0$$

From Equation A.7, we note that $P = \frac{AE}{c} V_o$, so that

$$\dot{P} = \frac{AE}{c} \dot{V}_o$$

Therefore, at time $t = 0$,

$$\dot{V}_o = \frac{KVc}{AE}$$

In summary, the boundary conditions at time $t = 0$ are given by Equations A.11 and A.12.

$$V_o = 0 \quad (A.11)$$

$$\dot{V}_o = \frac{KVc}{AE} \quad (A.12)$$

A4 Solving the Basic Differential Equation

The general solution of the differential Equation A.10 is obtained by combining the homogeneous solution V_h , and the particular solution V_p .

The particular solution to Equation A.10 is given by

$$V_p = \frac{cMg}{AE} \quad (A.13)$$

The homogeneous solution to Equation A.10 is determined as follows:

$$\ddot{V}_h + 2n\dot{V}_h + p^2V_h = 0 \quad (A.14)$$

where

$$n = \frac{cK}{2AE} = \frac{K}{2A} \sqrt{\frac{g}{E\rho}}$$

$$p^2 = \frac{K}{M} = \frac{Kg}{W}$$

$$\ddot{V}_h = \frac{d^2 V_h}{dt^2}$$

$$\dot{V}_h = \frac{dV_h}{dt}$$

We shall now investigate solutions for this case having the form

$$V_h = Ae^{mt} \quad (A.15)$$

By substituting Equation A.15 into Equation A.10, we obtain

$$m^2 + 2nm + p^2 = 0$$

and therefore

$$m = -n \pm \sqrt{n^2 - p^2} \quad (A.16)$$

Three possible variations to this solution will now be considered.

CASE I ($n < p$)

The first case is where n is less than p . When n is less than p , the roots of Equation A.17 are given by

$$m = -n \pm i\sqrt{p^2 - n^2}$$

The homogeneous solution to Equation A.11 then becomes

$$V_h = e^{-nt} (A_1 \sin t\sqrt{p^2 - n^2} + A_2 \cos t\sqrt{p^2 - n^2})$$

And the general solution is given by

$$V_o = V_h + \frac{cMg}{AE} \quad (A.17)$$

Applying the boundary conditions noted by Equations A.14 to A.17 we find

$$0 = A_2 + \frac{cMg}{AE}$$

$$A_2 = \frac{-cMg}{AE}$$

Applying the boundary conditions of Equation A.12 to Equation A.17 results in

$$\dot{V}_o = -ne^{-nt}(A_1 \sin t\sqrt{p^2 - n^2} + A_2 \cos t\sqrt{p^2 - n^2}) + e^{-nt}(A_1 \sqrt{p^2 - n^2} \cos t\sqrt{p^2 - n^2} - A_2 \sqrt{p^2 - n^2} \sin t\sqrt{p^2 - n^2})$$

$$\frac{KVc}{AE} = -nA_2 + A_1 \sqrt{p^2 - n^2}$$

$$A_1 = \left[\frac{KVc}{AE} - \frac{ncMg}{AE} \right] \frac{1}{\sqrt{p^2 - n^2}}$$

or

$$A_1 = \frac{c}{AE\sqrt{p^2 - n^2}} [KV - nMg]$$

Rewriting Equation A.17 using the values of A_1 , as noted above, yields

$$V_o = \frac{cKV}{AE\sqrt{p^2 - n^2}} e^{-nt} \sin t\sqrt{p^2 - n^2} + \frac{cMg}{AE} \left[1 - e^{-nt} [\cos t\sqrt{p^2 - n^2} + \frac{n}{\sqrt{p^2 - n^2}} \sin t\sqrt{p^2 - n^2}] \right] \quad (A.18)$$

Substituting Equation A.18 into Equation A.6 gives the final solution for the stress at the head of the pile when the value of n is less than p .

$$\sigma_o = \frac{-KVe^{-nt}}{A\sqrt{p^2 - n^2}} \sin t\sqrt{p^2 - n^2} + \frac{W}{A} \left[1 - e^{-nt} (\cos t\sqrt{p^2 - n^2} + \frac{n}{\sqrt{p^2 - n^2}} \sin t\sqrt{p^2 - n^2}) \right] \quad (A.19)$$

where

$$n = \frac{cK}{2AE} = \frac{K}{2A} \sqrt{\frac{g}{E\gamma}}$$

$$p = \sqrt{\frac{Kg}{W}}$$

Equation A.19 gives the solution for the stress at the head of the pile at all times after impact.

CASE II ($n = p$)

The second case is when n is equal to p in which case the solution of the homogeneous differential equation (Equation A.14) assumes the form

$$V_h = A_1 e^{-nt} + A_2 te^{-nt}$$

$$V_h = e^{-nt} (A_1 + A_2 t) \quad (A.20)$$

The complete solution for this case is given by

$$V_o = V_h + V_p$$

$$V_o = e^{-nt} (A_1 + A_2 t) + \frac{cMg}{AE} \quad (A.21)$$

Substituting the required boundary conditions given by Equation A.11 and A.12, we find that

$$0 = A_1 + \frac{cMg}{AE}$$

$$A_1 = \frac{-cMg}{AE}$$

Using the boundary condition given by Equation A.12, we determine

$$\dot{V}_o = -ne^{-nt} A_1 - ne^{-nt} A_2 t + A_2 e^{-nt}$$

When t is equal to 0, we find that

$$+ \frac{ncMg}{AE} + A_2 = \frac{KVc}{AE}$$

$$A_2 = \frac{KVc}{AE} - \frac{ncMg}{AE}$$

$$A_2 = \frac{c}{AE} (KV - nMg)$$

Rewriting Equation A.21, using the values of A_1 and A_2 , as given above, yields

$$V_o = e^{-nt} \left[\frac{-cMg}{AE} + \frac{ct}{AE} (KV - nMg) \right] + \frac{cMg}{AE} \quad (A.22)$$

Substituting Equation A.22 into Equation A.6 gives

$$\sigma_o = \frac{-t}{A} (KV - nMg) e^{-nt} - \frac{Mg}{A} (1 - e^{-nt})$$

or:

$$\sigma_o = \frac{-t}{A} (KV - nW) e^{-nt} - \frac{W}{A} (1 - e^{-nt}) \quad (A.23)$$

where

$$n = \frac{cK}{2AE} = \frac{K}{2A} \sqrt{\frac{g}{E\gamma}},$$

$$p = \sqrt{\frac{Kg}{W}}, \text{ and}$$

γ = unit weight of pile material

Equation (A.23) gives the compressive stress at the head of the pile, as a function of time for the case when n is equal to p .

CASE III ($n > p$)

The third and final case is where n is greater than p . For this condition, the solution of the homogeneous differential equation, given by Equation (A.14), assumes the form

$$V_h = e^{-nt} [A_1 e^{t\sqrt{n^2 - p^2}} + A_2 e^{-t\sqrt{n^2 - p^2}}]$$

or

$$V_h = e^{-nt} [A_1 \sinh t\sqrt{n^2 - p^2} + A_2 \cosh t\sqrt{n^2 - p^2}]$$

The general solution then becomes

$$V_o = V_h + V_p$$

$$V_o = e^{-nt} (A_1 \sinh t\sqrt{n^2 - p^2} + A_2 \cosh t\sqrt{n^2 - p^2}) + \frac{cMg}{AE} \quad (A.24)$$

Applying the boundary conditions required by Equation A.11 yields

$$0 = A_2 + \frac{cMg}{AE}$$

$$A_2 = \frac{-cMg}{AE}$$

Substituting the required boundary condition given by Equation A.12 then gives

$$\dot{V}_o = -ne^{-nt} (A_1 \sinh t\sqrt{n^2 - p^2} + A_2 \cosh t\sqrt{n^2 - p^2}) + e^{-nt} (A_1 \sqrt{n^2 - p^2} \cosh t\sqrt{n^2 - p^2} + A_2 \sqrt{n^2 - p^2} \sinh t\sqrt{n^2 - p^2})$$

then:

$$\frac{KVc}{AE} = -nA_2 + A_1 \sqrt{n^2 - p^2}$$

and:

$$A_1 = \left[\frac{KVc}{AE} - \frac{ncMg}{AE} \right] \frac{1}{\sqrt{n^2 - p^2}}$$

Rewriting Equation A.24 gives

$$V_o = \frac{KVc}{AE \sqrt{n^2 - p^2}} \sinh t\sqrt{n^2 - p^2} + \frac{cMg}{AE} \left[1 - e^{-nt} (\cosh t\sqrt{n^2 - p^2} + \frac{n \sinh t\sqrt{n^2 - p^2}}{\sqrt{n^2 - p^2}}) \right] \quad (A.25)$$

Substituting Equation A.25 into Equation A.6 gives

$$\sigma_o = \frac{-KV}{A \sqrt{n^2 - p^2}} e^{-nt} \sinh t\sqrt{n^2 - p^2} - \frac{W}{A} \left[1 - e^{-nt} (\cosh t\sqrt{n^2 - p^2} + \frac{n \sinh t\sqrt{n^2 - p^2}}{\sqrt{n^2 - p^2}}) \right] \quad (A.26)$$

where

$$n = \frac{K}{2A} \sqrt{\frac{g}{E\gamma}}, \text{ and}$$

$$p = \sqrt{\frac{Kg}{W}}$$

Equation A.26 gives the stress at the head of the pile as a function of time in the case where n is greater than p .

A5 Maximum Compressive Stress at the Head of the Pile

To compute the maximum compressive stress at the pile head, Equations A.19, A.23, and A.26 are required.

Numerical studies of these equations have shown that if the last term in each equation is omitted, little accuracy is lost, and the expression becomes relatively simple. Since it is necessary to know the time, t , at which the maximum stress occurs, Equations A.19, A.23, and A.26 will be differentiated with respect to time and set equal to 0. This in turn will allow the maximum

stress to be found. The following notations are again used:

$$\begin{aligned} W &= \text{the ram weight (lb)} \\ V &= \text{the ram impact velocity (in./sec)} = \sqrt{2gh} \\ K &= \text{cushion stiffness (lb per in.)} = \frac{A_c E_c}{t_c} \\ t &= \text{time (seconds)} \\ A &= \text{the cross-sectional area of the pile (in.}^2\text{)} \\ E &= \text{modulus of elasticity of the pile (psi)} \\ \gamma &= \text{unit weight of the pile (lb per in.}^3\text{)} \\ g &= \text{acceleration due to gravity (386 in. per sec}^2\text{)} \\ h &= \text{the free fall of the ram (in.)} \\ A_c &= \text{the cross-sectional area of the cushion (in.}^2\text{)} \\ E_c &= \text{the modulus of elasticity of the cushion (psi)} \\ t_c &= \text{cushion thickness (in.)} \\ n &= \frac{K}{2A} \sqrt{\frac{g}{E\gamma}} \\ p &= \sqrt{\frac{Kg}{W}} \end{aligned}$$

In order to further simplify the solutions, the following approximate equations for the maximum compressive stress are presented:

Case 1 (where n is less than p)

$$\sigma_o (\text{max}) = \frac{-KV}{A \sqrt{p^2 - n^2}} e^{-nt} \sin (t \sqrt{p^2 - n^2}) \quad (\text{A.27})$$

where t is given by the equation

$$\tan (t \sqrt{p^2 - n^2}) = \frac{\sqrt{p^2 - n^2}}{n}$$

Case 2 (where n is equal to p)

$$\sigma_o (\text{max}) = - \left[\frac{KV}{nA} - \frac{W}{A} \right] e^{-1} \quad (\text{A.28})$$

where the value of t was given by

$$t = \frac{1}{n}$$

Case 3 (where n is greater than p)

$$\sigma_o (\text{max}) = \frac{-KV}{A \sqrt{n^2 - p^2}} e^{-nt} \sinh (t \sqrt{n^2 - p^2}) \quad (\text{A.29})$$

where t is found from the expression

$$\tanh t \sqrt{n^2 - p^2} = \frac{\sqrt{n^2 - p^2}}{n}$$

Equations A.27, A.28, and A.29 can be used to determine the maximum compressive stress at the head of the pile. In most practical pile problems, n will be less than p , and Equation A.27 will most often be used, although this is not always the case.

For a given pile these equations can be used to determine the proper combination of ram weight, W ,

ram velocity, V , and the required cushion stiffness, K , in order to prevent excessive stresses at the head of the pile. In most cases, there is some minimum amount of driving energy which must be available to drive the pile. For example, the maximum energy output available to a drop hammer is given by its kinetic energy at the instant of impact. Therefore,

$$\text{K.E.} = W \frac{V^2}{2g}$$

should be equal to or greater than the energy required. It would appear that the most efficient way to increase hammer energy would be by increasing the ram velocity V . However, Equations A.27, A.28, and A.29 show that the maximum compressive stress at the head of the pile will increase proportionally with velocity. On the other hand, to increase driving energy the maximum compressive stress at the head of the pile increases slightly as W increases. It is therefore desirable (considering driving stresses) to increase the ram weight, W , if the pile driving situation requires that the driving energy be increased. Once the ram weight and its velocity at impact have been selected, the spring rate of the cushion (K) can be varied to hold the maximum compressive stress within allowable limits.

A6 Length of the Stress Wave

It is known that the magnitude of the reflected stresses in a pile will be a function of the length of the stress wave and the length of the pile. The length of this stress wave is easily found from Equations A.19, A.23, and A.26.

If the last term is again omitted in each of these equations, little accuracy is lost and relatively simple expressions are obtained for the stress at the head of the pile. Omitting the last term in Equation A.19 yields

$$\sigma_o = \frac{-KV}{A \sqrt{p^2 - n^2}} e^{-nt} \sin t \sqrt{p^2 - n^2} \quad (\text{A.30})$$

Equation A.30 is seen to equal 0 at time t equals 0 and again at

$$t = \frac{\pi}{\sqrt{p^2 - n^2}}$$

Thus, the second of these equations gives the duration of the impulse stress.

Noting Equation A.1 a, the stress wave velocity, c , is found to be

$$c = \sqrt{\frac{E}{\rho}}$$

The length of the stress wave, L_s , is then obtained from

$$L_s = ct = \frac{\pi \sqrt{\frac{E}{\rho}}}{\sqrt{p^2 - n^2}}$$

$$L_s = \pi \sqrt{\frac{Eg}{\gamma (p^2 - n^2)}} \text{ for } n < p \quad (\text{A.31})$$

Similarly use Equations A.23 and A.26 to establish that when $n = p$ and $n > p$ the stress wave is infinitely long

$$L_s = \infty$$

APPENDIX B

Wave Equation Computer Program Utilization Manual

B1 Introduction

This appendix describes the utilization of the computer program for the application of the one-dimensional wave equation to the investigation of a pile during driving.

The program can be used to obtain the following information for one blow of the pile driver's ram for any specified soil resistance:

1. Stresses in the pile.
2. Displacement of the pile (penetration per blow).
3. Static load capacity of the pile for specified soil resistance and distribution. This capacity is the static resistance at the time of driving and does not reflect soil set-up due to consolidation.

The program is valuable in that system parameters ignored before (in pile driving formulas) can be included, and their effects investigated. It makes possible an engineering evaluation of driving equipment and pile type, rather than relying only upon experience and judgement.

In order to simulate a given system, the following information is essential:

1. Pile driver.
 - a) energy and efficiency of hammer,
 - b) weight and dimensions of ram,
 - c) weight and dimensions of anvil (if included),
 - d) dimensions and mechanical properties of capblocks,
 - e) weight and dimensions of pile cap helmet,
 - f) and dimensions and mechanical properties of cushion.
2. Dimensions, weight, and mechanical properties of the pile.
3. Soil medium.
 - a) embedment of pile,
 - b) distribution of frictional soil resistance over the embedded length of the pile expressed as a percentage of the total static soil resistance,
 - c) Point soil resistance expressed as a percentage of the total static soil resistance,
 - d) ultimate elastic displacement for the soil on the side and point of pile,
 - e) and the damping constant for the soil on the side and point of the pile.

It should be recognized that the solution obtained with the program represents the results for one blow of

the hammer at the specified soil embedment and soil resistance.

The techniques for idealization can be categorized in three groups:

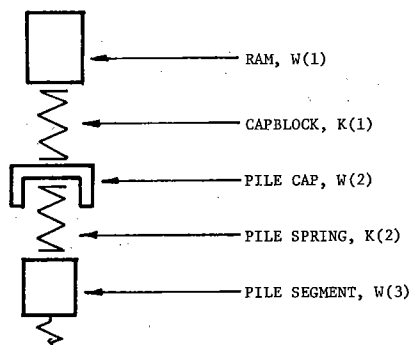
1. the hammer and driving accessories,
2. the pile, and
3. the soil.

B2 Idealization of Hammers

The program is formulated to handle drop hammers, single, double, and differential acting steam hammers and diesel hammers that operate on the head of the pile. The techniques presented in this section are general in scope and are presented for illustration. Appendix B gives the idealizations and pertinent information for the most common hammers.

Figures B1 through B3 describe the idealization for the following cases:

1. Case I — Ram, capblock, pile cap, and pile (Figure B1).
2. Case II — Ram, capblock, pile cap, cushion, and pile (Figure B2).
3. Case III — Ram, anvil, capblock, pile cap, and pile (Figure B3).



Calculations for idealization

$$W(1) = \text{weight of ram, (lb)}$$

$$K(1) = \frac{A(1) E(1)}{L(1)}, \text{ stiffness of the capblock, (lb/in)}$$

Where

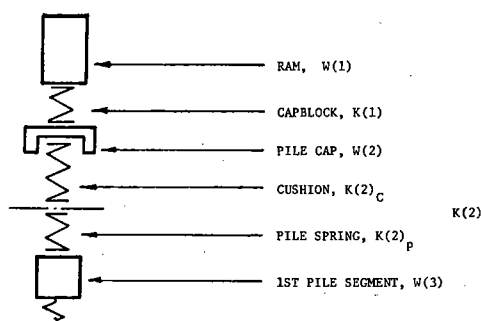
$$A(1) = \text{cross sectional area of the capblock, (in}^2\text{)}$$

$$E(1) = \text{modulus of elasticity of the capblock, (psi)}$$

$$L(1) = \text{thickness of the capblock, (in)}$$

Note: See Table 4.1 for capblock properties.

Figure B.1. Case I—ram, capblock, and pile cap.



Calculations for idealization

$W(1)$ = Weight of ram, (lb)

$K(1)$ = Stiffness of the Capblock, (lb/in.)

$K(2)_C$ = Stiffness of cushion, (lb/in.)

$K(2)_P$ = Stiffness of pile spring, (lb/in.)

$K(2) = \frac{K(2)_C \cdot K(2)_P}{K(2)_C + K(2)_P}$, combined stiffness of $K(2)_C$ and $K(2)_P$ in series.

Note: See Table 4.1 for capblock and cushion properties.

$$K_C = \frac{AE}{L}$$

where

A = cross-section area of cushion, in.²

E = secant modulus of elasticity of cushion material, psi

L = thickness of cushion, in.

Figure B.2. Case II—ram, capblock, pile cap, and cushion.

B3 Ram Kinetic Energies

The kinetic energy of the ram for specific hammer types can be calculated as follows:

1. Drop hammers and single acting steam hammers:

$$E_H = W(1) (h) (e_f) \quad (B.1)$$

where

E_H = ram kinetic energy, (ft-lb)

$W(1)$ = ram weight, (lb)

h = ram stroke, (ft)

e_f = hammer mechanical efficiency (usually between 0.75 and 0.85 for most single acting hammers).

2. Differential and double-acting steam hammers:

$$E_H = h \left[1 + \frac{P_{actual}}{P_{rated}} \cdot \frac{W(h)}{W(1)} \right] W(1) e_f \quad (B.2)$$

where

h = actual ram stroke, (ft)

P_{actual} = actual steam pressure, (psi)

P_{rated} = manufacturers rated steam pressure, (psi)

$W(h)$ = hammer housing weight, (lb)

$W(1)$ = ram weight, (lb)

e_f = efficiency is approximately 85% for these hammers.

3. Diesel hammers:

$$E_H = W(1) (h_e - C) \cdot (e_f) \quad (B.3)$$

where

h_e = actual ram stroke for open-end hammers, and the effective stroke (includes effect of bounce chamber pressure) for closed-end hammers, (ft). The energy E_H for the closed-end Link Belt hammers can be read directly from the manufacturer's chart using bounce chamber pressure),

e_f = efficiency of diesel hammers is approximately 100%

C = distance from bottom-dead-center of anvil to exhaust ports, (ft).

Work done on the pile by the diesel explosive force is automatically accounted for by using an explosive pressure (see Sample Problem and Table 2).

Calculations for idealization

$W(1)$ = weight of ram, (lb)

$K(1) = \frac{A(1) E(1)}{L(1)}$, stiffness of the capblock, (lb/in.)

Where

$A(1)$ = cross sectional area of the capblock, (in²)

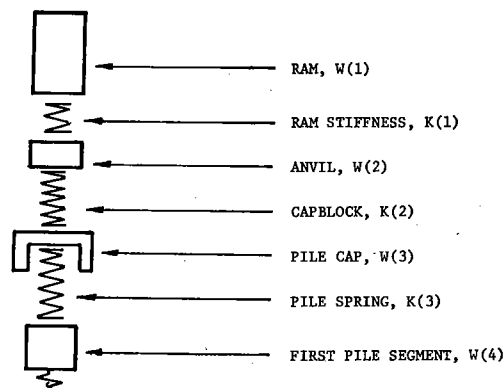
$E(1)$ = modulus of elasticity of the capblock (psi)

$L(1)$ = thickness of the capblock, (in)

Note: See Table 4.1 for capblock properties.

Calculations for idealization

$W(1)$ = Weight of ram, (lb)



Calculations for idealization

$W(1)$ = Weight of ram, (lb.)

$K(1) = \frac{A(1) E(1)}{L(1)}$, the stiffness of the ram, (lb./in.)

where $A(1)$ = ram cross sectional area, (in.)

$E(1)$ = modulus of elasticity of ram material, (psi)

$L(1)$ = length of ram, (in.)

This calculation assumes that the pile cap and anvil are rigid.

Figure B.3. Case III—ram, anvil, capblock, and pile cap.

$K(1)$ = Stiffness of the Capblock, (lb/in.)

$K(2)_c$ = Stiffness of cushion, (lb/in.)

$K(2)_p$ = Stiffness of pile spring, (lb/in.)

$K(2) = \frac{K(2)_c K(2)_p}{K(2)_c + K(2)_p}$, combined stiffness of $K(2)_c$ and $K(2)_p$ in series.

Note: See Table 4.1 for capblock and cushion properties.

$$K_c = \frac{AE}{L}$$

where

A = cross-sectional area of cushion, in.²

E = secant modulus of elasticity of cushion material, psi

L = thickness of cushion, in.

Calculations for idealization

$W(1)$ = Weight of ram, (lb)

$K(1) = \frac{A(1) E(1)}{L(1)}$, the stiffness of the ram, (lb/in.)

where

$A(1)$ = ram cross sectional area, (in.)

$E(1)$ = modulus of elasticity of ram material, (psi)

$L(1)$ = length of ram, (in.)

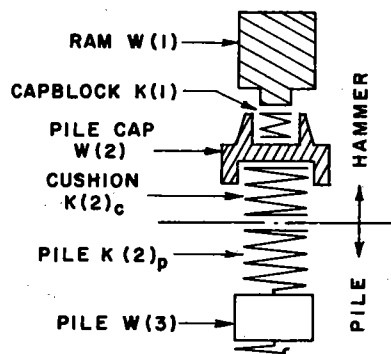
This calculation assumes that the pile cap is rigid.

In the hammer idealization, note that the parts composing the pile driver are physically separated, i.e., the ram is capable of transmitting compressive force to the anvil but not tension. The same is true of the interface between the anvil and pile cap, and the pile cap and the head of the pile. The program contains provisions for eliminating the capability of transmitting tensile forces between adjacent segments. The mechanics of this provision are more fully explained in the following section.

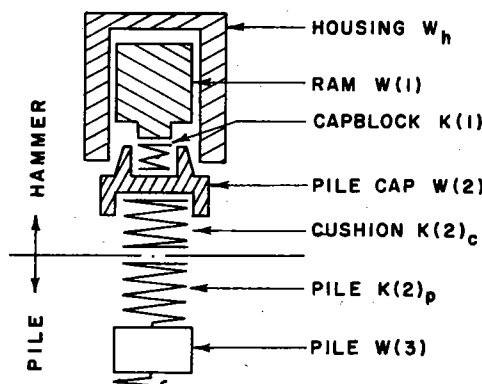
Tables B1 and B2 list the information needed for the simulation of the most common types of pile driving hammers.

B4 Methods of Including Coefficient of Restitution in Capblock and Cushion Springs

In the case where $K(1)$ is a capblock (Cases I, II, and III), and $K(2)$ is a cushion (Case II), it is desirable to include the energy loss due the coefficient of restitution of the particular material.



DROP HAMMERS
SINGLE ACTING STEAM HAMMERS
(A)



DOUBLE AND DIFFERENTIAL ACTING
STEAM HAMMERS
(B)

TABLE B1 DROP HAMMERS AND STEAM HAMMERS

HAMMER	TYPE	W (1) (LB.)	W (2)* (LB.)	W (h) (LB.)	K (1) (LB./IN.)	K (2)c (LB./IN.)	K (2)p (LB./IN.)	STROKE h, (FT.)	Prated (PSI)	EFF. e _f
MKT S3	A	3000	—	—	DEPENDS ON MATERIAL PROPERTIES & DIMENSIONS	DEPENDS ON MATERIAL PROPERTIES & DIMENSIONS	$K(2)_p = \frac{A(2)E(2)}{L(2)}$	3.00	—	0.80
MKT S5	A	5000	—	—				3.25	—	0.80
VULCAN 1	A	5000	1000	—				3.00	—	0.80
VULCAN 2	A	3000	1000	—				2.42	—	0.80
VULCAN 30C	B	3000	1000	4036				1.04	120	0.85
VULCAN 50C	B	5000	1000	6800				1.29	120	0.85
VULCAN 80C	B	8000	2000	9885				1.38	120	0.85
VULCAN 140C	B	14000	—	13984				1.29	140	0.85

* REPRESENTATIVE VALUES FOR PILE NORMALLY USED IN HIGHWAY CONSTRUCTION

In Figure B4 the coefficient of restitution is defined as

$$e = \sqrt{\frac{\text{Area BCD}}{\text{Area ABC}}} = \sqrt{\frac{\text{Energy output}}{\text{Energy input}}} \quad (\text{B.5})$$

In Case II it is necessary to combine springs $K(2)_c$ and $K(2)_p$ to determine the equivalent spring $K(2)$. In this instance it is also necessary to determine the coefficient of restitution of the combined springs. The stiffness of the spring in the restitution phase is the slope of the line DB in Figure B4.

$$K_{DB} = \frac{F_B}{\Delta_C - \Delta_D} \quad (\text{B.6})$$

Since,

$$\text{Energy output} = \text{Area BCD} = F_B (\Delta_C - \Delta_D)/2$$

$$\text{Energy input} = \text{Area ABC} = F_B (\Delta_C)/2$$

$$e^2 = \frac{F_B (\Delta_C - \Delta_D)}{F_B (\Delta_C)} = \frac{\frac{F_B}{\Delta_C}}{\frac{F_B}{(\Delta_C - \Delta_D)}} = \frac{K_{AB}}{K_{DB}}$$

or

$$K_{DB} = \frac{K_{AB}}{e^2} \quad (\text{B.7})$$

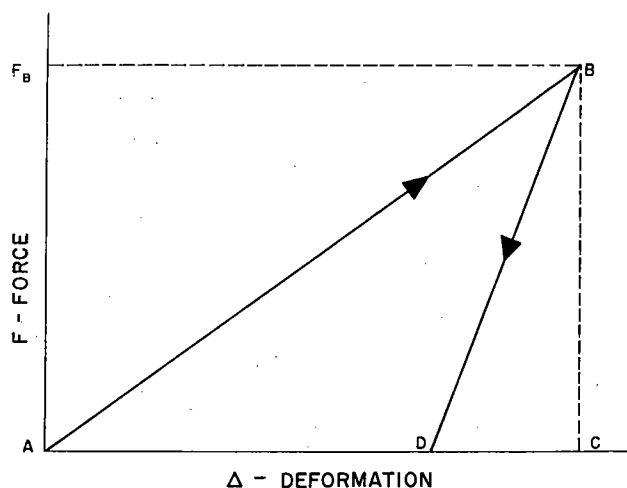
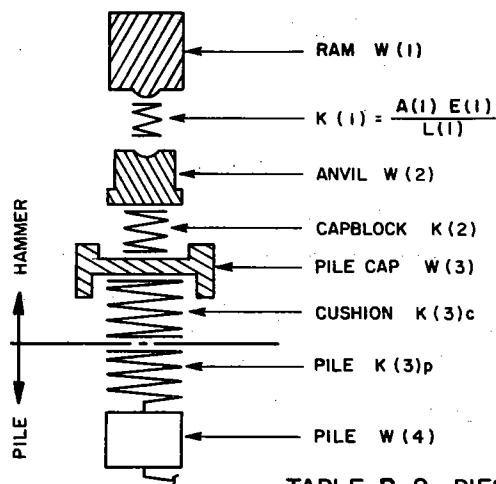


Figure B.4. Definition of coefficient of restitution.

The combined restitution stiffness of $K(2)_c$ and $K(2)_p$ can be determined from,

$$\frac{1}{K(2)} = \frac{1}{K(2)_c} + \frac{1}{K(2)_p} \quad (\text{for restitution phase DB in Figure B4})$$



NOTES FOR TABLE B.2

* for actual stroke use field observations (may vary from 4.0 to 8.0 ft.)

** determine from bounce chamber pressure ($h_g = E/W(1)$ where E = Indicated Energy)

† average values

TABLE B.2 - DIESEL HAMMERS

TYPE HAMMER	W(1) (LB.)	W(2) (LB.)	W(3) [†] (LB.)	K(1) x 10 ⁶ (LB./IN.)	K(2) x 10 ⁶ (LB./IN.)	K(3) _c	K(3) _p	MAX h_g (FT.)	C (FT.)	E_n (FT.-LB.)	EXPLOSIVE FORCE (LB.)	e_f
MKT DE-20	2000	640	1300		14.2	VARIES	$K(3) = \frac{A(3) E(3)}{L(3)}$	8.00*	0.92	$E_n = W(1)(h_g - C)$ DEPENDS ON RAM STROKE h_g	46300	1.00
MKT DE-30	2800	775	690	38.7	63.8			8.00*	1.04		98000	1.00
MKT DE-40	4000	1350	1000		101.0			8.00*	1.16		138000	1.00
DELMAG D 5	1100	330		18.5	13.6			8.00*	0.83		46300	1.00
DELMAG D 12	2750	816		31.5	18.6			8.00*	1.08		93700	1.00
DELMAG D 22	4850	1576		49.7	23.8			8.00*	1.08		158700	1.00
DELMAG D 44	9500	4081		106.2	56.5			8.00*	1.19		200000	1.00
LINK-BELT 180	1724	377	All sq. concrete	44.5	15.5			4.63**	0.64		81000	1.00
LINK-BELT 312	3857	1188	All wood	142.5	18.6			3.87**	0.50		98000	1.00
LINK-BELT 440	4000	705	All H-bearing	138.0	18.6			4.55**	1.25		98000	1.00
LINK-BELT 520	5070	1179	All pipe	108.5	18.6			5.20**	0.83		98000	1.00

from Equation (A-7),

$$\frac{e(2)^2}{K(2)} = \frac{e(2)_c^2}{K(2)_c} + \frac{e(2)_p^2}{K(2)_p}$$

$$e(2)^2 = \frac{K(2)}{K(2)_c K(2)_p} [e(2)_c^2 K(2)_p + e(2)_p^2 K(2)_c]$$

since

$$K(2) = \frac{K(2)_c K(2)_p}{K(2)_c + K(2)_p}$$

$$e(2) = \sqrt{\frac{1}{K(2)_c + K(2)_p} [e(2)_c^2 K(2)_p + K(2)_c e(2)_p^2]}$$

(B.8)

B5 Idealization of Piles

The idealization of the pile is handled by breaking the continuous pile into discrete segments. Each segment is represented by its weight and spring representing the total segment stiffness. In Figure B5, the weight representing the segment is assumed to be concentrated at the end of the segment away from the point of impact. This places the spring on top of the weight whose stiffness it represents, i.e., $K(2)$ is associated with $W(3)$.

Piles should be broken into segments not to exceed approximately 10 feet in lengths, but into not less than five segments. The stiffness of each pile segment spring is calculated from

$$K(m-1) = \frac{A(m) E(m)}{L(m)} \quad (B.9)$$

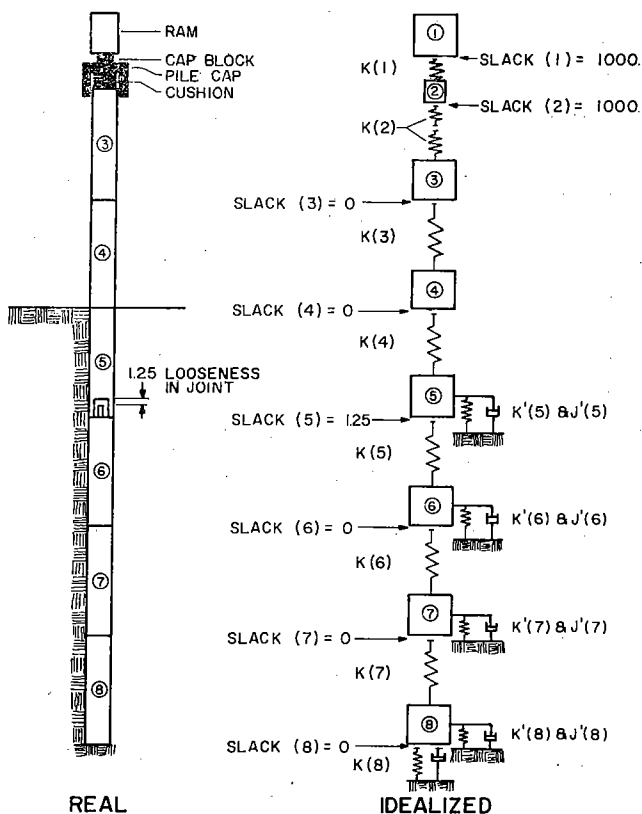


Figure B.5. Pile idealization.

where

$K(m-1)$ = spring stiffness for segment m , (lb/in.)

$A(m)$ = cross sectional area of segment m , (in.²)

$E(m)$ = modulus of elasticity of the material of segment m , (psi)

$L(m)$ = length of segment m , (in.)

The weight of each pile segment is calculated by

$$W(m) = A(m) L(m) \alpha$$

where

α = unit weight of pile material, (lb/in.)

If the pile is tapered, the average value of $A(m)$ should be used.

The program has provisions for handling cases where the physical construction of the pile prohibits the transmission of tensile stresses or is capable of transmitting tensile stresses only after a specified movement of a mechanical joint (joint slack or looseness). These conditions occur with certain types of pile splices. The program provides for this eventuality by entering the following:

- 1) If a joint (a joint is defined as the interface between two segments) can transmit tension, the slack or looseness is entered as SLACK (m) = 0. (Refer to Figure B5)
- 2) If a joint is completely loose, no tension can be transmitted and SLACK (m) should be made a very large number, i.e., SLACK (m) = 1000.0.
- 3) If a joint is capable of moving 1.25 in. before transmitting tension, SLACK (m) = 1.25, i.e., the physical value of the slack or looseness in a joint is entered in inches.

The SLACK (m) values are always associated with spring $K(m)$. In Figure B5, if tension can be transmitted across the interface between segments 3 and 4, the slack value would be associated with spring $K(3)$, i.e., SLACK (3) = 0.

The interfaces between the various parts composing the pile driver (ram, capblock, pile cap, its.) which cannot transmit tension are also handled by setting the SLACK values equal to 1000.

B6 Explanation of Data Input Sheets

Data for the Pile Driving Analysis program is entered on two sheets. Page 1 contains data pertaining to the physical parameters of a particular pile. Page 2 is used to vary the soil, pile driver, or cushion characteristics for the pile described on page 1. Examples of the data sheets follow the explanation.

Page 1

Case No. = Any combination of up to six alphabetic or numerical characters used for identifying information. These characters will identify all problems associated with the pile data entered on sheets 1 and 2.

No. of Probs. = Total number of problems listed on page 2.

1/DELTA T = This space may be left blank in most cases as the program calculates the critical time interval from the parameters of the system. The value calculated is

$$1/\text{DELTA } T = 2(19.698 \sqrt{K/W})$$

If, however, one desires to use a specific 1/DELTA T, it may be entered. The program will then compare the entered value with the critical value calculated by the above formula and use the larger of the two. This is done so that the user cannot inadvertently enter a value too small and hence introduce instability into the numerical process.

P = Total number of weights including ram of hammer, follower, and helmet, etc.

SLACK (1) = This indicates a specified looseness between W(1) and W(2) in inches. This is the amount of movement required before K(1) will take tension. If there is complete tensile freedom of K(1), then enter SLACK (1) = 1000. Leave blank if option 3 is "2".

SLACK (2),

SLACK (3) = see notes on Slack (1).

Option 1 = This is an option for the manual entry of the cross sectional area of each segment.

(a) Enter "1" and all AREAS will automatically be set equal to 1.00. In this case, draw a horizontal line through all AREA rows on the middle portion of page 1. If "1" is used, do not enter areas in AREA rows.

(b) Enter "2" if the cross sectional area of each segment is to be entered manually in the AREA rows. In this case enter AREAS (1) to (P) inclusive.

Option 2 = This is an option for the manual entry of soil resistances.

(a) Enter "2" if the soil resistances (expressed as a percentage of the total soil resistance) are to be entered manually in the RU rows. The RU values are entered from (1) to (P + 1) inclusive. Note that (P + 1) is the point resistance and all others are side resistances. The total of all RU percentages entered must total 100%.

(b) Enter "1" if the soil resistances are not listed in the RU rows but are indicated under Option 12 on page 2.

Option 3 = This is an option for manual entry of the SLACK values.

(a) Enter "1" if SLACK values from SLACK (4) to SLACK (P - 1) are all 0.00 (indicating K(4) to K(P - 1) can take tension). In this case only SLACK (1) to SLACK (3) are entered in row 1. Draw a horizontal line through all SLACK rows in the lower portion of page 1. In this case do not enter any values in the Slack rows.

(b) Enter "2" if SLACK values are to be entered manually. In this case, SLACK (1) to SLACK (3) in row 1 may be left blank.

Option 4 = This is an option on the routine used to simulate the material behavior of springs K(1), K(2), and K(3).

(a) Enter "1" for use of Smith's routine 3 and 4.

(b) Enter "2" for use of Texas A&M's routine.⁴ It is suggested that

Option 4 = 2. Option 4 may be left blank in which case it is automatically set equal to 2.

IPRINT

= This is an option on the amount of data printed out when the long form output is used (Option 15 = 2). If Option 15 = 2, IPRINT is the print interval expressed as the number of time intervals. As an example, if a print out is required every 10th time interval, 10 would be entered for IPRINT. If Option 15 is "1" or "3", leave IPRINT blank.

NSEG 1

= NSEG 1 is the mass number of the first pile segment. If NSEG 1 is left blank, NSEG 1 = 2 will be used by the program.

The total weight of each segment, in pounds, is entered in the rows marked W(2), W(3), . . . W(24). The weights, W's, are entered for 2 to P inclusive. Note that W(1) is not entered as it will be included on page 2.

The spring stiffness of each segment, in lb/in., is entered in the rows marked K(1), K(2), . . . K(24). The stiffnesses, K's, are entered from 1 to P - 1 inclusive. Spring K(P) is the soil spring at the pile tip and is calculated by the program from the soil data entered on Page 2.

If Option 1 = 2, the average area of each segment must be entered in the rows marked A(1), A(2), . . . A(24). The units of A should be consistent with the stress units desired in the output. The basic force unit of the output is the pound. The areas, A's, are entered from 1 to P inclusive. A(P - 1) and A(P) in most instances will be the same. Areas of segments of the hammer are usually entered as A(1) = 1.00, etc., since stress values obtained for these segments are not usually of concern. If Option 1 = 1, the area row should be marked through with a solid horizontal line indicating no data cards are to be included.

If Option 2 = 2, the side soil resistance on each segment, expressed as a percentage of the total soil resistance, is entered in the rows marked RU(1), RU(2), . . . RU(24). The soil resistances, RU's, are entered from 1 to P + 1 inclusive. The value of RU (P + 1) is the pile tip resistance. Mark out all rows when Option 2 = 1.

If Option 3 = 2, the physical slack or looseness, expressed in inches, is entered in each row marked SLACK (1), SLACK (2), . . . SLACK (24). SLACK's are entered from 1 to P - 1 inclusive. If there is no slack, enter 0.0; if there is complete looseness, enter 1000.0. SLACK (P) is automatically set equal to 1000.0 since the point soil spring cannot take tension. If Option 3 = 1, mark out all rows.

Note that the forms have 24 spaces for W's, K's, A's, RU's, and SLACK's. The program is capable of handling a pile with a maximum of 149 segments. Additional cards may be added to each parameter as needed.

Page 2

W(1) = The weight of the pile driver's ram in pounds.

NC = The number of the spring for which K(NC) is being varied.

K(NC) = The spring constant of the spring being varied in lbs/in. Only one spring can take on variable values per case.

EFF = The efficiency of the pile hammer.
 ENERGY = Kinetic energy of the falling ram calculated by Equation B-1, B-2, or B-3.
 ERES (1) = The coefficient of restitution of spring K(1)
 ERES (2) = The coefficient of restitution of spring K(2)
 ERES (3) = The coefficient of restitution of spring K(3)
 RU (TOTAL) = This space should be used only when Option 11 = 2. In this case RU (TOTAL) is the desired ultimate pile resistance in pounds. When Option 11 = 1, leave this entry blank.
 % RU (TOTAL AT POINT) = The percentage of the total pile soil resistance, RU(TOTAL), under the point of the pile. This value is entered as a percentage.
 MO = If Option 12 is "1" or "2", enter the number of the first pile segment acted upon by soil resistance. This space may be left blank if Option 12 = 3, i.e., RU's are read in on page 1.
 Q POINT = Quake of the soil at the point. Normally "0.10" is used.
 Q SIDE = Quake of the soil on the side of the pile. Normally "0.10" is used.
 J POINT = Damping constant for the soil at the point.

J SIDE = Damping constant for the soil on the side of the pile.
 FEXP = The diesel explosive force (in pounds) which acts on the ram and anvil of a diesel hammer. In the case where no explosive force exists, as with drop hammers or steam hammers, leave FEXP blank.
 Option 11 = This option provides for single or multiple calculations.
 (a) Enter "1" if multiple calculations for RU(TOTAL) VS BLOW/IN., data are desired. The computer will assign suitable values of RU (TOTAL). Leave RU(TOTAL) space on page 2 blank.
 (b) Enter "2" if single calculation is to be made with RU(TOTAL) value entered on page 2.
 Option 12 = This option is used for designation of the distribution of side friction on the pile.
 (a) Enter "1" for a uniform distribution of side friction from segment MO to P.
 (b) Enter "2" for a triangular distribution of side friction from segment MO to P.
 (c) Enter "3" if Option 2 = 2, i.e., RU values are entered on page 1.
 Option 13 = This option provides for computer plotted curves using the data gen-

PILE DRIVING ANALYSIS TEXAS A & M UNIVERSITY										OPTIONS				BY: _____ DATE: _____		PAGE # 1 OF 2	
CASE NO.	NO. OF PROBS.	1/DELTA	T	P	SLACK (1)	SLACK (2)	SLACK (3)	AREAS				IPRINT USED WHEN OPTION 13=2	NSEGI	60	70	80	
								1	2	3	4						
LBS.																	
W (1)	W (2)	W (3)	W (4)	W (5)	W (6)	W (7)	W (8)										
W (9)	W (10)	W (11)	W (12)	W (13)	W (14)	W (15)	W (16)										
W (17)	W (18)	W (19)	W (20)	W (21)	W (22)	W (23)	W (24)										
LBS./IN.																	
K (1)	K (2)	K (3)	K (4)	K (5)	K (6)	K (7)	K (8)										
K (9)	K (10)	K (11)	K (12)	K (13)	K (14)	K (15)	K (16)										
K (17)	K (18)	K (19)	K (20)	K (21)	K (22)	K (23)	K (24)										
SQ. IN.																	
AREA (1)	AREA (2)	AREA (3)	AREA (4)	AREA (5)	AREA (6)	AREA (7)	AREA (8)										
AREA (9)	AREA (10)	AREA (11)	AREA (12)	AREA (13)	AREA (14)	AREA (15)	AREA (16)										
AREA (17)	AREA (18)	AREA (19)	AREA (20)	AREA (21)	AREA (22)	AREA (23)	AREA (24)										
%																	
RU (1) %	RU (2) %	RU (3) %	RU (4) %	RU (5) %	RU (6) %	RU (7) %	RU (8) %										
RU (9) %	RU (10) %	RU (11) %	RU (12) %	RU (13) %	RU (14) %	RU (15) %	RU (16) %										
RU (17) %	RU (18) %	RU (19) %	RU (20) %	RU (21) %	RU (22) %	RU (23) %	RU (24) %										
INCHES																	
SLACK (1)	SLACK (2)	SLACK (3)	SLACK (4)	SLACK (5)	SLACK (6)	SLACK (7)	SLACK (8)										
SLACK (9)	SLACK (10)	SLACK (11)	SLACK (12)	SLACK (13)	SLACK (14)	SLACK (15)	SLACK (16)										
SLACK (17)	SLACK (18)	SLACK (19)	SLACK (20)	SLACK (21)	SLACK (22)	SLACK (23)	SLACK (24)										

NOTES: ONE OR MORE PROBLEMS MUST BE LISTED ON PAGE 2

W's AND AREAS 1 TO P INCL.; K's AND SLACK'S 1 TO P-1 INCL.; RU'S 1 TO P+1 INCL. (P+1 IS % RU UNDER POINT OF PILE.)

erated for RU(TOTAL) VS BLOW/IN. (Option 11 = 1).

(a) Enter "1" for computer plot of data. If no plot is desired, leave blank.

Option 14 = This is used to include or exclude gravity in the calculations.

(a) Enter "1" if the forces of gravity are to be included in the calculations.

(b) Enter "2" if the forces of gravity are to be excluded from the calculation. This alternate in effect excludes the weight of the pile from the calculations. It is used when the pile driver is in a horizontal position or for an extreme batter.

Option 15 = This option provides for versatility in the output format.

(a) Enter "1" for a normal data printout.

(b) Enter "2" for extra detail in printout. This alternate gives pertinent stresses, deformations, velocities, etc., at the print interval, specified as IPRINT on page 1.

(c) Enter "3" for short output. This alternate gives only a tabular summary of BLOW/IN. VS RU(TOTAL). Option 15 = 3 should be used only when Option 11 = 2.

SPECIAL NOTE Where anything listed for Problem 1 is to be repeated for Problem 2, 3, etc., draw an arrow down through the last problem to indicate repetition.

B7 Comments on Data Input

On page 2 of the input forms, provisions are made for varying the stiffness of any spring, K(1) through K(P - 1), in the hammer or pile idealization. This is accomplished by entering the number of the spring to be changed in the NC column and then the stiffness of spring K(NC) in the K(NC) column. As soon as this problem is completed, the spring stiffnesses, K(NC) will be reset automatically to the value on page 1 of the input forms.

The program is capable of handling pile idealizations with a maximum of 149 segments. There is no limit on the number of problems that can be run for each case.

Sample Problem

Consider the pile shown in Figure B-6.

Pile: 16 in. square prestressed concrete pile, 26 ft in length. The modulus of the concrete is 7.82×10^6 psi and its unit weight is 154 lb/ft³. The pile is assumed to be embedded for its full length.

Pile hammer: Hypothetical diesel hammer with 4850 lb ram with an input ram kinetic energy of 39,800 ft lb. The explosive force produced by the diesel fuel is 158,700 lb. The stiffness of the ram is given as 42.25×10^6 lb/in. The anvil is assumed rigid and weighs 1150 lb. The capblock stiffness is 24.5×10^6 lb/in.

PILE DRIVING ANALYSIS TEXAS A&M UNIVERSITY															BY :	DATE :	PAGE # 2 OF 2
PROB	W(I) POUNDS	NC	K(NC) POUNDS/INCH	EFF.	ENERGY	ERES (1)	ERES (2)	ERES (3)	RU (TOTAL) POUNDS	% AT POINT	MO	Q POINT	Q SIDE	J POINT	J SIDE	FEXP	OPTIONS 11 12 13 14 15
1																	
2																	
3																	
4																	
5																	
6																	
7																	
8																	
9																	
10																	
11																	
12																	
13																	
14																	
15																	
16																	
17																	
18																	
19																	
20																	

NOTE: IF OPTION #11 = 1, RU(TOTAL) NOT REQUIRED

NO OF CALCULATIONS
RESISTANCE
PLOT
GRAVITY
PRINT OUT

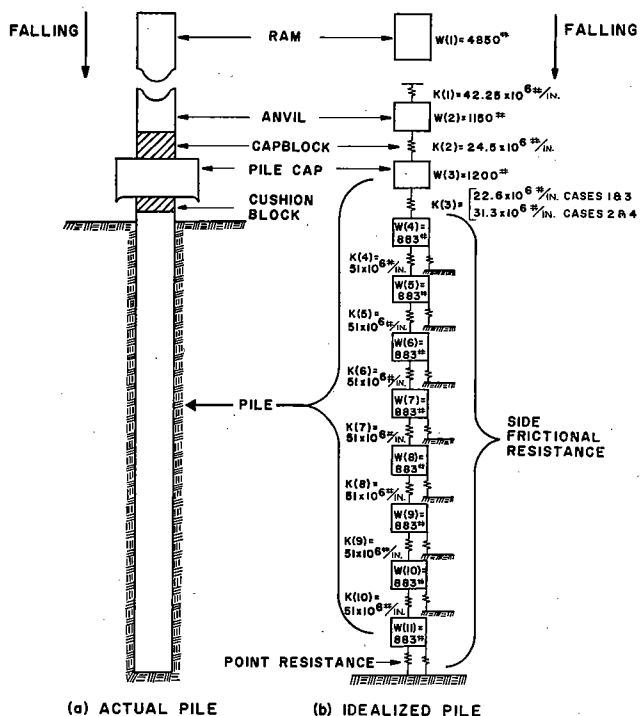


Figure B.6. Sample problem.

In order to illustrate the utilization of the input data sheets and explain the output data sheets, four problems are considered.

Problem 1 and Problem 2 are concerned with the driving effects produced by two different cushions. The object of these two cases is to determine the dynamic-static resistance curves (RU(TOTAL) VS BLOWS/IN.) for one blow of the hammer. In Problem 1, the cushion is assumed to have a cross sectional area equal to that of the pile, is $6\frac{1}{4}$ in. thick and has a modulus of elasticity of 1.0×10^6 psi. In Problem 2 the cushion area and properties are the same as in Problem 1, but the thickness is $3\frac{1}{8}$ in. In Problem 1 and 2 the soil side friction is assumed to have a triangular distribution with 10% point resistance. The soil constants are:

- (a) $Q = Q' = 0.10$ in.
- (b) $J = 0.15$ sec./ft.
- (c) $J' = 0.05$ sec./ft.

Problems 3 and 4 illustrate the use of program to investigate the penetration of a pile to 200 tons of static soil resistance produced by one blow of the hammer. In Problem 3 the soil resistance is distributed uniformly along the side with 10% at the point. The cushion is the same as in Case 1. In Problem 4 the soil has a triangular distribution along the side with 10% soil resistance (same as Problem 2). The cushion is the same as in Problem 2. Problem 4 will also illustrate the use of the output option (OPTION 15).

The following calculations illustrate the computations for the hammer and pile idealization.

- (a) Pile: The pile is broken into eight equal length segments of 39 in. The spring stiffness for each segment is,

$$K(3)_p = \frac{A(3)_p E(3)_p}{L(3)_p}$$

where

$$A(3)_p = 254 \text{ in.}^2$$

$$E(3)_p = 7.32 \times 10^6 \text{ psi}$$

$$L(3)_p = 39 \text{ in.}$$

therefore

$$K(3)_p = \frac{(254)(7.32 \times 10^6)}{39} = 51.0 \times 10^6 \text{ lb/in.}$$

- (b) Cushion: Spring K(3) in Figure B6 (b) represents the combined stiffness of the cushion and first pile segment.

In Problem 1 and 3

$$K(3)_c = \frac{A(3)_c E(3)_c}{L(3)_c}$$

where

$$A(3)_c = 254 \text{ in.}^2$$

$$E(3)_c = 1.00 \times 10^6 \text{ psi}$$

$$L(3)_c = 6.25 \text{ in.}$$

then

$$K(3)_c = \frac{(254)(1 \times 10^6)}{6.25} = 40.5 \times 10^6 \text{ lb/in.}$$

The combined stiffness of $K(3)_c$ and $K(3)_p$ is

$$K(3) = \frac{K(3)_c \times K(3)_p}{K(3)_c + K(3)_p} = \frac{(40.5)(51.0)(10^6)}{(40.5 + 51.0)(10^6)}$$

$$K(3) = 22.6 \times 10^6 \text{ lb/in.}$$

The coefficient of restitution for the combined springs is assumed to be 0.50.

For Problem 2 and 4 similar calculation yields

$$K(3) = 31.3 \times 10^6 \text{ lb/in.}$$

The output data sheets are completed as follows:

Page 1 (Same for all 4 problems)

No. of Problems = 4, there are 4 problems to be solved on page 2.

1/DELTA T = 0.0, since the program will calculate the correct value.

P = 11, there are 11 weights (3 for the hammer and 8 for the pile).

SLACK'S = all set equal to 1000 since there is complete looseness between the ram, anvil, capblock, pile cap, cushion, and pile head.

OPTION 1 = 2, all areas are entered manually in AREA rows.

OPTION 2 = 1, since OPTION 12 is used to describe the soil distribution.

OPTION 3 = 1, all pile segments are connected, hence SLACK (4) to SLACK (10) = 0.0.

OPTION 4 = left blank since it is desired to use the A&M routine.

IPRINT = 10, in Problem 4, OPTION 15 = 2, it is desired to print output every 10 iterations.

NSEG1 = 4, the first pile segment, see Figure B6 (b).

W'S = enter the weight of each element in lb. Note that W(1) is blank since it will be entered on page 2.

K'S = enter all spring stiffnesses for the pile system considered to be basic, i.e., the program will automatically reset the stiffnesses to these values after each problem on page 2.

A'S = enter all cross sectional areas of pile segments only.

Page 2—Problem 1

W(1) = 4850 lb., the ram weight.

NC = 3, the cushion spring number, see Figure B6 (b).

K(NC) = K(3) = 22,500,000, the stiffness of the combined springs.

EFF = 1.00, diesel hammers are considered to be 100% efficient.

ENERGY = 39,800, the input energy for this particular hammer blow.

ERES(1) = 0.60, coefficient of restitution of steel on steel impact.

ERES(2) = 0.80, coefficient of restitution of cap-block material.

ERES(3) = 0.50, coefficient of restitution of combined cushion and first pile spring.

RU(TOTAL) = leave blank, since OPTION 11 = 1, i.e., the program will generate suitable values for curve generation.

% AT POINT MO = 10%.

MO = 4, the first pile segment with side soil resistance.

QPOINT = 0.10, Q.

QSIDE = 0.10, Q'.

JPOINT = 0.15, J.

JSIDE = 0.05, J'.

FEXP = 158,700, lb. the diesel explosive force.

OPTION 11 = 1, for program generated RU(TOTAL) VS BLOWS/IN. curve.

OPTION 12 = 2, for triangular side soil resistance distribution.

OPTION 13 = leave blank since computer plotted curve is not desired.

OPTION 14 = 1, to indicate gravity.

OPTION 15 = 1, for normal data output.

Page 2, Problem 2

Only the value of K(3), is changed.

NC = 3

K(NC) = 31,300,000.

K(3) = 3.

Page 2, Problem 3

The value of K(3) and the OPTIONS are changed.

NC = 3.

K(NC) = K(3) = 22,500,000.

RU(TOTAL) = 400,000 lb for a 200 ton total static soil resistance.

OPTION 11 = 2, for single calculation using RU (TOTAL) = 400,000.

OPTION 12 = 1, for uniform side soil resistance distribution.

Page 2, Problem 4

In this problem the cushion and the options are changed.

NC = 3

K(NC) = K(3) = 31,300,000

OPTION 12 = 2, for triangular side soil resistance distribution.

OPTION 15 = 2, for output at interval expressed by IPRINT on page 1.

PILE DRIVING ANALYSIS TEXAS A & M UNIVERSITY										OPTIONS				BY: <i>A. Aggie</i> DATE: <i>8/2/67</i>		PAGE #1 OF 2	
CASE NO.	NO. OF PROBS	I/DELTA	T	P	SLACK (1)	SLACK (2)	SLACK (3)	AREAS				PRINT USED WHEN OPTION 15=2	NSEG	TO	BO		
								1	2	3	4						
4PS 10 4		0.0		11	1000	1000	1000	211	110	4							
LBS.																	
W (1)	W (2)	W (3)	W (4)	W (5)	W (6)	W (7)	W (8)										
1150	1200	883	883	883	883	883	883										
W (9)	W (10)	W (11)	W (12)	W (13)	W (14)	W (15)	W (16)										
883	883	883															
W (17)	W (18)	W (19)	W (20)	W (21)	W (22)	W (23)	W (24)										
LBS./IN.																	
K (1)	K (2)	K (3)	K (4)	K (5)	K (6)	K (7)	K (8)										
42200000	24500000	22600000	51000000	51000000	51000000	51000000	51000000										
K (9)	K (10)	K (11)	K (12)	K (13)	K (14)	K (15)	K (16)										
51000000	51000000																
K (17)	K (18)	K (19)	K (20)	K (21)	K (22)	K (23)	K (24)										
SQ. IN.																	
AREA (1)	AREA (2)	AREA (3)	AREA (4)	AREA (5)	AREA (6)	AREA (7)	AREA (8)										
1.0	1.0	254	254	254	254	254	254										
AREA (9)	AREA (10)	AREA (11)	AREA (12)	AREA (13)	AREA (14)	AREA (15)	AREA (16)										
254	254	254															
AREA (17)	AREA (18)	AREA (19)	AREA (20)	AREA (21)	AREA (22)	AREA (23)	AREA (24)										
% RU																	
RU (1) %	RU (2) %	RU (3) %	RU (4) %	RU (5) %	RU (6) %	RU (7) %	RU (8) %										
RU (9) %	RU (10) %	RU (11) %	RU (12) %	RU (13) %	RU (14) %	RU (15) %	RU (16) %										
RU (17) %	RU (18) %	RU (19) %	RU (20) %	RU (21) %	RU (22) %	RU (23) %	RU (24) %										
INCHES																	
SLACK (1)	SLACK (2)	SLACK (3)	SLACK (4)	SLACK (5)	SLACK (6)	SLACK (7)	SLACK (8)										
SLACK (9)	SLACK (10)	SLACK (11)	SLACK (12)	SLACK (13)	SLACK (14)	SLACK (15)	SLACK (16)										
SLACK (17)	SLACK (18)	SLACK (19)	SLACK (20)	SLACK (21)	SLACK (22)	SLACK (23)	SLACK (24)										

NOTES: ONE OR MORE PROBLEMS MUST BE LISTED ON PAGE 2

W'S AND AREAS 1 TO P INCL.; K'S AND SLACK'S 1 TO P-1 INCL.; RU'S 1 TO P+1 INCL. (P+1 IS % RU UNDER POINT OF PILE.)

PILE DRIVING ANALYSIS TEXAS A&M UNIVERSITY					BY : A. Aggie		DATE : 8/31/67		PAGE # 2 OF 2								
PROB	W(I) POUNDS	N C	K(NC) POUNDS/INCH	EFF.	ENERGY	ERES (1)	ERES (2)	ERES (3)	RU (TOTAL) POUNDS	% AT POINT	MO	Q POINT	Q SIDE	J POINT	J SIDE	FEXP	OPTIONS 11 12 13 14 15
1	4850.	3	22500000	100	3980000	0.60	0.80	0.50		10		40100	100	15005		158706	12 11
2			31300000														12 11
3			22500000						400000								21 11
4			31300000						400000								22 12
5																	
6																	
7																	
8																	
9																	
10																	
11																	
12																	
13																	
14																	
15																	
16																	
17																	
18																	
19																	
20																	

NOTE: IF OPTION #11 = 1, RU(TOTAL) NOT REQUIRED

NO. OF CALCULATIONS
RESISTANCE
PLOT
GRAVITY
PRINT OUT

The output for the four sample problems are shown in Figures B7 through B-11. Figure B7 is the output for one point on the RU(TOTAL) VS BLOWS/IN. curve generated for Problem 1. The block of data on the upper part of the figure is a printout of the input

data. The RU(TOTAL) value of 1,040,962.1 is the total static soil resistance for which this problem was run. This value was generated by the program and is only one point of 10 used to develop the data for the total RU(TOTAL) VS BLOWS/INCH curve shown in

TEXAS A * M UNIVERSITY										PILE DRIVING ANALYSIS										CASE NO.HSP 10										PROBLEM NO. 1 OF 4									
1/DELTA T P OPTIONS										1 2 3 4 11 12 13 14 15										EXP. FORCE																			
9443.9 11										2 1 1 2 0 1 1										158700.																			
ENERGY HAMMER EFFICIENCY										RU(TOTAL) PERCENT UNDER POINT MO Q(POINT) Q(SIDE) J(POINT) J(SIDE) N2																													
39800.00 1.00										1040962.1 10.0 4 0.10 0.10 0.15 0.05 125																													
M	W(M)	K(M)	AREA(M)	RU(M)	SLACK(M)	ERES(M)	VSTART(M)	KPRIME(M)																															
1	4850.000	0.4220000E 08	1.000	0.0	1000.000	0.60	22.99	0.0																															
2	1150.000	0.2450000E 08	1.000	0.0	1000.000	0.80	0.0	0.0																															
3	1200.000	0.2250000E 08	254.000	0.0	1000.000	0.50	0.0	0.0																															
4	883.000	0.5100000E 08	254.000	14638.531	0.0	1.00	0.0	0.1463853E 06																															
5	883.000	0.5100000E 08	254.000	43915.594	0.0	1.00	0.0	0.4391561E 06																															
6	883.000	0.5100000E 08	254.000	73192.625	0.0	1.00	0.0	0.7319265E 06																															
7	883.000	0.5100000E 08	254.000	102469.687	0.0	1.00	0.0	0.1024697E 07																															
8	883.000	0.5100000E 08	254.000	131746.750	0.0	1.00	0.0	0.1317467E 07																															
9	883.000	0.5100000E 08	254.000	161023.812	0.0	1.00	0.0	0.1610238E 07																															
10	883.000	0.5100000E 08	254.000	190300.875	0.0	1.00	0.0	0.1903009E 07																															
11	883.000	0.1040962E 07	254.000	219577.937	1000.000	1.00	0.0	0.2195780E 07																															
12	-0.0	-0.0	-0.0	104096.125	-0.0	-0.0	-0.0	0.0																															

SEGMENT	AREA	TIME N	MAX C. STRESS	TIME N	MAX T. STRESS	DMAX(M)	DM(M)	V(M)
1	1.000	4	2883699.	0	-0.0	0.487338	0.486179	-0.50
2	1.000	7	2245092.	0	-0.0	0.430214	0.430214	4.07
3	254.000	11	7432.	42	-0.0	0.359616	0.359616	-1.17
4	254.000	13	7324.	0	-0.0	0.238627	0.223646	-3.80
5	254.000	15	7107.	0	-0.0	0.231331	0.211913	-1.14
6	254.000	17	6883.	0	-0.0	0.215890	0.204061	0.57
7	254.000	19	6633.	34	1.	0.203751	0.198904	-2.68
8	254.000	21	6344.	34	172.	0.190195	0.188150	-2.55
9	254.000	23	5834.	29	1973.	0.182027	0.174308	0.39
10	254.000	35	4195.	30	2491.	0.172878	0.168807	-0.03
11	254.000	27	1320.	0	-0.0	0.167608	0.166761	-1.43
PERMANENT SET OF PILE = 0.06760806 INCHES								
NUMBER OF BLOWS PER INCH = 14.79113579								
TOTAL INTERVALS = 49								

Figure B.7. Normal output (option 15=1) for Prob. 1.

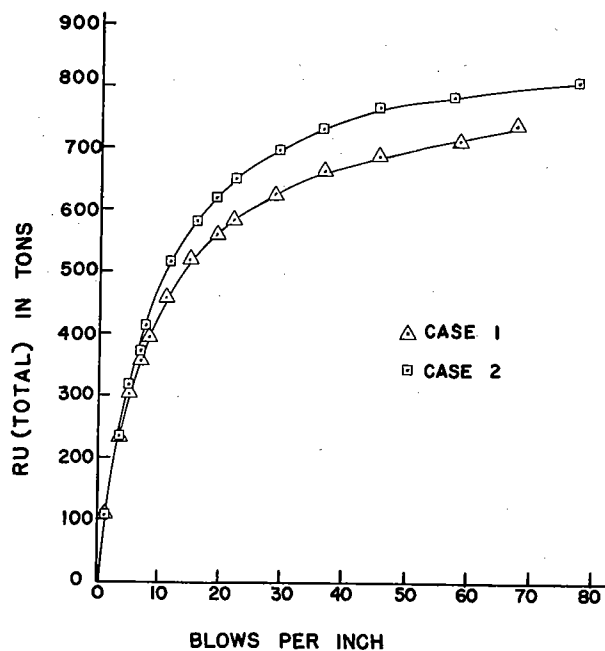


Figure B.8. Effect of varying cushion stiffness.

Figure B8. The second block of data shows the maximum compressive and tensile stresses and the maximum displacement of each segment. The column labeled TIMEN is the time interval at which the maximum compressive stress (MAX C STRESS) occurred, i.e., the maximum compressive stress of 7432 psi occurred in segment 5 at time interval 11 (11/9443.9 sec.). Similar

data is printed for each point on the RU(TOTAL) VS BLOWS/IN. shown in Figure B8.

Figure B9 shows the summary of the data for the RU(TOTAL) VS BLOWS/IN. for Problems 1 and 2. Data of this type can be used to construct curves like that shown in Figure B8. These curves can be used to compare the effects of cushion stiffness (the cushion stiffness, $K(3)_0$, in Problem 2 was twice that in Problem 1). Note the stiffer cushion (Problem 2) produces the most efficient driving since for a specified resistance the penetration per blow is larger (BLOWS/IN. is smaller).

Figure B-10 is a typical output when RU(TOTAL) is specified. The maximum penetration of the point of the pile under one blow of the hammer is 0.473011 in., listed under DMAX(M), and the permanent set is 0.473011-0.100000 (the ground quake Q) or 0.373011 in. Note that the input data is listed as well as the maximum stresses and the displacement of each segment.

Figure B-11 is a sampling of the output when data is desired at some specified interval (OPTION 15 = 2, IPRINT = 1). The input information is listed in the first block of data. The next two blocks show the stresses at time interval N = 0 and N = 1. The data is defined as follows:

- D(M) = displacement of each mass point, (in.),
- C(M) = the compression in each spring, (in.),
- STRESS(M) = stress in each segment, (psi),
- F(M) = force in each spring, (lb),
- R(M) = force in each soil spring, (lb),
- W(M) = weight of each segment, (lb),
- V(M) = velocity of each segment, (fps),
- DPRIME(M) = elastic displacement of soil, (in.),

PILE DRIVING ANALYSIS				CASE NUMBER	HSP 10	PROBLEM NUMBER		
QPOINT = 0.10				JPOINT = 0.15				
BLCWS PER	IN.	RUTOTAL	POINT FORCE	MAX C STRESS	SEG	MAX T STRESS	SEG	
1.0733	213593.-	107.T	92981.	7321.	4	4411.	10	
3.3072	462346.-	231.T	185557.	7322.	4	3706.	10	
4.9401	601539.-	301.T	232773.	7322.	4	3358.	10	
6.6525	708095.-	354.T	266561.	7323.	4	3112.	10	
8.1351	785875.-	393.T	285066.	7323.	4	2955.	10	
10.7809	917031.-	459.T	312727.	7324.	4	2708.	10	
14.7911	1040962.-	520.T	335193.	7324.	4	2491.	10	
18.8100	1118220.-	559.T	350215.	7324.	4	2362.	10	
21.5075	1166279.-	583.T	359397.	7324.	4	2285.	10	
28.2780	1255360.-	628.T	375508.	7325.	4	2148.	10	
36.2405	1321145.-	661.T	386685.	7325.	4	2051.	10	
44.9512	1371145.-	686.T	394790.	7325.	4	1981.	10	
58.1772	1421145.-	711.T	402573.	7325.	4	1908.	10	
67.8860	1471145.-	736.T	410044.	7325.	4	1836.	10	

PILE DRIVING ANALYSIS				CASE NUMBER	HSP 10	PROBLEM NUMBER		2
QPOINT = 0.10				JPOINT = 0.15				
BLCWS PER IN.	RUTOTAL	POINT FORCE	MAX C STRESS	SEG	MAX T STRESS	SEG		
1.0377	213593.-	107.T	96645.		7664.	4	4171.	10
3.1615	470888.-	235.T	196306.		7663.	4	3412.	10
4.8150	622323.-	311.T	247556.		7662.	4	3083.	10
6.5367	736804.-	368.T	283048.		7662.	4	2857.	10
7.5466	819918.-	410.T	307190.		7661.	4	2703.	10
11.4121	1025674.-	513.T	361561.		7661.	4	2352.	10
15.8643	1158745.-	579.T	392988.		7660.	4	2145.	10
18.7758	1233466.-	617.T	409456.		7660.	4	2035.	10
22.0974	1297626.-	649.T	420576.		7659.	4	1950.	10
29.3317	1394207.-	697.T	430297.		7659.	4	1840.	10
36.8446	1460959.-	730.T	436023.		7659.	4	1766.	10
45.1832	1510959.-	755.T	439816.		7659.	4	1713.	10
57.8852	1560959.-	780.T	443210.		7658.	4	1663.	10
77.6870	1610959.-	805.T	446224.		7658.	4	1613.	10

Figure B.9. Summary output for RU (total) vs blows/in. (option 11=1) for Prob. 1 and 2.

TEXAS A * M UNIVERSITY				PILE DRIVING ANALYSIS				CASE NO.HSP 10				PROBLEM NO. 3 OF 4					
1/DELTA T P OPTIONS				1	2	3	4	11	12	13	14	15	EXP. FORCE				
9443.9 11				2	1	1	2	2	1	0	1	1	158700.				
ENERGY	HAMMER	EFFICIENCY		RU(TOTAL)		PERCENT UNDER POINT		MO	Q(POINT)		Q(SIDE)		J(POINT) J(SIDE)		N2		
39800.00	1.00			400000.0		10.0		4	0.10		0.10		0.15 0.05		142		
M	W(M)	K(M)		AREA(M)		RU(M)		SLACK(M)	ERES(M)		VSTART(M)		KPRIME(M)				
1	4850.000	0.4220000E 08	08	1.000		0.0		1000.000	0.60		22.99		0.0				
2	1150.000	0.2450000E 08	08	1.000		0.0		1000.000	0.80		0.0		0.0				
3	1200.000	0.2250000E 08	08	254.000		0.0		1000.000	0.50		0.0		0.0				
4	883.000	0.5100000E 08	08	254.000		45000.000		0.0	1.00		0.0		0.4500001E 06		06		
5	883.000	0.5100000E 08	08	254.000		45000.000		0.0	1.00		0.0		0.4500001E 06		06		
6	883.000	0.5100000E 08	08	254.000		45000.000		0.0	1.00		0.0		0.4500001E 06		06		
7	883.000	0.5100000E 08	08	254.000		45000.000		0.0	1.00		0.0		0.4500001E 06		06		
8	883.000	0.5100000E 08	08	254.000		45000.000		0.0	1.00		0.0		0.4500001E 06		06		
9	883.000	0.5100000E 08	08	254.000		45000.000		0.0	1.00		0.0		0.4500001E 06		06		
10	883.000	0.5100000E 08	08	254.000		45000.000		0.0	1.00		0.0		0.4500001E 06		06		
11	883.000	0.3999999E 06	06	254.000		45000.000		1000.000	1.00		0.0		0.4500001E 06		06		
12	-0.0	-0.0		-0.0		39999.984		-0.0	-0.0		-0.0		0.0				
SEGMENT	AREA	TIME N	MAX C STRESS	TIME N	MAX T STRESS	D(M)		D(M)		V(M)							
1	1.000	4	2883701.	0	-0.0	0.502888		0.375493		-4.67							
2	1.000	7	2245095.	93	-0.0	0.688212		0.688212		1.00							
3	254.000	11	7445.	97	-0.0	0.608394		0.606307		1.22							
4	254.000	13	7258.	41	2537.	0.497042		0.495229		-2.50							
5	254.000	15	7017.	39	3001.	0.489747		0.489520		-0.17							
6	254.000	17	6826.	38	2655.	0.484540		0.484376		1.46							
7	254.000	19	6656.	35	2477.	0.481653		0.481653		0.52							
8	254.000	21	6493.	34	3081.	0.479475		0.479301		-0.90							
9	254.000	23	6133.	29	3078.	0.474198		0.473951		0.21							
10	254.000	24	4278.	30	4194.	0.475263		0.470868		1.83							
11	254.000	27	647.	0	-0.0	0.473911		0.473011		-1.43							
PERMANENT SET OF PILE =				0.37391138 INCHES				NUMBER OF BLOWS PER INCH =				2.67442989				TOTAL INTERVALS =	98

Figure B.10. Normal output for single RU (total) (option 11 = 2) for Prob. 3.

KPRIME(M) = soil spring stiffness, (lb/in.),
 FMAXC(M) = maximum compressive force in segment, (lb), and
 FMAXT(M) = maximum tensile force in segment, (lb).

Time interval N = 0 is for the pile under the influence of gravity alone. The particular output listed in Figure B-11 shows that the point of the pile of Problem 4 would penetrate 0.002353 in. under gravity alone.

TEXAS A * M UNIVERSITY				PILE DRIVING ANALYSIS				CASE NO.HSP 10				PROBLEM NO. 4 OF 4				
1/DELTA T P OPTIONS				1	2	3	4	11	12	13	14	15	EXP. FORCE			
9443.9 11				2	1	1	2	2	2	0	1	2	158700.			
ENERGY	HAMMER	EFFICIENCY		RU(TOTAL)		PERCENT UNDER POINT		MO		Q(POINT)		Q(SIDE)		J(POINT) J(SIDE)		N2
39800.00	1.00			400000.0		10.0		4		0.10		0.10		0.15 0.05		140
M	W(M)	K(M)		AREA(M)		RU(M)		SLACK(M)		ERES(M)		VSTART(M)		KPRIME(M)		
1	4850.000	0.4220000E 08	08	1.000		0.0		1000.000		0.60		22.99		0.0		
2	1150.000	0.2450000E 08	08	1.000		0.0		1000.000		0.80		0.0		0.0		
3	1200.000	0.3130000E 08	08	254.000		0.0		1000.000		0.50		0.0		0.0		
4	883.000	0.5100000E 08	08	254.000		5625.000		0.0		1.00		0.0		0.5625002E 05		05
5	883.000	0.5100000E 08	08	254.000		16875.000		0.0		1.00		0.0		0.1687500E 06		06
6	883.000	0.5100000E 08	08	254.000		28125.000		0.0		1.00		0.0		0.2812501E 06		06
7	883.000	0.5100000E 08	08	254.000		39375.000		0.0		1.00		0.0		0.3937501E 06		06
8	883.000	0.5100000E 08	08	254.000		50625.000		0.0		1.00		0.0		0.5062501E 06		06
9	883.000	0.5100000E 08	08	254.000		61875.000		0.0		1.00		0.0		0.6187502E 06		06
10	883.000	0.5100000E 08	08	254.000		73125.000		0.0		1.00		0.0		0.7312502E 06		06
11	883.000	0.3999999E 06	06	254.000		84375.000		1000.000		1.00		0.0		0.8437502E 06		06
12	-0.0	-0.0		-0.0		39999.984		-0.0		-0.0		-0.0		0.0		
TIME INTERVAL N = 0				NET PENETRATION = 0.0				N1 = 140		N2 =						
SEGMENT M	D(M)	C(M)		STRESS(M)	F(M)	R(M)	W(M)	V(M)	DPRIME(M)	KPRIME(M)	FMAXC(M)	FMAXT(M)				
1	0.002919	0.0		0.0	0.0	0.0	4850.00	22.988647	0.000566	0.0	0.0	0.0				
2	0.002919	0.000047		1150.	1150.	0.0	1150.00	0.0	0.000566	0.0	0.0	0.0				
3	0.002873	0.000075		9.	2350.	0.0	1200.00	0.0	0.000519	0.0	0.0	0.0				
4	0.002797	0.000061		12.	3101.	132.	883.00	0.0	0.000444	56250.	0.0	0.0				
5	0.002737	0.000070		14.	3586.	397.	883.00	0.0	0.000383	168750.	0.0	0.0				
6	0.002666	0.000075		15.	3808.	662.	883.00	0.0	0.000313	281250.	0.0	0.0				
7	0.002592	0.000074		15.	3764.	927.	883.00	0.0	0.000238	393750.	0.0	0.0				
8	0.002518	0.000068		14.	3455.	1191.	883.00	0.0	0.000164	506250.	0.0	0.0				
9	0.002450	0.000057		11.	2882.	1456.	883.00	0.0	0.000097	618750.	0.0	0.0				
10	0.002394	0.000040		8.	2044.	1721.	883.00	0.0	0.000040	731250.	0.0	0.0				
11	0.002353	0.0		4.	941.	1986.	883.00	0.0	0.0	843750.	0.0	0.0				
TIME INTERVAL N = 1				NET PENETRATION = 0.0				N1 = 140		N2 =						
SEGMENT M	D(M)	C(M)		STRESS(M)	F(M)	R(M)	W(M)	V(M)	DPRIME(M)	KPRIME(M)	FMAXC(M)	FMAXT(M)				
1	0.032130	0.029211		1232689.	1232689.	0.0	4850.00	22.126266	0.000566	0.0	1232689.	0.0				
2	0.002919	0.000047		1150.	1150.	0.0	1150.00	3.651348	0.000566	0.0	1150.	0.0				
3	0.002873	0.000075		9.	2350.	0.0	1200.00	0.000000	0.000519	0.0	2350.	0.0				
4	0.002797	0.000061		12.	3101.	132.	883.00	-0.000000	0.000444	56250.	3101.	0.0				
5	0.002737	0.000070		14.	3586.	397.	883.00	-0.000000	0.000383	168750.	3586.	0.0				
6	0.002666	0.000075		15.	3808.	662.	883.00	0.000000	0.000313	281250.	3808.	0.0				
7	0.002592	0.000074		15.	3764.	927.	883.00	0.000000	0.000238	393750.	3764.	0.0				
8	0.002518	0.000068		14.	3455.	1191.	883.00	0.000000	0.000164	506250.	3455.	0.0				
9	0.002450	0.000057		11.	2882.	1456.	883.00	-0.000000	0.000097	618750.	2882.	0.0				
10	0.002394	0.000040		8.	2044.	1721.	883.00	0.000000	0.000040	731250.	2044.	0.0				
11	0.002353	0.0		4.	941.	1986.	883.00	-0.000000	0.0	843750.	941.	0.0				

APPENDIX C

OS-360 Fortran IV Program Statements

The listing that follows is known as an XREF listing. Each statement is numbered, for reference, consecutively from the first to the last statement. The variables and program statement numbers are indexed by their reference number. This listing facilitates finding each

variable in the program and makes the logic much easier to follow.

A flow diagram of the program logic is included for reference.

```

C      TEXAS A * M UNIVERSITY
C      PILE DRIVING ANALYSIS BY THE WAVE EQUATION
C      TEXAS A AND M PROGRAM REVISED 12/1/65 BY EAS
C      PERMANENT SET, BLOWS PER INCH
C      LOOSE, TIGHT, OR LIMITED MOTION AT JOINTS
C      MAXIMUM STRESSES OR FORCES
C      IOPT USED FOR OPTION.
C      I, JT, JTM, LAMP, LAY, LT, LACK, ARE USED FOR CONTROL
C      X AT END OF NAME = LAST PRECEDING VALUE EXCEPT IN MAX = MAXIMUM
C      N ALWAYS MEANS NUMBER OF TIME INTERVAL.
C      NOTATION FOLLOWS SMITHS ASCE PAPER CLOSELY. TO DECODE NOTE THAT
C      NFMAXT = NO. OF TIME INTERVAL WHERE FORCE = MAXIMUM IN TENSION
ISN 0002 5000 REAL JPOINT, JSIDE, K, KPRIME, NPASS, NP1, KHOLD, CASE*8
ISN 0003 5001 INTEGER P, PPLUS1, PLESS1, PROBS, PROBS
ISN 0004 5002 DIMENSION AREA(150), C(150), CX(150), CMAX(150), D(150), DX(150),
      1, CMAX(150), DPRIME(150), ERES(150), F(150), FX(150), FMAXC(150),
      2, FMAXT(150), K(150), KPRIME(150), LAM(150), NDMAX(150),
      3, NFMAXC(150), NFMAXT(150), R(150), RU(150), SLACK(150),
      4, UBLOWS(150), UFMAXC(150), URUTTL(150), V(150),
      5, W(150), RULIST(150), RUHIL(30), RWENR(30), RWMICH(30),
      6, XPLOT(50), YPLOT(50), STRESS(150), KHOLD(150),
      7, FCMAX(50), NCMAX(50), FTMAX(50), NTMAX(50)
      24 OF EACH OF ABOVE SUFFICIENT FOR USUAL PROBLEMS
C----- INPUT --- GENERAL
ISN 0005 5010 READ(5,5113) CASE, PROBS, TTDELTA, P, SLACK(1), SLACK(2), SLACK(3), IOPT1,
      1 ICPT2, IOPT3, IOPT4, IPRINT, NSEG1
ISN 0006 WRITE(6,5003)
ISN 0007 5003 FORMAT(1H1)
ISN 0008 IF(TTDELTA.LE.0.) TTDELTA=1.0
ISN 0010 IF(IOPT4.LE.0) IOPT4=2
ISN 0012 IF(IPRINT.LE.0) IPRINT=1
ISN 0014 IF(NSEG1.LE.0) NSEG1=2
ISN 0016 TTDELTA=TTDELTA
ISN 0017 5020 DELTAT = 1./TTDELTA
ISN 0018 5021 PPLUS1 = P+1
ISN 0019 5022 PLESS1 = P-1
ISN 0020 5030 READ (5,5114)(W(M),M=1,P)
ISN 0021 5031 W(PPLUS1) = -0.0
C----- CALCULATE PILE WEIGHT
ISN 0022 WPILE=0.
ISN 0023 DO 6 JT=NSG1,P
ISN 0024 6 WPILE=WPILE+W(JT)
ISN 0025 5040 READ (5,5115)(K(M),M=1,PLESS1)
      C K(P) IS DETERMINED AT 5184
ISN 0026 5041 K(PPLUS1) = -0.0
ISN 0027 5083 DO 5084 M=1,P
ISN 0028 KHOLD(M)=K(M)
ISN 0029 5084 AREA(M) = 1.0
ISN 0030 5086 AREA(PPLUS1) = -0.0
ISN 0031 5087 IF(IOPT1-2)5090,5088,5088
ISN 0032 5088 READ (5,5114)(AREA(M),M=1,P)
ISN 0033 IF(AREA(1).LE.0.) AREA(1)=1.0
ISN 0035 IF(AREA(P).LE.0.) AREA(P)=1.0
ISN 0037 5090 IF(IOPT2-2)5100,5092,5092
ISN 0038 5092 READ (5,5116)(RULIST(M),M=1,PPLUS1)
ISN 0039 5100 IF(IOPT3-2)5101,5104,5104
ISN 0040 5101 DO 5102 M=4,PLESS1
ISN 0041 5102 SLACK(M) = 0.0
ISN 0042 5103 GO TO 5105
ISN 0043 5104 READ (5,5114)(SLACK(M),M=1,PLESS1)
ISN 0044 5105 SLACK(P) = 1000.0
ISN 0045 5106 SLACK(PPLUS1) = -0.0
ISN 0046 5110 DO 5111 M=4,P
ISN 0047 5111 ERES(M) = 1.0
ISN 0048 5112 ERES(PPLUS1) = -0.0
ISN 0049 5113 FORMAT(A6,I3,F10.4,I3,3F7.3,4I1,1X,I3,I2)
ISN 0050 5114 FORMAT(8F10.3)
ISN 0051 5115 FORMAT(8F10.0)
ISN 0052 5116 FORMAT(8F10.7)
ISN 0053 5117 FORMAT (I2,F8.2,I1,F9.0,F3.2,F6.0,3F3.2,F9.1,F4.1,I3,4F3.2,F9.0,
      1,511)
ISN 0054 5118 FORMAT(1H0,5H CASE,A7,4X,5H PROBS,A6,74H RU PERCENTAGES ON DATA SHE
      1ET PAGE 1 SHOULD TOTAL 100.0 BUT ACTUALLY TOTAL,F15.7)
C----- DO 5570 SOLVES PROBLEMS ONE AFTER ANOTHER
ISN 0055 NC=1
ISN 0056 5120 DO 5570 I=1,PROBS
ISN 0057 K(INC)=KHOLD(INC)
ISN 0058 5121 READ(5,5117) PROBS,W(1),NC,K(INC),EFF,ENERGY,ERES(1),ERES(2),ERES(3)
      1, RUSUM, PERCENT, MO, QPOINT, QSIDE, JPOINT, JSIDE, FEXP, IOPT11,
      2 ICPT12, IOPT13, IOPT14, IOPT15
      IF(IOPT12.LE.0) IOPT12=3
      VSTART= SQRT(64.4*EFF*(ENERGY/W(1)))
      DO 9009 M=1,50
      FTMAX(M)=0.
      9009 FCMAX(M)=0.
      NKENT=0
ISN 0059 5140 RUTTLX = 0.0
ISN 0061 5141 BLWSX = 0.0
ISN 0062 5150 V(1) = VSTART
ISN 0063 5152 LT = 0
ISN 0064 C----- FIRST DETERMINE VALUE OF RUTOTL
ISN 0065 5154 IF(IOPT11-2)5151,5160,5151
ISN 0066
ISN 0067
ISN 0068
ISN 0069
ISN 0070

```



```

C      FOR CURVE PLOTTING
5151 RUTOTL = W(1)* V(1)**2/12.0
ISN 0071
ISN 0072
C      FOR SINGLE PROBLEM
5160 RUTOTL=RUSUM
ISN 0073
ISN 0074
C      COMPUTER CYCLES FROM 707 NEAR END OF PROGRAM
701 SLOPE = (RUTOTL-RUTTLX)/(BLOWS-BLOWSX)
SLOPE=AMAX1(10000.,SLOPE)
ISN 0075
ISN 0076
ISN 0077
IF(BLOWS-7.0)5164,702,702
ISN 0078
5164 IF(10PT4-2)5165,703,703
ISN 0079
702 IF(BLOWS-20.0)704,704,705
ISN 0080
5165 DB = 1.00
ISN 0081
GC TO 706
ISN 0082
703 DB = 1.25
ISN 0083
GC TO 706
ISN 0084
704 DB = 2.5
ISN 0085
GC TO 706
ISN 0086
705 DB = 5.0
ISN 0087
GC TO 706
ISN 0088
706 RUTTLX = RUTOTL
RUTOTL = RUTTLX+(DB*SLOPE)
ISN 0089
BLOWSX = BLOWS
ISN 0090
C---- SECOND DETERMINE ALL VALUES OF RU(M)
5170 DO 13 M=1,M0
ISN 0091
13 RU(M) = 0.0
ISN 0092
5171 RUPINT = (PERCNT/100.0)*RUTOTL
ISN 0093
5172 IF(10PT12-2)143,146,5176
ISN 0094
C      FOR UNIFORM DISTRIBUTION
143 DO 144 M=M0,P
ISN 0095
144 RU(M) = (RUTOTL-RUPINT)/FLOAT(P-M0+1)
ISN 0096
5173 RU(PPLUS1) = RUPINT
ISN 0097
GC TO 713
ISN 0098
C      FOR TRIANGULAR DISTRIBUTION
146 DO 145 M=M0,P
ISN 0099
145 RU(M) = (2.0*(RUTOTL-RUPINT)*(FLOAT(M-M0)+0.5))/(FLOAT(P-M0+1))**2
ISN 0100
5175 RU(PPLUS1) = RUPINT
ISN 0101
GC TO 713
ISN 0102
C      FOR DISTRIBUTION PER RU LIST ON DATA SHEET
5176 TOTAL = 0.0
ISN 0103
DO 5177 M=1,PPLUS1
ISN 0104
5177 TOTAL = TOTAL+RU(LIST(M))
ISN 0105
5178 IF((ABS(TOTAL-100.0))-2.0)5180,5180,5179
ISN 0106
5179 WRITE (6,5118)CASE,PROB,TOTAL
ISN 0107
GC TO 5570
ISN 0108
5180 DO 5181 M=1,PPLUS1
ISN 0109
5181 RU(M) = (RU(LIST(M))/100.0)*RUTOTL
ISN 0110
GC TO 713
ISN 0111
C---- THIRD DETERMINE STARTING VALUES OF V(M)
713 V(1)=VSTART
ISN 0112
DO 180 M=2,P
ISN 0113
180 V(M) = 0.0
ISN 0114
5183 V(PPLUS1) = -0.0
ISN 0115
C---- FOURTH DETERMINE VALUE FOR K(P)
5184 K(P) = RU(PPLUS1)/QPOINT
ISN 0116
C      FIFTH CHANGE CYCLE COUNT
5186 LT = LT + 1
ISN 0117
C----CHECK ON DELTAT
CALL DELTCK(INPASS,TTDELT,P,W,K,TDELTA,DELTAT,N2)
ISN 0118
C----END DELTAT CHECK
C---- ASSIGN OTHER VALUES REQUIRED (TEXAS A AND M REPI)
DO 5218 M=1,P
ISN 0119
32 KPRIME(M) =RU(M)/QSIDE
ISN 0120
C(M) = 0.0
ISN 0121
F(M) = 0.0
ISN 0122
CMAX(M) = 0.0
ISN 0123
LAMP(M)=1
ISN 0124
D(M) = 0.0
ISN 0125
NFMAXC(M) = 0
ISN 0126
NFMAXT(M) = 0
ISN 0127
DMAX(M) = 0.0
ISN 0128
NDMAX(M) = 0
ISN 0129
FMAXC(M) = 0.0
ISN 0130
FMAXT(M) = 0.0
ISN 0131
R(M) = 0.0
ISN 0132
5218 DPRIME(M) = 0.0
ISN 0133
KPRIME(PPLUS1)=0.
ISN 0134
DPRIMP = 0.0
ISN 0135
LAMP = 1
ISN 0136
C---- SIXTH PRINT INPUT FOR ONE PROBLEM
5190 WRITE (6,5200)CASE,PROB,PROBS
ISN 0137
5191 WRITE (6,5201)
ISN 0138
5192 WRITE(6,5202) TDELTA,P,10PT1,10PT2,10PT3,10PT4, 10PT11,
ISN 0139
1 10PT12,10PT13,10PT14,10PT15,FEXP
ISN 0140
5193 WRITE (6,5203)
ISN 0141
5194 WRITE(6,5204) ENERGY,EFF,RUTOTL,PERCNT,M0,QPOINT,QSIDE,JPOINT,JSI
1DE,N2
ISN 0142
5195 WRITE (6,5205)
ISN 0143
5196 WRITE (6,5206)(M,W(M),K(M),AREA(M),RU(M),SLACK(M),ERES(M),
1 V(M),KPRIME(M),M=1,PPLUS1)
ISN 0144
5200 FORMAT(///27H TEXAS A * M UNIVERSITY ,3X,22H PILE DRIVING ANALY
1SIS,4X,9H CASE NO.,A7,3X,12H PROBLEM NO.,14,3H OF,14)
ISN 0145
5201 FORMAT(2X10H 1/DELTA T3X1HP4X62HOPTIONS 1 2 3 4
1 11 12 13 14 1510X10HEXP. FORCE)
ISN 0146
5202 FORMAT(F11.1,15,11X4I5,10X5I5,F18.0)
ISN 0147
5203 FORMAT(113H ENERGY HAMMER EFFICIENCY RU(TOTAL) PERCENT UN

```

```

      1DER POINT MO Q(POINT) Q(SIDE) J(POINT) J(SIDE) N2)
ISN 0148 5204. FORMAT(2F10.2,10X F12.1,F16.1,I11,F10.2,F9.2,F10.2,F9.2,I7)
ISN 0149 5206. FORMAT(13, F14.3,E15.7,F10.3,2F14.3,F9.2,F11.2,E15.7)
ISN 0150 5205. FORMAT(3H M,7X,5H W(M),7X,5H K(M),7X,8H AREA(M),6X,6H RU(M),7X,4I
      1H SLACK(M) ERES(M) VSTART(M) KPRIME(M))
C----- EFFECT OF GRAVITY BEFORE RAM STRIKES--TEXAS A AND M SMITHS GRAVITY
ISN 0151 5258 IF(IOPT14-2)5220,5221,5221
ISN 0152 5220 WTCTAL = 0.0
ISN 0153 RTOTAL = 0.0
ISN 0154 DO 5 JT=2,PPLUS1
ISN 0155 WTCTAL = WTOTAL + W(JT)
ISN 0156 5 RTOTAL = RTOTAL + RU(JT)
ISN 0157 DO 8 JT = 2,PLESS1
ISN 0158 R(JT) = (RU(JT)*WTOTAL)/RTOTAL
ISN 0159 8 F(JT) = F(JT-1)+W(JT)-R(JT)
ISN 0160 IF(K(P))67,66,67
ISN 0161 66 IF(KPRIME(P))67,63,67
ISN 0162 67 D(P) = (F(PLESS1)+W(P))/(KPRIME(P)+K(P))
ISN 0163 IF(QSIDE-D(P))64,65,65
ISN 0164 64 R(P) = RU(P)
ISN 0165 F(P) = F(PLESS1) + W(P) - R(P)
ISN 0166 U(P) = F(P)/K(P)
ISN 0167 GO TO 63
ISN 0168 65 R(P) = U(P)*KPRIME(P)
ISN 0169 F(P) = D(P)*K(P)
ISN 0170 63 CONTINUE
ISN 0171 DO 111 JT = 1,PLESS1
ISN 0172 JTM = P-JT
ISN 0173 C(JTM) = F(JTM)/K(JTM)
ISN 0174 D(JTM) = D(JTM+1)+C(JTM)
ISN 0175 DPRIME(JTM) = D(JTM)-WTOTAL*QSIDE/RTOTAL
ISN 0176 111 CONTINUE
ISN 0177 DO 8000 M=1,P
ISN 0178 8000 STRESS(M)=F(M)/AREA(M)
ISN 0179 5221 N=0
ISN 0180 LAY = 1
ISN 0181 5230 IF(IOPT15-2)5240,5231,5240
ISN 0182 5231 WRITE(6,5234)N,DPRIME,N2
ISN 0183 5232 WRITE (6,5235)
ISN 0184 5233 WRITE(6,5236)(M,D(M),C(M),STRESS(M),F(M),R(M),W(M),V(M),DPRIME(M),
      NKPRIME(M),FMAXC(M),FMAXT(M),M=1,P)
ISN 0185 NKCNT=0
ISN 0186 5234. FORMAT(/,18H TIME INTERVAL N =16,7X18HNET PENETRATION = F10.6,
      17X5HNI = 15,5X5HN2 = 15)
ISN 0187 5235. FORMAT(120H SEGMENT M D(M) C(M) STRESS(M) F(M)
      1 R(M) W(M) V(M) DPRIME(M) KPRIME(M) FMAXC(M) FMAXT(M))
ISN 0188 5236. FORMAT(18,F11.6,F10.6,F11.0,2F10.0,F10.2,2F10.6,3F10.0)
C----- DYNAMIC COMPUTATION BASED ON SMITHS PAPER MODIFIED (TEXAS REPN)
ISN 0189 5240 LACK = 1
ISN 0190 5241 DO 68 M=1,P
ISN 0191 C 68 IS BETWEEN 5439 AND 5440
ISN 0192 U(M) = D(M)+V(M)*12.0*DELTAT
ISN 0193 IF(DMAX(M)-U(M))20,21,21
ISN 0194 20 DMAX(M) = D(M)
ISN 0195 NDMAX(M) = N + 1
ISN 0196 21 CX(M) = C(M)
ISN 0197 IF(M-P)34,5400,34
ISN 0198 34 C(M) = U(M)-D(M+1)-V(M+1)*12.0*DELTAT
ISN 0199 C STATEMENT 34 MUST USE A COMPUTED VALUE FOR THE ACTUAL D(M+1)
ISN 0200 5242 IF(C(M))5243,30,30
ISN 0201 5243 IF(ABS(C(M))-SLACK(M))5244,5244,5246
ISN 0202 5244 C(M) = 0.0
ISN 0203 5245 GO TO 30
ISN 0204 5246 C(M) = C(M)+SLACK(M)
ISN 0205 C NOTE THAT ONLY A NEGATIVE VALUE OF C(M) RESULTS FROM 5246
ISN 0206 30 FX(M) = F(M)
ISN 0207 C A TEXAS ROUTINE FOR B(M) IS OMITTED HERE
ISN 0208 5250 IF(IOPT4-2)5300,36,5300
ISN 0209 C----- 36 TO 35 IS A TEXAS ROUTINE REPLACING SMITH ROUTINE 3 OR 4
ISN 0210 36 IF(ABS(ERES(M)-1.0)-.00001)38,38,14
ISN 0211 38 F(M) = C(M)*K(M)
ISN 0212 GO TO 5400
ISN 0213 14 IF(C(M)-CX(M))12,35,15
ISN 0214 15 F(M) = FX(M)+((C(M)-CX(M))*K(M))
ISN 0215 GO TO 35
ISN 0216 12 F(M) = FX(M)+((C(M)-CX(M))*K(M)/ERES(M)**2)
ISN 0217 35 F(M) = AMAX1(0.0,F(M))
ISN 0218 GO TO 5400
ISN 0219 C A TEXAS ROUTINE FOR GAMMA IS OMITTED HERE
ISN 0220 C----- SMITH ROUTINE 3 OR 4
ISN 0221 5300 IF(ERES(M)-1.00)5302,5301,5301
ISN 0222 5301 F(M) = C(M)*K(M)
ISN 0223 GO TO 5400
ISN 0224 5302 IF(C(M))5303,5303,5304
ISN 0225 5303 F(M) = 0.0
ISN 0226 GO TO 5400
ISN 0227 5304 IF(C(M)-CMAX(M))5306,5305,5305
ISN 0228 5305 CMAX(M) = C(M)
ISN 0229 F(M) = C(M)*K(M)
ISN 0230 GO TO 5400
ISN 0231 5306 F(M) = (K(M)/ERES(M)**2)*C(M)-(1./ERES(M)**2-1.)*K(M)*CMAX(M)
ISN 0232 F(M) = AMAX1(F(M),0.0)
ISN 0233 GO TO 5400
ISN 0234 5400 IF(M.GT.1) GO TO 48
ISN 0235 IF(IFEXP.LE.0.) GO TO 48
ISN 0236 NPI=N+1

```

```

ISN 0232      IF(NP1.GT.(0.0125/DELTAT)) GO TO 46
ISN 0234      IF(NP1-0.01/DELTAT)46,46,90
ISN 0235      46 IF(F(1)-FX(1))47,48,48
ISN 0236      47 F(1)=AMAX1(F(1),FEXP,0.)
ISN 0237      GO TO 48
ISN 0238      90 F(1)=AMAX1(0.0,FEXP*(1.0-(DELTAT*(NP1-0.01/DELTAT)/0.0025)))
ISN 0239      48 IF(KPRIME(M))50,55,50
ISN 0240      50 IF(DPRIME(M)-D(M)+QSIDE)51,52,52
ISN 0241      51 DPRIME(M) = D(M)-QSIDE
ISN 0242      52 CONTINUE
ISN 0243      IF(DPRIME(M)-D(M)-QSIDE)53,53,54
ISN 0244      54 DPRIME(M) = D(M)+QSIDE
ISN 0245      53 CONTINUE
ISN 0246      5410 LAP = LAM(M)
ISN 0247      GO TO(10,57),LAP
ISN 0248      10 IF(D(M)-DPRIME(M)-QSIDE)56,57,57
ISN 0249      56 R(M) = (D(M)-DPRIME(M))*KPRIME(M)*(1.0+JSIDE*V(M))
ISN 0250      GO TO 55
ISN 0251      57 R(M) = (D(M)-DPRIME(M)+JSIDE*QSIDE*V(M))*KPRIME(M)
ISN 0252      LAM(M) = 2
ISN 0253      55 CONTINUE
ISN 0254      73 IF(M-P)71,74,71
ISN 0255      74 IF(DPRIMP-D(P)+QPOINT)75,76,76
ISN 0256      75 DPRIMP = D(P)-QPOINT
ISN 0257      76 CONTINUE
ISN 0258      LAMP = LAMP
ISN 0259      GO TO (77,78),LAMP
ISN 0260      77 IF(D(P)-DPRIMP-QPOINT)79,78,78
ISN 0261      79 F(P) = (D(P)-DPRIMP)*K(P)*(1.0+JPOINT*V(P))
ISN 0262      GO TO 171
ISN 0263      78 F(P) = (D(P)-DPRIMP+JPOINT*QPOINT*V(P))*K(P)
ISN 0264      LAMP = 2
ISN 0265      171 F(P) = AMAX1(0.0,F(P))
ISN 0266      71 CONTINUE
C      GRAVITY OPTION
ISN 0267      5420 IF(1OPT14-2)5421,5423,5423
ISN 0268      5421 IF(LACK-2)58,72,72
ISN 0269      58 V(1) = V(1)-(F(1)+R(1)-W(1))*32.17*DELTAT/W(1)
ISN 0270      LACK = 2
ISN 0271      GO TO 5429
ISN 0272      72 V(M) = V(M)+(F(M)-F(M)-R(M)+W(M))*32.17*DELTAT/W(M)
ISN 0273      5422 GO TO 5429
ISN 0274      5423 IF(LACK-2)5424,5427,5427
ISN 0275      5424 V(1) = V(1)-(F(1)+R(1))*32.17*DELTAT/W(1)
ISN 0276      5425 LACK = 2
ISN 0277      GO TO 5429
ISN 0278      5427 V(M) = V(M)+(F(M)-F(M)-R(M))*32.17*DELTAT/W(M)
ISN 0279      5429 CONTINUE
ISN 0280      IF(M.GT.1) GO TO 5430
ISN 0282      IF(F(1).LE.0..AND.V(1).LE.-0.1) V(1)=-VSTART
ISN 0284      5430 FMAXC(M) = AMAX1(FMAXC(M),F(M))
ISN 0285      FMAXT(M) = AMIN1(FMAXT(M),F(M))
ISN 0286      5439 IF(FMAXC(M)-F(M))166,167,166
ISN 0287      167 NFMAXC(M) = N+1
ISN 0288      166 IF(FMAXT(M)-F(M))168,69,68
ISN 0289      69 NFMAXT(M) = N+1
ISN 0290      68 STRESS(M)=F(M)/AREA(M)
ISN 0291      N=N+1
C      THIS IS END OF DO 68 STARTING AT 5241
ISN 0292      5440 IF(1OPT15-2)5444,5441,5444
ISN 0293      5441 IF(N-1)7000,7001,7000
ISN 0294      7000 NKONT=NKONT+1
ISN 0295      IF(NKONT-1PRINT)5444,7001,5444
ISN 0296      7001 WRITE (6,5234)N,DPRIMP,N2
ISN 0297      WRITE (6,5235)
ISN 0298      WRITE(6,5236)(M,D(M),C(M),STRESS(M),F(M),R(M),W(M),V(M),DPRIME(M),
      IKPRIME(M),FMAXC(M),FMAXT(M),N=1,P)
ISN 0299      7003 NKONT=0
ISN 0300      5444 GO TO (5443,192),LAY
ISN 0301      5443 IF((V(P)+0.1).GT.0.) GO TO 192
ISN 0303      WV=0.0
ISN 0304      DO 193 JA=NSEG1,P
ISN 0305      193 WV=WV+W(JA)*V(JA)
ISN 0306      IF(V(1).LT.0..AND.WV.LT.0..AND.DMAX(P).GT.D(P)) GO TO 190
ISN 0308      GO TO 192
ISN 0309      190 LAY=2
ISN 0310      GO TO (192,194,192),1OPT15
ISN 0311      194 WRITE(6,5234)N,DPRIMP,N2
ISN 0312      WRITE(6,5235)
ISN 0313      WRITE(6,5236)(M,D(M),C(M),STRESS(M),F(M),R(M),W(M),V(M),DPRIME(M),
      IKPRIME(M),FMAXC(M),FMAXT(M),N=1,P)
ISN 0314      192 IF(V(2)/VSTART-3.1)61,60,60
ISN 0315      60 WRITE (6,105)
ISN 0316      105 FORMAT(74H THE RATIO OF THE VELOCITY OF W(2) TO THE VELOCITY OF T
      THE RAM EXCEEDS 3.1)
ISN 0317      GO TO 5570
ISN 0318      61 IF(V(P)/VSTART-3.1)163,62,62
ISN 0319      62 WRITE (6,106)
ISN 0320      GO TO 5570
ISN 0321      106 FORMAT(74H THE RATIO OF THE VELOCITY OF W(P) TO THE VELOCITY OF T
      THE RAM EXCEEDS 3.1)
C --- END OF TEXAS REPN
ISN 0322      163 CONTINUE
ISN 0323      IF(LAY.EQ.2) GO TO 5447
ISN 0325      IF(N-N2)5240,5447,5447
C---- 5240 CYCLES FOR NEXT TIME INTERVAL

```

```

ISN 0326 5447 DO 5449 M=1,P
ISN 0327 5448 FMAXC(M) = FMAXC(M)/AREA(M)
ISN 0328 5449 FMAXT(M)=FMAXT(M)/(-AREA(M))
ISN 0329 GC TO(5442,5442,5553),IOPT15
ISN 0330 5442 WRITE (6,2105)
ISN 0331 5550 WRITE(6,2106)(M,AREA(M),NFMAXC(M),FMAXC(M),NFMAXT(M),FMAXT(M),DMAX
1(M),D(M),V(M),M=1,P)
BLWS=0.0
ISN 0332 5553 IF(DPRIMP.GT.0.0) BLWS=1.0/DPRIMP
ISN 0333 5551 UBLWS(LT) = BLWS
ISN 0334 URUTTL(LT) = RUTOTL
ISN 0337 UFMAXC(LT) = FMAXC(P)*AREA(P)
C INITIAL U ABOVE IDENTIFIES FIGURES USED IN SUMMARY
ISN 0338 GO TO(5552,5552, 150),IOPT15
ISN 0339 5552 WRITE (6,2107)DPRIMP,BLWS,N
ISN 0340 2105 FCRMAT(//103H SEGMENT AREA TIME N MAX C STRESS TIME N
1 MAX T STRESS CMAX(M) D(M) V(M))
ISN 0341 2106 FCRMAT(13,F15.3,18,F12.0,114,F12.0,F16.6,F10.6,F13.2)
ISN 0342 2107 FCRMAT(24H PERMANENT SET OF PILE =F15.8, 38H INCHES NUMBER OF B
1LWS PER INCH = F16.8,22H TOTAL INTERVALS = 18)
ISN 0343 150 CONTINUE
ISN 0344 5558 DO 5563 M=NSEG1,P
ISN 0345 FTMAX(LT)=AMAX1(FTMAX(LT),FMAXT(M))
ISN 0346 FCMAX(LT)=AMAX1(FCMAX(LT),FMAXC(M))
ISN 0347 IF(FCMAX(LT)-FMAXC(M))5560,5561,5560
ISN 0348 5561 NCMAX(LT)=M
ISN 0349 5560 IF(FTMAX(LT)-FMAXT(M))5563,5562,5563
ISN 0350 5562 NFMAX(LT)=M
ISN 0351 5563 CONTINUE
ISN 0352 5555 IF(10PT11-2)5556,5570,5570
ISN 0353 5556 IF (DPRIMP-0.001)59,707,707
ISN 0354 707 IF (BLWS-60.0)701,701,59
ISN 0355 59 CONTINUE
ISN 0356 WRITE (6,803) CASE,PROB
ISN 0357 WRITE (6,804) QPOINT,JPOINT
ISN 0358 WRITE (6,805)
ISN 0359 DO 801 J=1,LT
ISN 0360 URUTON=URUTTL(J)/2000.
ISN 0361 801 WRITE(6,802) UBLWS(J),URUTTL(J),URUTON,UFMAXC(J),FCMAX(J),NCMAX(J
2),FTMAX(J),NFMAX(J)
ISN 0362 802 FCRMAT(4XF7.4,F10.0,1H-F5.0,1HTF13.0,F13.0,4X12,F13.0,4X12)
ISN 0363 803 FCRMAT (1H0,10X,22H PILE DRIVING ANALYSIS,
1 10X,12H CASE NUMBER,3X,A6,10X,15H PROBLEM NUMBER,3X,I3)
ISN 0364 804 FCRMAT(19X,9H0POINT = F5.2,11X,9HJPOINT = F5.2)
ISN 0365 805 FCRMAT(2X13HBLWS PER IN.2X7HROUTOTALX11HPOINT FORCE2X12HMAX C STR
1ESS2X3HSEGC2X12HMAX T STRESS2X3HSEGC//)
C-----PLOTING ROUTINE
ISN 0366 IF(10PT13-1)5570,5574,5574
ISN 0367 5574 CALL DRAW(WTOTA,URUTON,UBLWS,LT,CASE,PROB)
C-----END PLOTING ROUTINE
ISN 0368 5570 WRITE(6,5572)
C DO 5570 STARTS AT 5120
ISN 0369 5572 FORMAT(1H1)
ISN 0370 5571 GO TO 5010
ISN 0371 END

```

*****F O R T R A N C R O S S R E F E R E N C E L I S T I N G*****

SYMBOL	INTERNAL STATEMENT NUMBERS																
C	0004	0121	0173	0174	0184	0195	0197	0198	0199	0200	0202	0202	0206	0208	0209	0211	0215
D	0221	0222	0224	0298	0313												
F	0004	0125	0162	0163	0166	0168	0169	0174	0174	0175	0184	0191	0191	0192	0193	0197	0197
	0243	0244	0248	0249	0251	0255	0256	0260	0261	0263	0298	0306	0313	0331			
	0004	0122	0159	0159	0162	0165	0165	0166	0169	0173	0178	0184	0203	0206	0209	0211	0212
	0218	0222	0224	0225	0225	0235	0236	0236	0238	0261	0263	0265	0265	0269	0272	0272	0275
I	0282	0284	0285	0286	0288	0290	0298	0313									
J	0056																
K	0359	0360	0361	0361	0361	0361	0361	0361	0361	0118	0143	0160	0162	0166	0169	0173	0206
	0002	0004	0925	0026	0028	0057	0058	0116									
M	0222	0224	0224	0261	0263												
	0020	0020	0020	0025	0025	0025	0027	0028	0028	0029	0032	0032	0032	0038	0038	0038	0040
	0043	0043	0046	0047	0062	0063	0064	0091	0092	0095	0096	0099	0100	0100	0104	0105	0109
	0113	0114	0119	0120	0120	0121	0122	0123	0124	0125	0126	0127	0128	0129	0130	0131	0132
	0143	0143	0143	0143	0143	0143	0143	0143	0143	0143	0177	0178	0178	0178	0184	0184	0184
	0184	0184	0184	0184	0184	0184	0184	0184	0184	0190	0191	0191	0191	0192	0192	0193	0194
	0195	0196	0197	0197	0197	0197	0198	0199	0199	0200	0202	0202	0202	0203	0203	0205	0206
	0206	0208	0209	0209	0209	0209	0209	0211	0211	0211	0211	0211	0211	0212	0212	0214	0215
	0217	0218	0220	0220	0221	0221	0222	0222	0222	0224	0224	0224	0224	0224	0224	0225	0225
	0239	0240	0240	0241	0241	0243	0243	0244	0244	0246	0248	0248	0249	0249	0249	0249	0251
	0251	0251	0251	0252	0254	0272	0272	0272	0272	0272	0272	0278	0278	0278	0278	0278	0280
	0284	0284	0284	0285	0285	0285	0286	0286	0287	0288	0288	0289	0290	0290	0290	0298	0298
	0298	0298	0298	0298	0298	0298	0298	0298	0298	0298	0313	0313	0313	0313	0313	0313	0313
	0313	0313	0313	0313	0313	0326	0327	0327	0327	0328	0328	0328	0331	0331	0331	0331	0331
N	0331	0331	0331	0331	0344	0345	0346	0347	0348	0349	0350						
P	0179	0182	0194	0231	0287	0289	0291	0291	0293	0296	0311	0325	0339				
	0003	0005	0018	0019	0020	0023	0027	0032	0035	0035	0044	0046	0095	0096	0099	0100	0113
	0119	0139	0160	0161	0162	0162	0162	0162	0163	0164	0164	0165	0165	0166	0166	0166	0168
	0168	0169	0169	0169	0172	0177	0184	0190	0196	0254	0255	0256	0260	0261	0261	0261	0263
	0263	0264	0265	0265	0298	0301	0304	0306	0306	0313	0318	0326	0331	0337	0337	0344	
K	0004	0132	0158	0159	0164	0165	0168	0184	0249	0251	0269	0272	0275	0278	0298	0313	
V	0004	0068	0071	0112	0114	0115	0143	0184	0191	0197	0249	0251	0261	0263	0269	0269	0272
	0275	0278	0278	0282	0282	0298	0301	0305	0306	0313	0314	0318	0331				
W	0004	0020	0021	0024	0058	0061	0071	0118	0143	0155	0159	0162	0165	0184	0269	0269	0272
	0275	0298	0305	0313													
CX	0004	0195	0208	0209	0211												
DB	0060	0082	0084	0086	0089												
DX	0004																
FX	0004	0203	0209	0211	0235												
JA	0304	0305	0305														
JT	0023	0024	0154	0155	0156	0157	0158	0158	0159	0159	0159	0159	0171	0172			
LT	0069	0117	0117	0135	0136	0137	0145	0145	0146	0146	0147	0148	0149	0150	0151	0152	
MC	0058	0091	0095	0096	0099	0100	0100	0141									
NC	0055	0057	0057	0058	0058												
NZ	0118	0141	0182	0296	0311	0325											
RU	0004	0092	0096	0097	0100	0101	0110	0116	0120	0143	0156	0158	0164				

*****F O R T R A N C R O S S R E F E R E N C E L I S T I N G*****

SYMBOL	INTERNAL STATEMENT NUMBERS															
WV	0303	0305	0305	0306												
ABS	0106	0199	0205													
EFF	0058	0061	0141													
JTM	0172	0173	0173	0173	0174	0174	0174	0175	0175							
LAM	0004	0124	0246	0252												
LAP	0246	0247														
LAY	0180	0300	0309	0323												
NP1	0002	0231	0232	0234	0238											
AREA	0004	0029	0030	0032	0033	0033	0035	0035	0143	0176	0290	0327	0328	0331	0337	
CASE	0002	0005	0107	0137	0356	0367										
CMAx	0004	0123	0220	0221	0224											
DMAx	0004	0128	0192	0193	0306	0331										
DRAW	0367															
ERES	0004	0047	0048	0058	0058	0058	0143	0205	0211	0214	0224	0224				
FLXP	0058	0139	0229	0236	0238											
LACK	0189	0268	0270	0274	0276											
LAMP	0136	0258	0258	0259	0264											
PROB	0003	0058	0107	0137	0356	0367										
SORT	0061															
AMAX1	0076	0212	0225	0236	0238	0265	0284	0345	0346							
AMIN1	0285															
BLOWS	0075	0077	0079	0090	0332	0333	0335	0339	0354							
FCMAX	0004	0064	0346	0346	0347	0361										
FLUAT	0096	0100	0100													
FMAXC	0004	0130	0184	0284	0284	0286	0298	0313	0327	0327	0331	0337	0346	0347		
FMAXT	0004	0131	0184	0285	0285	0288	0298	0313	0328	0328	0331	0345	0349			
FTMAX	0004	0063	0345	0345	0349	0361										
IOP11	0005	0031	0139													
IOP12	0005	0037	0139													
IOP13	0005	0039	0139													
IOP14	0005	0010	0010	0079	0139	0204										
JSIDE	0002	0058	0141	0249	0251											
KHOLD	0002	0004	0028	0057												
NOMAX	0004	0348	0361													
NOMAX	0004	0129	0194													
NKUNT	0065	0185	0294	0294	0295	0299										
NPASS	0007	0118														
NSEGI	0005	0014	0014	0023	0304	0344										
NTMAX	0004	0350	0361													
PROBS	0003	0005	0056	0137												
QSIDE	0058	0120	0141	0163	0175	0240	0241	0243	0244	0248	0251					
RUHIL	0004															
RUSUM	0058	0073														
RWENR	0004															
SLACK	0304	0005	0005	0005	0041	0043	0044	0045	0143	0199	0202					
SLOPE	0075	0076	0076	0089												

*****F O R T R A N C R O S S R E F E R E N C E L I S T I N G*****

SYMBOL	INTERNAL STATEMENT NUMBERS															
TOTAL	0103	0105	0105	0106	0107											
WFILE	0022	0024	0024													
XPLOT	0004															
YPLUT	0004															
BLOWSX	0067	0075	0090													
DELTAT	0017	0118	0191	0197	0232	0234	0238	0238	0269	0272	0275	0278				
DELTCK	0118															
DPRIME	0004	0133	0175	0184	0240	0241	0243	0244	0248	0249	0251	0298	0313			
DPRIMP	0135	0182	0255	0256	0260	0261	0263	0296	0311	0333	0333	0339	0353			
ENERGY	0058	0061	0141													
IOP11	0058	0070	0139	0352												
IOP12	0058	0059	0059	0094	0139											
IOP13	0058	0139	0366													
IOP14	0058	0139	0151	0267												
IOP15	0058	0139	0181	0292	0310	0329	0338									
IPRINT	0005	0012	0012	0295												
JPRINT	0002	0058	0141	0261	0263	0357										
KPRIME	0002	0004	0120	0134	0143	0161	0162	0168	0184	0239	0249	0251	0298	0313		
NEMAXC	0004	0126	0287	0331												
NEMAXT	0004	0127	0289	0331												
PERCNT	0058	0093	0141													
PLESS1	0003	0019	0025	0040	0043	0157	0162	0165	0171							
PPLUS1	0003	0018	0021	0025	0030	0038	0045	0048	0097	0101	0104	0109	0115	0116	0134	0143
QPOINT	0058	0116	0141	0255	0256	0260	0263	0357								
RTOTAL	0153	0156	0156	0158	0175											
RULIST	0004	0038	0105	0110												
RUPINT	0093	0096	0097	0100	0101											
RUTITL	0071	0073	0075	0088	0089	0093	0096	0100	0110	0141	0336					
RUTTLX	0066	0075	0088	0089												
RWNICH	0304															
STRESS	0004	0178	0184	0290	0298	0313										
TDELTA	0016	0017	0118	0139												
TIDELT	0005	0008	0008	0016	0118											
UNFLOWS	0004	0335	0361	0367												
UFMAXC	0004	0337	0361													
URUTON	0360	0361														
URUTTL	0004	0336	0360	0361	0367											
VSTART	0061	0068	0112	0282	0314	0318										
WTOTAL	0152	0155	0155	0158	0175	0367										

*****F O R T R A N C R O S S R E F E R E N C E L I S T I N G*****

LABEL	DEFINED	REFERENCES
5	0156	0154
6	0024	0023
8	0159	0157
10	0248	0247
12	0211	0208
13	0092	0091
14	0208	0205
15	0209	0208
20	0193	0192
21	0195	0192 0192
30	0203	0198 0198 0201
32	0120	
34	0197	0196 0196
35	0212	0208 0210
36	0205	0204
38	0206	0205 0205
46	0235	0234 0234
47	0236	0235
48	0239	0227 0229 0232 0235 0235 0237
50	0240	0239 0239
51	0241	0240
52	0242	0240 0240
53	0245	0243 0243
54	0244	0243
55	0253	0239 0250
56	0249	0248
57	0251	0247 0248 0248
58	0269	0268
59	0355	0353 0354
60	0315	0314 0314
61	0318	0314
62	0319	0318 0318
63	0170	0161 0167
64	0164	0163
65	0168	0163 0163
66	0161	0160
67	0162	0160 0160 0161 0161
68	0290	0190 0288 0288
69	0289	0288
71	0266	0254 0254
72	0272	0268 0268
73	0254	
74	0255	0254
75	0256	0255
76	0257	0255 0255
77	0260	0259

*****F O R T R A N C R O S S R E F E R E N C E L I S T I N G*****

LABEL	DEFINED	REFERENCES
78	0263	0259 0260 0260
79	0261	0260
90	0238	0234
105	0316	0315
106	0321	0319
111	0176	0171
143	0095	0094
144	0096	0095
145	0100	0099
146	0099	0094
150	0343	0338
163	0322	0318
166	0288	0286 0286
167	0287	0286
171	0265	0262
180	0114	0113
190	0309	0306
192	0314	0300 0301 0308 0310 0310
193	0305	0304
194	0311	0310
701	0075	0354 0354
702	0079	0077 0077
703	0082	0078 0078
704	0084	0079 0079
705	0086	0079
706	0088	0081 0083 0085 0087
707	0354	0353 0353
713	0112	0098 0102 0111
801	0361	0359
802	0362	0361
803	0363	0356
804	0364	0357
805	0365	0358
2105	0340	0330
2106	0341	0331
2107	0342	0339
5003	0007	0006
5010	0005	0370
5020	0017	
5021	0018	
5022	0019	
5030	0020	
5031	0021	
5040	0025	
5041	0026	
5083	0027	

*****FORTRAN CROSS REFERENCE LISTING*****

LABEL	DEFINED	REFERENCES
5084	0029	0027
5086	0030	
5087	0031	
5088	0032	0031 0031
5090	0037	0031
5092	0038	0037 0037
5100	0039	0037
5101	0040	0039
5102	0041	0040
5103	0042	
5104	0043	0039 0039
5105	0044	0042
5106	0045	
5110	0046	
5111	0047	0046
5112	0048	
5113	0049	0005
5114	0050	0020 0032 0043
5115	0051	0025
5116	0052	0038
5117	0053	0058
5118	0054	0107
5120	0056	
5121	0058	
5140	0066	
5141	0067	
5150	0068	
5151	0071	0070 0070
5152	0069	
5153	0072	
5154	0070	
5160	0073	0070
5164	0078	0077
5165	0080	0078
5170	0091	0072 0074
5171	0093	
5172	0094	
5173	0097	
5175	0101	
5176	0103	0094
5177	0105	0104
5178	0106	
5179	0107	0106
5180	0109	0106 0106
5181	0110	0109
5183	0115	

*****FORTRAN CROSS REFERENCE LISTING*****

LABEL	DEFINED	REFERENCES
5184	0116	
5186	0117	
5190	0137	
5191	0138	
5192	0139	
5193	0140	
5194	0141	
5195	0142	
5196	0143	
5200	0144	0137
5201	0145	0138
5202	0146	0139
5203	0147	0140
5204	0148	0141
5205	0150	0142
5206	0149	0143
5218	0133	0119
5220	0152	0151
5221	0179	0151 0151
5230	0181	
5231	0182	0181
5232	0183	
5233	0184	
5234	0186	0182 0296 0311
5235	0187	0183 0297 0312
5236	0188	0184 0298 0313
5240	0189	0181 0181 0325
5241	0190	
5242	0198	
5243	0199	0198 0199
5244	0200	0199 0199
5245	0201	
5246	0202	0199
5250	0204	
5258	0151	
5300	0214	0204 0204
5301	0215	0214 0214
5302	0217	0214
5303	0218	0217 0217
5304	0220	0217
5305	0221	0220 0220
5306	0224	0220
5400	0227	0196 0207 0213 0216 0219 0223 0226
5410	0246	
5420	0267	
5421	0268	0267

*****FORTRAN CROSS REFERENCE LISTING*****

LABEL	DEFINED	REFERENCES
5422	0273	
5423	0274	0267 0267
5424	0275	0274
5425	0276	
5427	0278	0274 0274
5429	0279	0271 0273 0277
5430	0284	0280
5439	0286	
5440	0292	
5441	0293	0292
5442	0330	0329 0329
5443	0301	0300
5444	0300	0292 0292 0295 0295
5447	0326	0323 0325 0325
5448	0327	
5449	0328	0326
5550	0331	
5551	0335	
5552	0339	0338 0338
5553	0333	0329
5555	0352	
5556	0353	0352
5558	0344	
5560	0349	0347 0347
5561	0348	0347
5562	0350	0349
5563	0351	0344 0349 0349
5570	0368	0056 0108 0317 0320 0352 0352 0366
5571	0370	
5572	0369	0368
5574	0367	0366 0366
7000	0294	0293 0293
7001	0296	0293 0295
7003	0299	
8000	0178	0177
9009	0064	0062

OS/360 FORTRAN H

```

COMPILER OPTICNS - NAME=. MAIN,OPT=00,LINECNT=50,SOURCE,EBCDIC,NULIST,NODECK,LOAD,NOMAP,NOEDIT,IO,XREF
ISN 0002      SUBROUTINE DRAW(WTOTAL,URUTTL,UBLWS,LT,CASE,PROB)
ISN 0003      DIMENSION URUTTL(150),UBLWS(150),YPLT(51),XPLOT(51)
ISN 0004      5574 YPLT(1)=WTOTAL
ISN 0005      XPLOT(1)=0.
ISN 0006      LTP1=LT+1
ISN 0007      DO 5573 IP=1,LT
ISN 0008      YPLT(IP+1)=URUTTL(IP)/2000.
ISN 0009      5573 XPLOT(IP+1)=UBLWS(IP)
ISN 0010      YMAX=YPLT(LTP1)
ISN 0011      N2=N2
ISN 0012      IF(YMAX.LE.400.) GO TO 3
ISN 0014      IF(YMAX.LE.800.) GO TO 4
ISN 0016      IF(YMAX.LE.1600.) GO TO 5
ISN 0018      IF(YMAX.LE.3200.) GO TO 6
ISN 0020      3 DY=50.
ISN 0021      GO TO 10
ISN 0022      4 DY=100.
ISN 0023      GO TO 10
ISN 0024      5 DY=200.
ISN 0025      GO TO 10
ISN 0026      6 DY=400.
ISN 0027      10 DX=10.
ISN 0028      PPRUB=PROB
ISN 0029      RETURN
ISN 0030      END
  
```

*****FORTRAN CROSS REFERENCE LISTING*****

SYMBOL	INTERNAL STATEMENT NUMBERS
DX	0027
DY	0020 0022 0024 0026
IP	0007 0008 0008 0009 0009
LT	0002 0006 0007
N2	0011 0011
CASE	0002
DRAW	0002
LTP1	0006 0010
PRUB	0002 0028
YMAX	0010 0012 0014 0016 0018
PPRUB	0028
XPLOT	0003 0004 0009
YPLT	0003 0004 0008 0010
UBLWS	0002 0003 0009
URUTTL	0002 0003 0008
WTOTAL	0002 0004

*****FORTRAN CROSS REFERENCE LISTING*****

LABEL	DEFINED	REFERENCES
3	0020	0012
4	0022	0014
5	0024	0016
6	0026	0018
10	0027	0021 0023 0025
5573	0009	0007
5574	0004	

***** END OF COMPILATION *****

OS/360 FORTRAN H

```

COMPILER OPTIONS - NAME= MAIN,OPT=00,LINECT=50,SOURCE,EBUDIC,NOLIST,NODECK,LOAD,NOMAP,NOEDIT,ID,XREF
ISN 0002 SUBROUTINE DELTCK(NPASS,TDELTA,P,W,K,TDELTA,DELTA1,N2)
ISN 0003 REAL K,NPASS
ISN 0004 INTEGER P,PLESS1
ISN 0005 DIMENSION W(150),K(150),DELTA1(300)
ISN 0006 PLESS1=P-1
ISN 0007 N=2*P-1
ISN 0008 SUM=0.
ISN 0009 TMIN=1.
ISN 0010 TDELTA=TDELTA
ISN 0011 DELTA1=1./TDELTA
ISN 0012 DO 1 M=1,PLESS1
ISN 0013 DELTA1(M)=SQRT(W(M+1)/K(M))/19.648
ISN 0014 NN=PLESS1+M
ISN 0015 1 DELTA1(NN)=SQRT(W(M)/K(M))/19.648
ISN 0016 IF(K(P).GT.0.) GO TO 2
ISN 0018 DELTA1(N)=1.0
ISN 0019 GO TO 3
ISN 0020 2 DELTA1(N)=SQRT(W(P)/K(P))/19.648
ISN 0021 3 DO 4 M=1,N
ISN 0022 4 TMIN=AMIN1(TMIN,DELTA1(M))
ISN 0023 IF(TMIN/2.-DELTA1)5,6,6
ISN 0024 5 DELTA1=TMIN/2.
ISN 0025 TDELTA=1.0/DELTA1
ISN 0026 6 DO 7 M=1,N
ISN 0027 7 SUM=SUM+DELTA1(M)
ISN 0028 N2=4.0*SUM/(2.0*DELTA1)
ISN 0029 RETURN
ISN 0030 END

```

*****FORTRAN CROSS REFERENCE LISTING*****

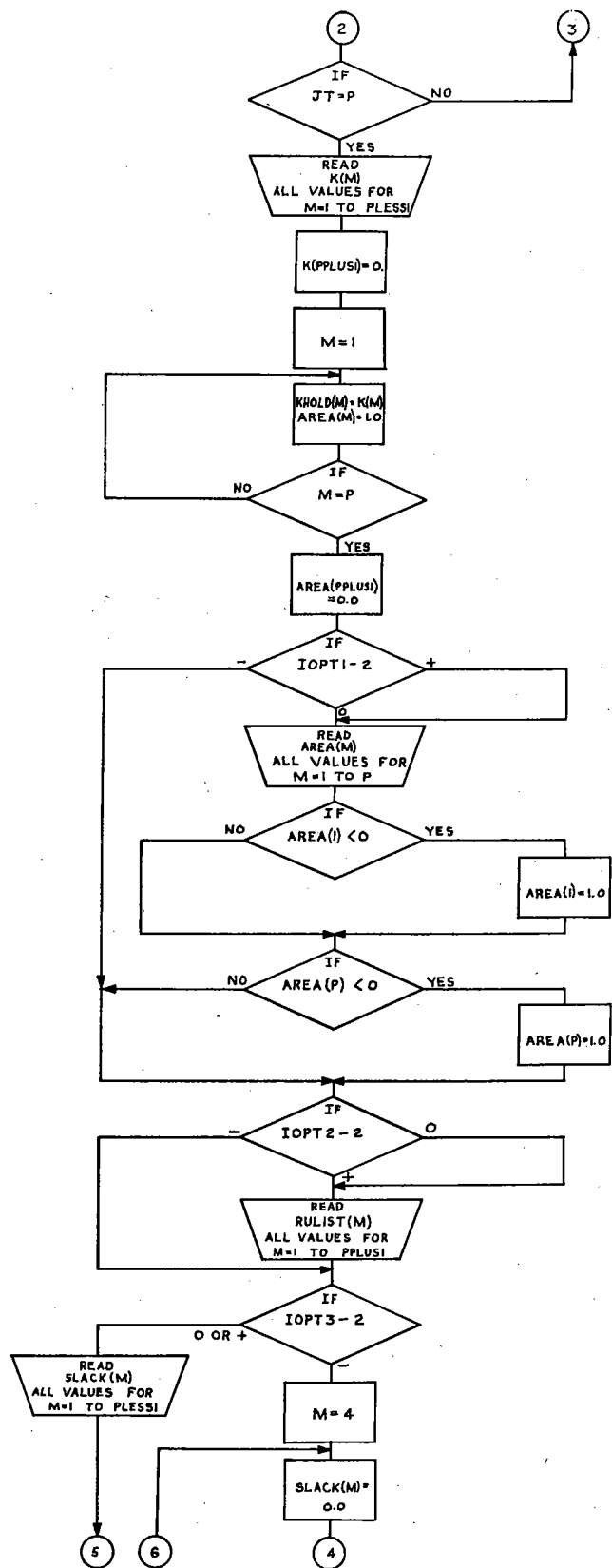
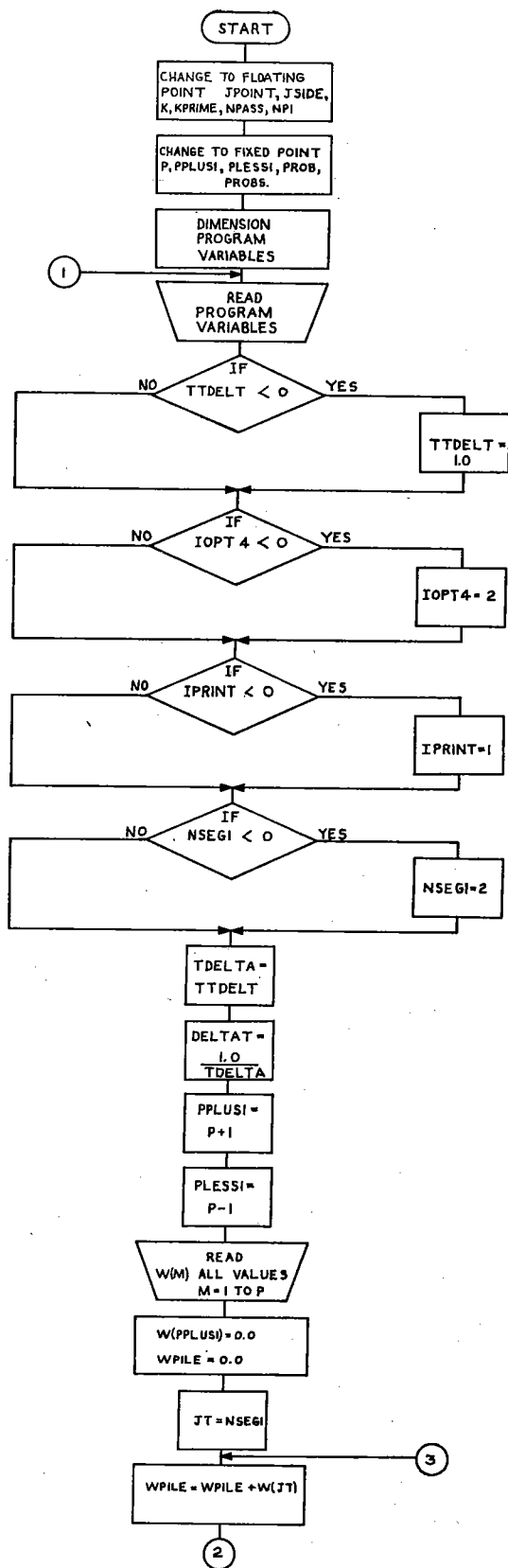
SYMBOL	INTERNAL	STATEMENT	NUMBERS
K	0002	0003	0005 0013 0015 0016 0020
M	0012	0013	0013 0013 0014 0015 0015 0021 0022 0026 0027
N	0007	0018	0020 0021 0026
P	0002	0004	0006 0007 0016 0020 0020
W	0007	0005	0013 0015 0020
NN	0014	0015	
N2	0002	0026	
SUM	0008	0027	0028
SQRT	0013	0015	0020
TMIN	0009	0022	0023 0024
AMIN1	0022		
DELTA1	0005	0013	0015 0018 0020 0022 0027
NPASS	0002	0003	
DELTA1	0002	0011	0023 0024 0025 0028
DELTCK	0007		
PLESS1	0004	0006	0012 0014
TDELTA	0002	0010	0011 0025
TDELTA	0002	0010	

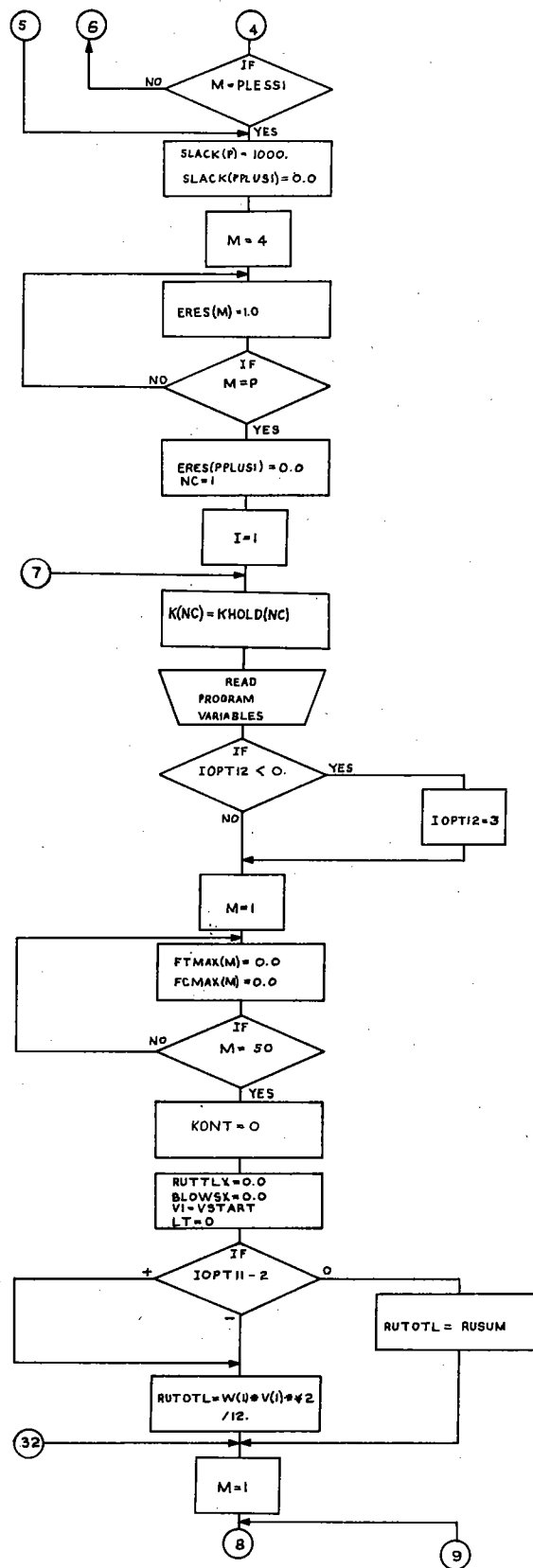
*****FORTRAN CROSS REFERENCE LISTING*****

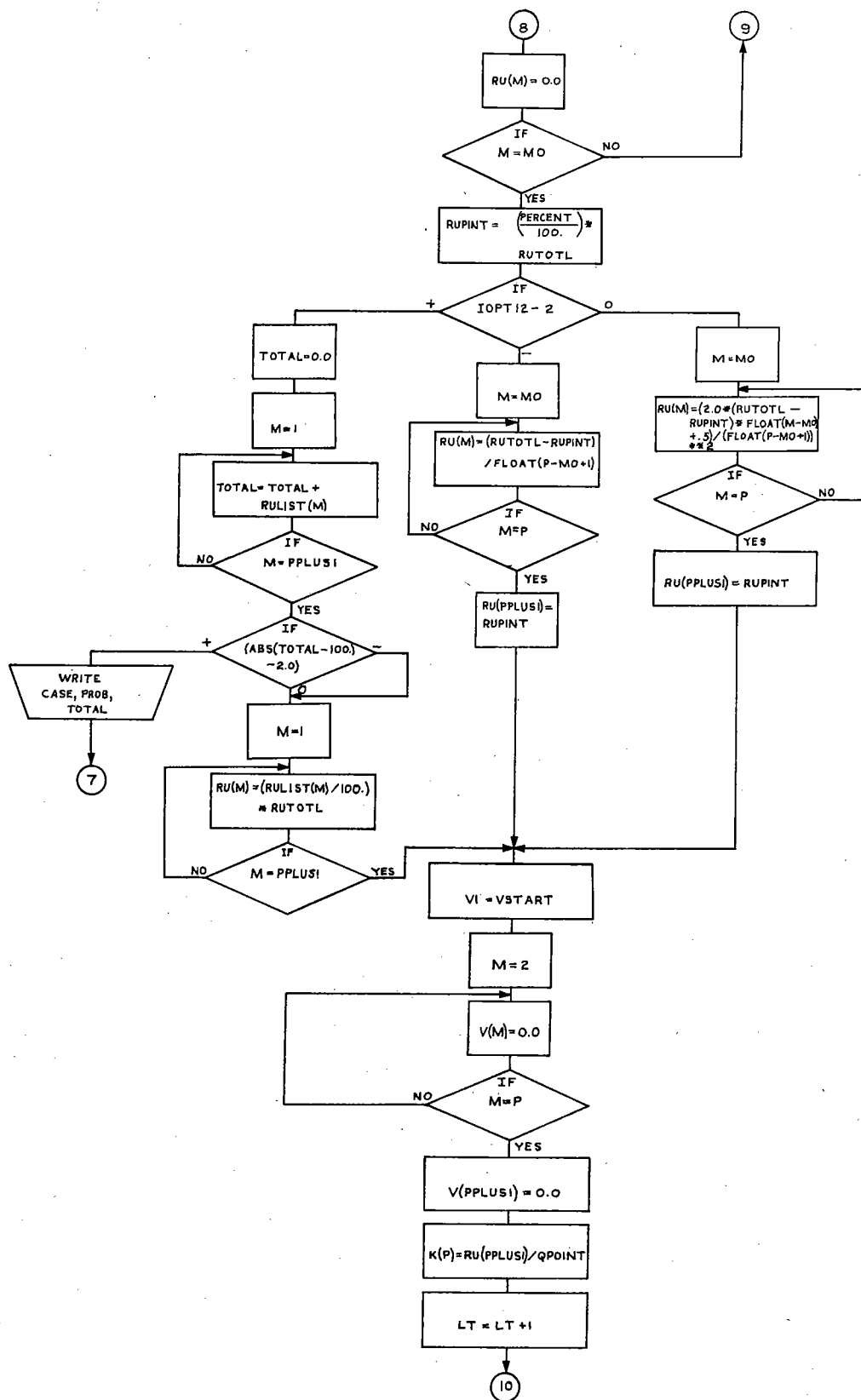
LABEL	DEFINED	REFERENCES
1	0015	0012
2	0020	0016
3	0021	0019
4	0022	0021
5	0024	0023
6	0026	0023 0023
7	0027	0026

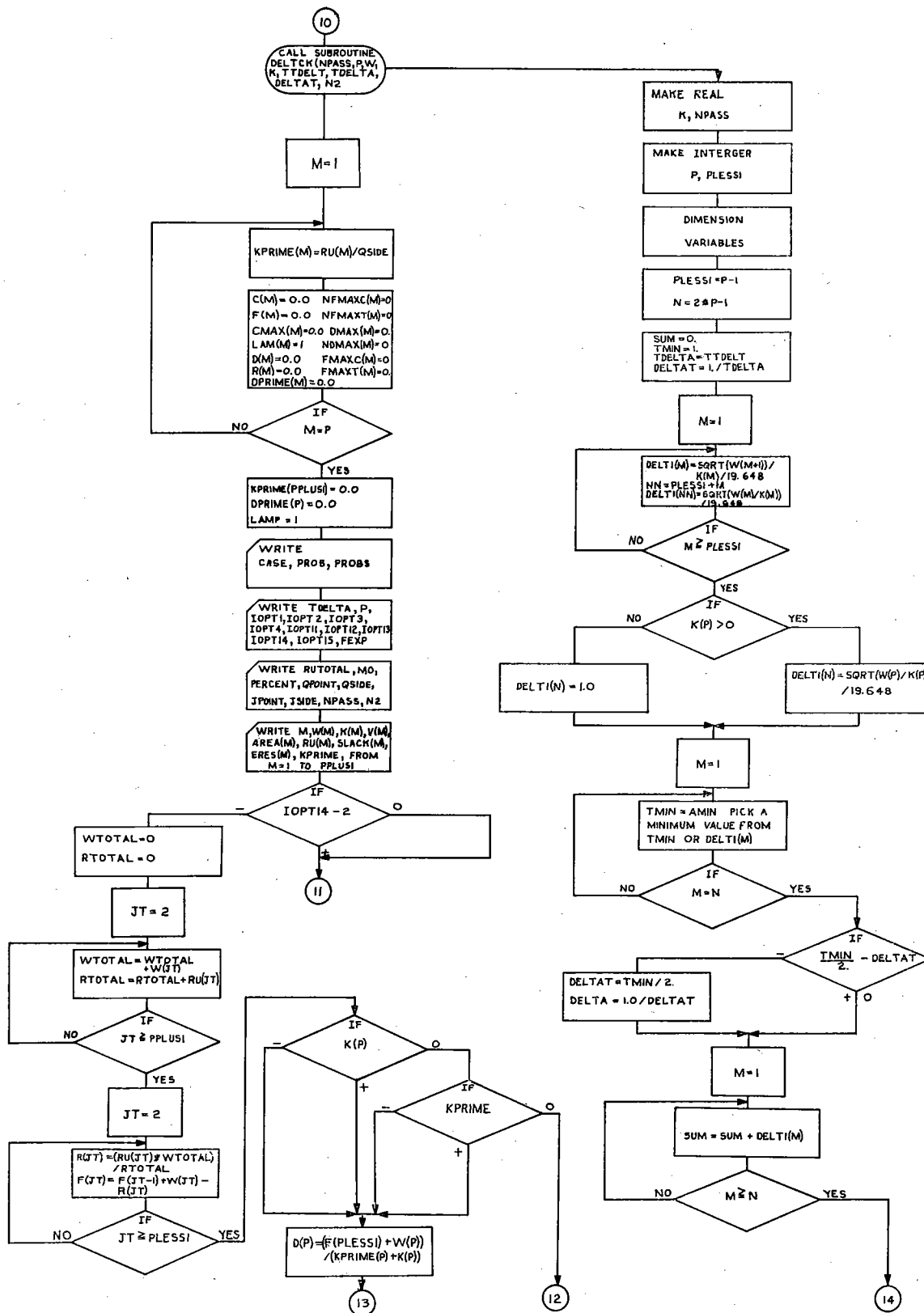
***** END OF COMPILATION *****

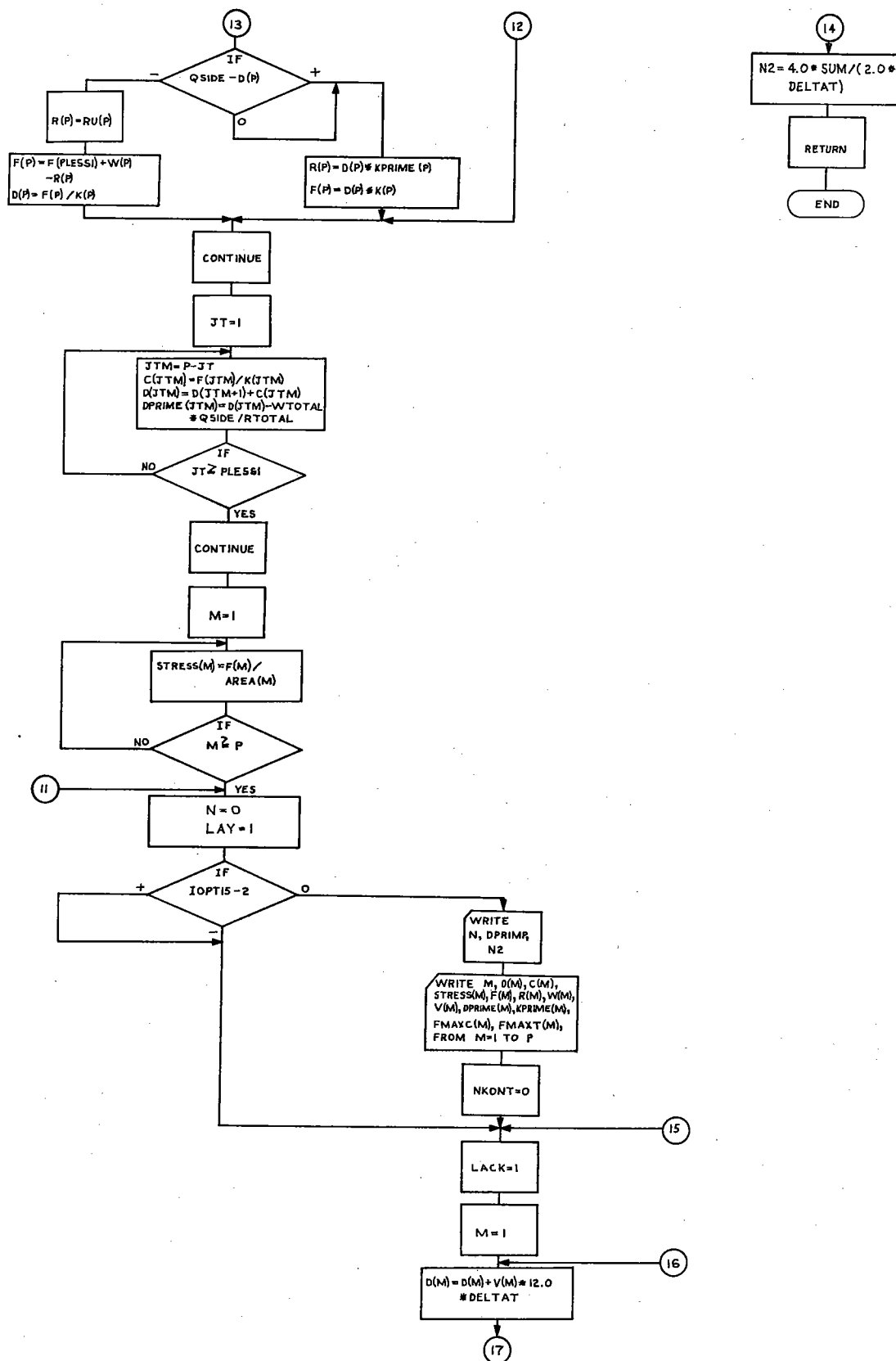
IEF2851	SYS68134.T145405.RP001.A49394.R0000444	DELETED
IEF2851	VOL SER NOS= 555555.	
IEF2851	SYS68134.T145405.RP001.A49394.R0000445	DELETED
IEF2851	VOL SER NOS= STUBAU.	
IEF2851	SYSOUT	SYSOUT
IEF2851	VOL SER NOS=	
IEF2851	SYS68134.T145405.RP001.A49394.LOADSET	PASSED
IEF2851	VOL SER NOS= 666666.	
IEF2851	SYS68134.T145405.RP001.A49394.LOADSET	DELETED
IEF2851	VOL SER NOS= 666666.	



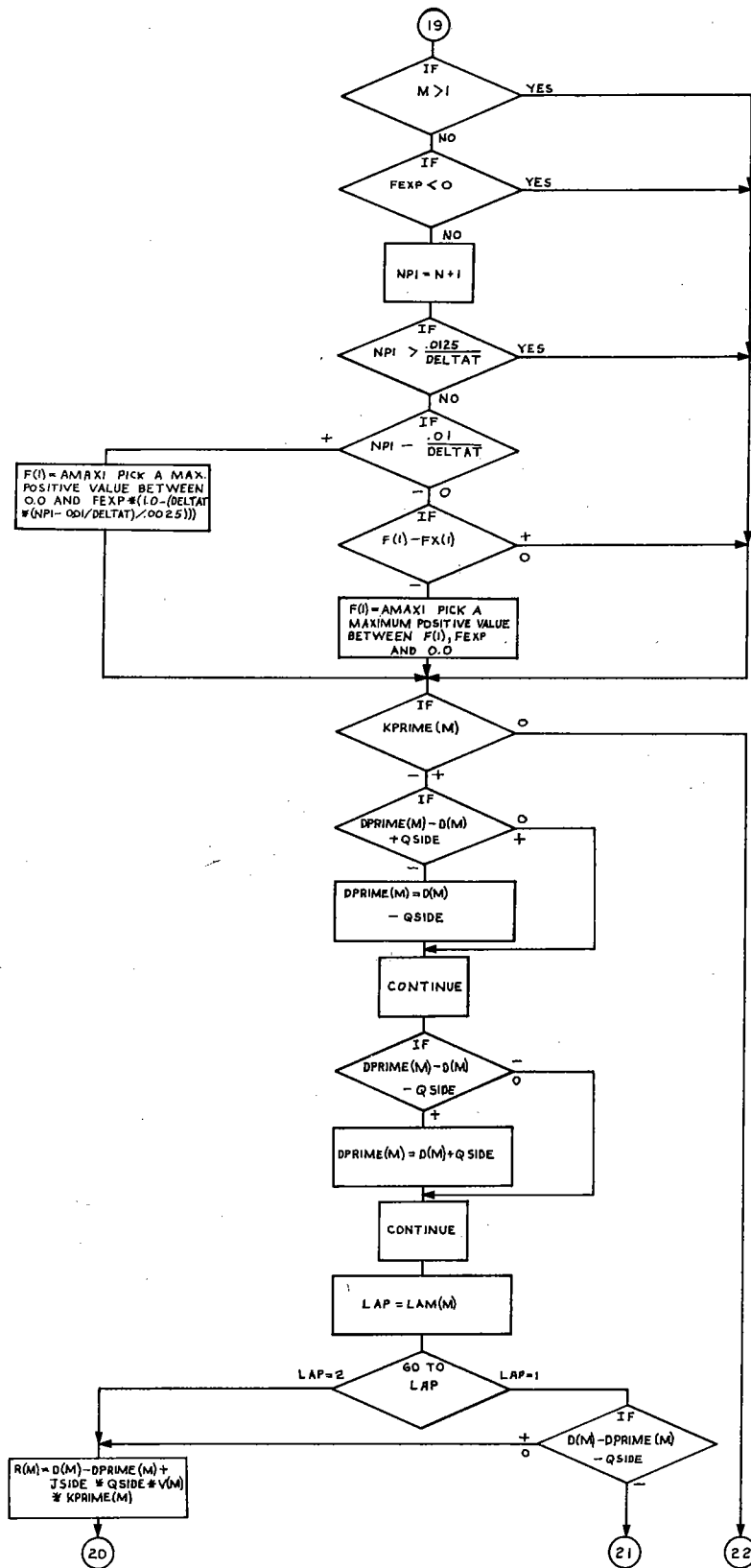




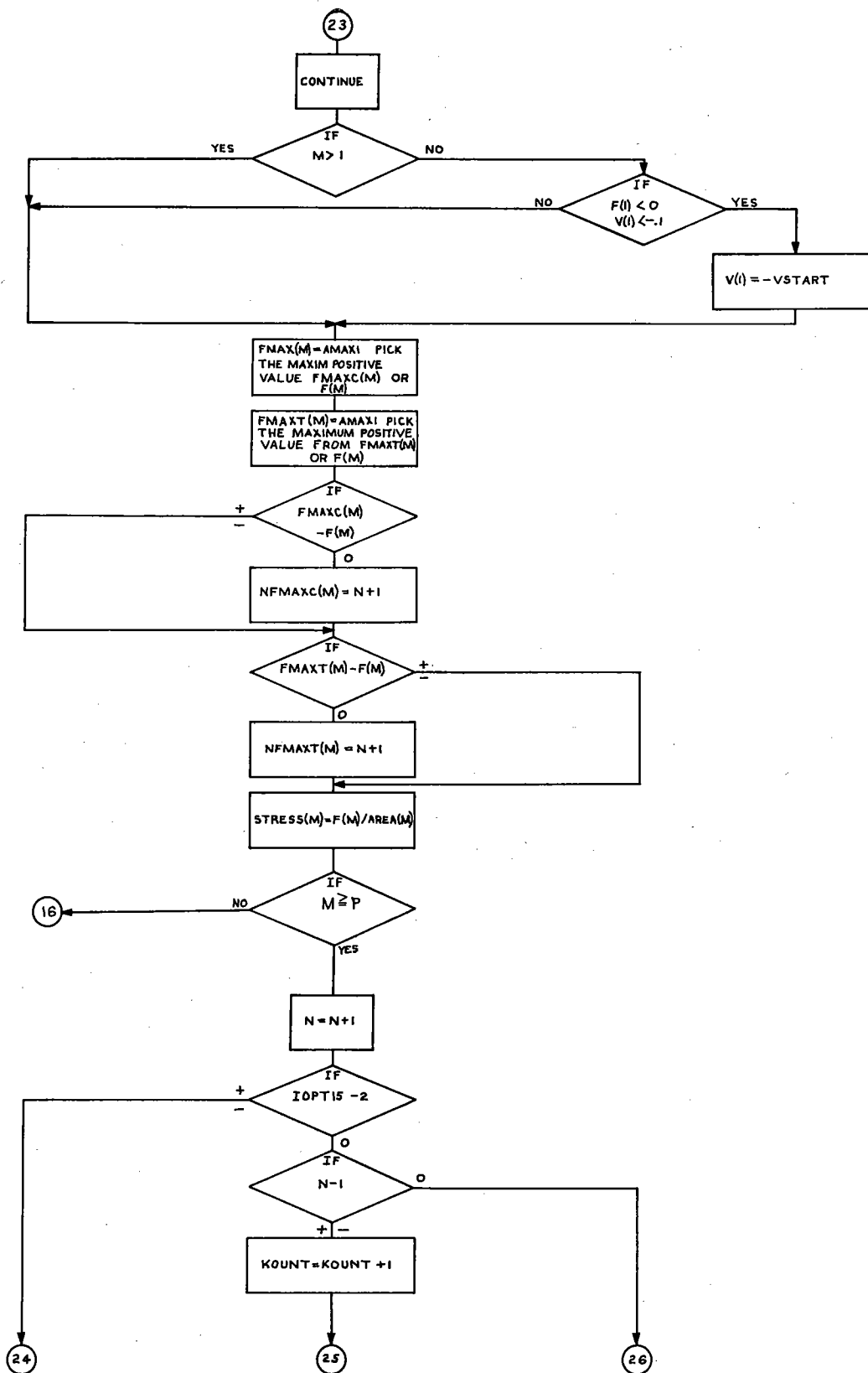


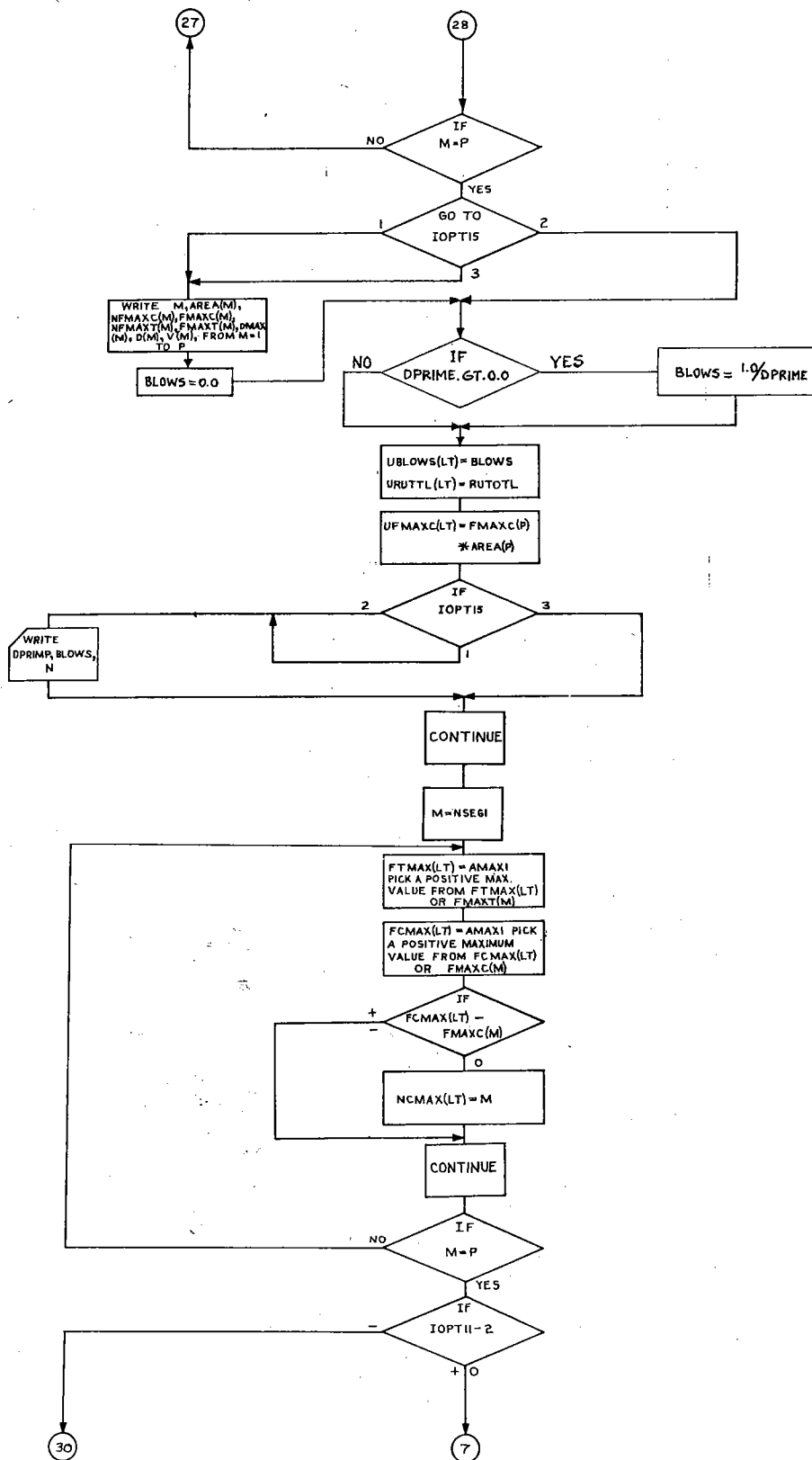


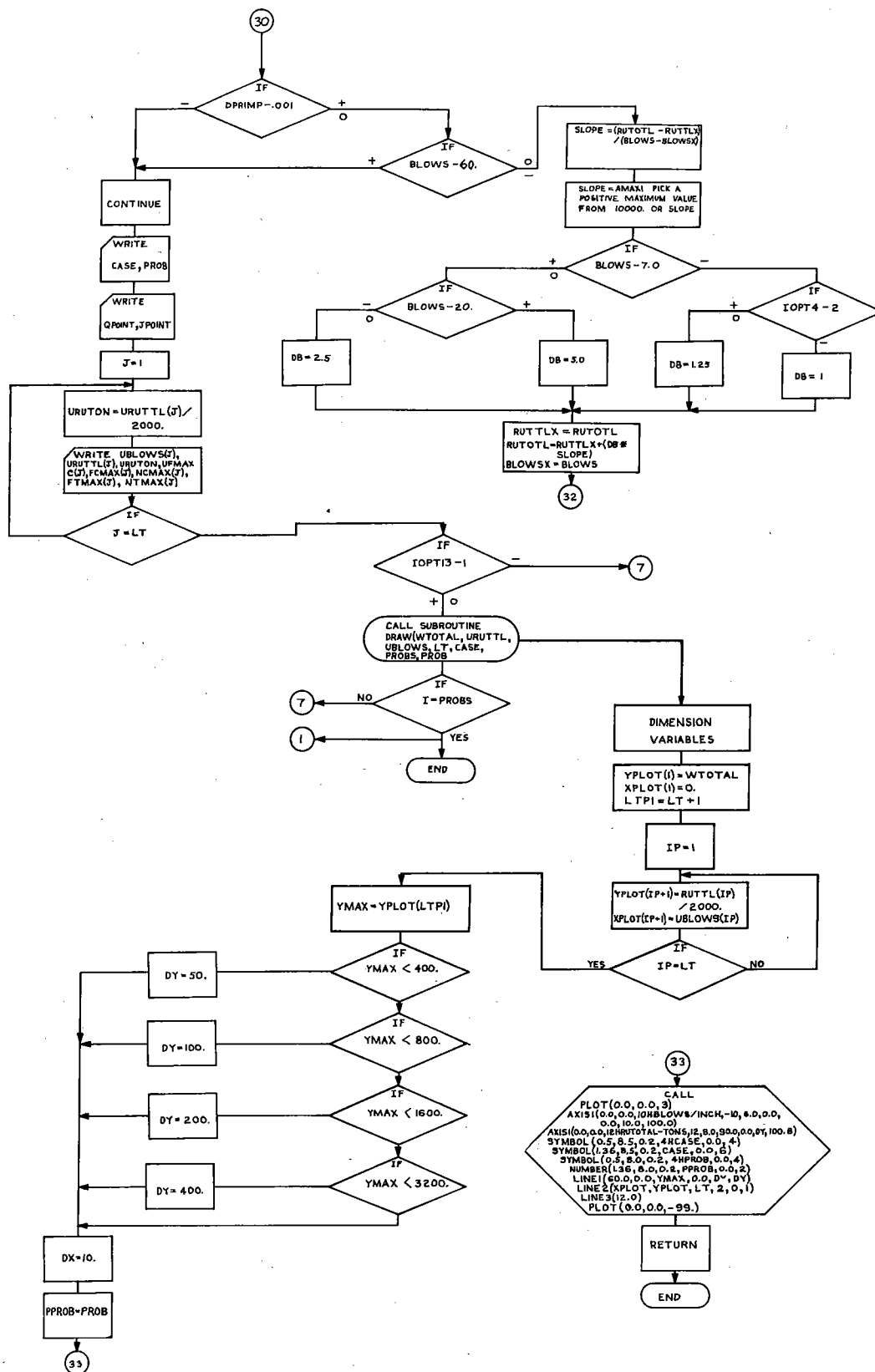












REFERENCES

- 1.1 Isaacs, D. V., "Reinforced Concrete Pile Formula," *Inst. Aust. Eng. J.*, Vol. 12, 1931.
- 1.2 Smith, E. A. L., "Pile Driving Impact," *Proceedings, Industrial Computation Seminar*, September, 1950, International Business Machines Corp., New York, N.Y., 1951, p. 44.
- 1.3 Smith, E. A. L., "Pile Driving Analysis by the Wave Equation," *Proceedings, ASCE*, August, 1960.
- 2.1 Isaacs, D. V., "Reinforced Concrete Pile Formula," *Inst. Aust. Eng. J.*, Vol. 12, 1931.
- 2.2 Smith, E. A. L., "Pile Driving Impact," *Proceedings, Industrial Computation Seminar*, September, 1950, International Business Machines Corp., New York, N.Y., 1951, p. 44.
- 2.3 Smith, E. A. L., "Pile Driving Analysis by the Wave Equation," *Proceedings, ASCE*, August, 1960.
- 2.4 Dunham, C. W., *Foundations of Structures*, McGraw-Hill Book Company, New York, 1962.
- 2.5 Chellis, R. D., *Pile Foundations*, McGraw-Hill Book Co., New York, 1951.
- 2.6 Fowler, J. W., "Chesapeake Bay Bridge-Tunnel Project," *Civil Engineering*, December, 1963.
- 2.7 Chellis, R. D., *Pile Foundations*, McGraw-Hill Book Co., New York, 1951.
- 2.8 Leonards, G. A., *Foundation Engineering*, McGraw-Hill Book Co., New York, 1962.
- 2.9 Janes, R. L., "Driving Stresses in Steel Bearing Piles," *Dissertation at Illinois Institute of Technology*, June, 1955.
- 2.10 Cummings, A. E., "Dynamic Pile Driving Formulas," *Journal of the Boston Society of Civil Engineers*, January, 1940.
- 2.11 Gardner, S. V. and Holt, D., "Some Experiences with Prestressed Concrete Piles," *Proceedings of the Institute of Civil Engineers, London*, Vol. 18, January, 1961.
- 2.12 Glanville, W. H., Grime, G., Fox, E. N., and Davies, W. W., "An Investigation of the Stresses in Reinforced Concrete Piles During Driving," *British Bldg. Research Board Technical Paper No. 20*, D.S.I.R., 1938.
- 2.13 Heising, W. P., Discussion of "Impact and Longitudinal Wave Transmission" by E. A. L. Smith, *Transactions, ASME*, August, 1955, p. 963.
- 3.1 Rand, Mogens, "Explosion Adds Driving Force to Diesel Hammer," *Engineering Contract Record*, December, 1960.
- 3.2 Housel, W. S., "Pile Load Capacity: Estimates and Test Results," *Journal of the Soil Mechanics and Foundations Division, ASCE*, Proc. Paper 4483, September, 1965.
- 3.3 Lowery, L. L., Hirsch, T. J. and Samson, C. H., "Pile Driving Analysis—Simulation of Hammers, Cushions, Piles and Soils," *Research Report 33-9*, Texas Transportation Institute, August, 1967.
- 6.1 Chan, P. C., Hirsch, T. J. and Coyle, H. M., "A Laboratory Study of Dynamic Load-Deformation and Damping Properties of Sands Concerned with a Pile-Soil System," *Texas Transportation Institute, Research Report No. 33-7*, June, 1967.
- 6.2 Reeves, G. N., Coyle, H. M., and Hirsch, T. J., "Investigation of Sands Subjected to Dynamic Loading," *Texas Transportation Institute, Research Report No. 33-7A*, December, 1967.
- 6.3 Airhart, T. P., Hirsch, T. J. and Coyle, H. M., "Pile-Soil System Response in Clay as a Function of Excess Pore Water Pressure and Other Soil Properties," *Texas Transportation Institute, Research Report No. 33-8*, September, 1967.
- 6.4 Chellis, R. D., *Pile Foundations*, McGraw-Hill Book Co., New York, 1951.
- 6.5 Smith, E. A. L., "Pile Driving Analysis by the Wave Equation," *Transactions, ASCE*, Paper No. 3306, Vol. 127, Part I, 1962.
- 6.6 Forehand, P. W. and Reese, J. L., "Pile Driving Analysis Using the Wave Equation," *Master of Science in Engineering Thesis, Princeton University*, 1963.
- 6.7 Mansur, C. I., "Pile Driving and Loading Test," *Presented at ASCE Convention, New York*, October 22, 1964.
- 7.1 Lowery, L. L., Jr., Edwards, L. C., and Hirsch, T. J., "Use of the Wave Equation to Predict Soil Resistance on a Pile During Driving," *Texas Transportation Institute, Research Report 33-10*, August, 1968.
- 7.2 Moseley, E. T., "Test Piles in Sand at Helena, Arkansas, Wave Equation Analysis," *Foundation Facts*, Vol. 3, No. 2, Raymond International, Concrete Pile Division, New York, 1967.
- 8.1 Samson, C. H., Hirsch, T. J. and Lowery, L. L., "Computer Study of The Dynamic Behavior of Piling," *Journal of the Structural Division, Proceedings, ASCE*, Paper No. 3608, ST4, August, 1963, p. 413.
- 8.2 Heising, W. P., Discussion of "Impact and Longitudinal Wave Transmission" by E. A. L. Smith, *Transactions, ASME*, August, 1955, p. 963.
- 8.3 Smith, E. A. L., "Pile Driving Analysis by the Wave Equation," *Transactions, ASCE*, Vol. 127, 1962, Part I, p. 1145.
- 8.4 Hirsch, T. J., "A Report on Stresses in Long Prestressed Concrete Piles During Driving," *Research Report No. 27*, Texas Transportation Institute, September, 1962.

- 8.5 Hirsch, T. J., "A Report on Field Tests of Prestressed Concrete Piles During Driving," Progress Report, Project No. 2-5-62-33, Texas Transportation Institute, August, 1963.
- 8.6 Lowery, L. L., Hirsch, T. J. and Samson, C. H., "Pile Driving Analysis—Simulation of Hammers, Cushions, Piles and Soils," Research Report No. 33-9, Texas Transportation Institute, August, 1967.
- 9.1 Hirsch, T. J., "A Report on Computer Study of Variables which Affect the Behavior of Concrete Piles During Driving," Progress Report, Project No. 2-5-62-33, Texas Transportation Institute, August, 1963.
- 9.2 Hirsch, T. J., and Samson, C. H., "Driving Practices for Prestressed Concrete Piles," Research Report 33-3, Texas Transportation Institute, April, 1965.
- 9.3 McClelland, B., Focht, J., and Emrich, W., "Problems in Design and Installation of Heavily Loaded Pipe Piles," Presented to ASCE Specialty Conference on Civil Engineering in the Oceans, San Francisco, September, 1967.
- 9.4 Lowery, L. L., Hirsch, T. J. and Edwards, T. C., "Use of the Wave Equation to Predict Soil Resistance on a Pile During Driving," Research Report No. 33-10, Texas Transportation Institute, April, 1967.
- 9.5 Lowery, L. L., Hirsch, T. J. and Samson, C. H., "Pile Driving Analysis—Simulation of Hammers, Cushions, Piles and Soils," Research Report No. 33-9, Texas Transportation Institute, August, 1967.
- B1. Smith, E. A. L., "Pile Driving Analysis by the Wave Equation," *Journal of the Soil Mechanics and Foundations Division*, Proceedings of the American Society of Civil Engineers, Proc. Paper 2574, SM4, August, 1960, pp. 35-61.
- B2. Hirsch, T. J., and Edwards, T. C., "Impact Load-Deformation Properties of Pile Cushioning Materials," Research Report 33-4, Project 2-5-62-33, Piling Behavior, Texas Transportation Institute, Texas A&M University, College Station, Texas, May, 1966, p. 12.
- B3. Smith, E. A. L., "Pile Driving Analysis by the Wave Equation," *Journal of the Soil Mechanics and Foundations Division*, Proceedings of the American Society of Civil Engineers, Proc. Paper 2574, SM4, August, 1960, p. 47.
- B4. Samson, C. H., Hirsch, T. J., and Lowery, L. L., "Computer Study of Dynamic Behavior of Piling," *Journal of the Structural Division*, Proceedings of the American Society of Civil Engineers, Proceedings Paper 3608, ST4, August, 1963, p. 419.
- B5. Smith, E. A. L., "Pile Driving Analysis by the Wave Equation," *Journal of the Soil Mechanics and Foundations Division*, Proceedings of the American Society of Civil Engineers, Proc. Paper 2574, SM4, August, 1960, p. 44.